

**DYE REMOVAL BY NANO-SIZED METAL COATED
ELECTRODES**

Reza SHAHBAZI
Master Dissertation

Graduate School of Sciences
Nanotechnology Program
June-2012

JÜRİ VE ENSTİTÜ ONAYI

Reza Shahbazi'nin “Nano Boyutlu Metal Kaplı Elektrotlarla Boyar Madde Giderimi” başlıklı **Nanoteknoloji** Anabilim Dalındaki, Yüksek Lisans Tezi 12.06.2012 tarihinde, aşağıdaki jüri tarafından Anadolu Üniversitesi Lisansüstü Eğitim Öğretim ve Sınav Yönetmeliğinin ilgili maddeleri uyarınca değerlendirilerek Kabul edilmiştir.

	Adı-Soyadı	İmza
Üye (Tez Danışmanı) :	Doç. Dr. YUSUF YAVUZ
Üye :	Prof. Dr. ALİ SAVAŞ KOPARAL
Üye :	Prof. Dr. AYDIN DOĞAN

Anadolu Üniversitesi Fen Bilimleri Enstitüsü Yönetim Kurulu'nun
..... tarih ve sayılı kararıyla onaylanmıştır.

Enstitü Müdürü

ABSTRACT

Master of Science Thesis

DYE REMOVAL BY NANO-SIZED METAL COATED ELECTRODES

Reza SHAHBAZI

Anadolu University
Graduate School of Sciences
Nanotechnology Program

Supervisor: Assoc./Prof. Dr. Yusuf YAVUZ
2012, 103 pages

Textile processing industries are widespread in developing countries. Among the various processes in the textile industry, the dyeing process uses large volumes of water for dyeing, fixing and washing. Textile industry wastewater is characterized by suspended particles, salts, high pH and high chemical oxygen demand (COD) concentrations that discarding of these toxic wastewaters to the environment will cause a major problem. Nanotechnology techniques and materials have been prosperous in many fields and about wastewater treatment boron-doped diamond (BDD) electrodes have been successful in dye removing processes. In this study, electrochemical oxidation of Reactive Black 5 (RB5) dye using bipolar trickle tower (BTT) reactor and Raschig ring shaped boron-doped diamond (BDD) electrodes in recirculated batch mode was fulfilled. One half of the BDD electrodes act as anode and the other half as cathode. Different parameters affect the dye removing process that has been studied during experiments. Experimental parameters like flow rate, sodium sulfate concentration (Na_2SO_4) as supporting electrolyte, initial pH, current density and initial dye concentration were examined. The best experimental conditions obtained were as follows: current density 1 mA/cm^2 , natural pH, flow rate 100 mL/min , Na_2SO_4 concentration 0.02 mol/L . After determining best experimental conditions TOC, COD and toxicity studies have been performed to prove the reliability of this process. Under these conditions, 97% color, ~51% COD and 29.3% TOC removal were achieved. Toxicity of RB5 solution was also decreased relatively to its initial toxicity value at the same conditions.

Keywords: Electrochemical Oxidation, Reactive Black 5 Dye, Boron-Doped Diamond, Toxicity, Bipolar Trickle Tower Reactor



ÖZET

Yüksek Lisans Tezi

NANO BOYUTLU METAL KAPLI ELEKTROTLARLA BOYAR MADDE GİDERİMİ

Reza SHAHBAZİ

Anadolu Üniversitesi
Fen Bilimleri Enstitüsü
Nanoteknoloji Anabilim Dalı

Danışman: Doç. Dr. Yusuf YAVUZ
2012, 103 sayfa

Tekstil endüstrisi geliştirmekte olan ülkelerde çok yaygındır. Tekstil endüstrisinin farklı süreçleri arasında, boyama sürecinde, boyama, sabitleme ve yıkama için çok miktarda su sarf edilmektedir. Tekstil atık suyunun karakteristiği asılı parçacıklar, tuzlar, yüksek pH ve yüksek kimyasal oksijen ihtiyacı (KOİ) derişimidir. Bu toksik atık suların çevreye deşarj edilmesi önemli problemlere neden ola bilir. Nanoteknoloji teknikleri ve malzemeleri farklı alanlarda başarılı olmuştur ve atık su arıtımında bor kaplı elmas (BDD) elektrotlar renk giderim süreçlerinde başarı ile kullanılmıştır. Bu çalışmada, tıkaç akım reaktörde, bor katkılı elmas elektrotlar kullanılarak Reactive Black 5 (RB5) boyarmaddesinin elektrokimyasal yükseltgemesi gerçekleştirilmiştir. Bor katkılı elmas elektrotların yarısı anot ve yarısı katot olarak davranıyor. Farklı parametreler arıtım sürecini etkiliyor ki deneyler sırasında araştırılmıştır. Akış hızı, destek elektrolit olarak sodyum sülfat derişimi (Na_2SO_4), başlangıç pH, akım yoğunluğu ve başlangıç boyar madde derişimi gibi deneysel parametreler incelendi. Elde edilen en iyi şartlar şöyledir: akım yoğunluğu 1 mA/cm^2 , doğal pH, akış hızı 100 mL/min , sodyum sülfat derişimi 0.02 mol/L . En iyi deneysel şartlar elde edildikten sonra sürecin güvenilirliğini kanıtlamak için toplam organik karbon (TOC), KOİ ve toksisite çalışmaları yapılmıştır. Bu şartlar altında, %97 renk, ~%51 KOİ ve %29,3 TOK giderimi elde edilmiştir. RB5 boyar maddesinin toksisitesi de başlangıç toksisite oranına göre azalmıştır.

Anahtar Kelimeler: Elektrokimyasal Yükseltgeme, Reactive Black 5 (RB5)
Boyarmadde, Bor Kaplı Elmas, Toksisite, Tıkaç Reaktör

ACKNOWLEDGMENT

I do thank my professors Dr. Yusuf Yavuz as my thesis supervisor and Prof. Dr. Ali Savaş Koparal as my advisor. They helped me a lot during my thesis. Without their help it wasn't possible to overcome problems. Also I learned the real meaning of Nano world and how the things behave differently in the Nano world, thanks to their infinite knowledge.

Reza SHAHBAZİ

June, 2012

CONTENTS

	<u>Page</u>
ABSTRACT	i
ÖZET	ii
ACKNOWLEDGMENT	iii
CONTENTS	iv
ORDER OF FIGURES	vii
ORDER OF TABLES	xi
SYMBOLS AND ABBREVIATIONS	xv
1. TITLE AND AIM OF THE STUDY	1
2. INTRODUCTION	2
2.1. Classification of Dyes	3
2.2. Dye Removing Processes and Techniques	3
2.3. Current Methods for Pollutant Treatment.....	6
2.3.1. Incineration and pyrolysis	8
2.3.2. Air stripping	9
2.3.3. Microbial treatment	9
2.3.4. Precipitation and coagulation	10
2.3.5. Chemical treatment.....	11
2.3.6. Adsorption	11
2.3.7. Membrane processes	12
2.3.8. Distillation	12
2.4. Advanced Oxidation Processes.....	12
2.5. Electrochemical Technologies for Wastewater Treatment	13
2.5.1. Electrodeposition.....	13
2.5.2. Electrocoagulation.....	14

2.5.3. Electroflotation	15
2.6. Positive Features of Electrochemical Approaches to Pollution Control.....	15
2.7. Electrochemical Oxidation: An Alternative in Wastewater Treatment	16
2.7.1. Direct anodic oxidation	16
2.7.2. Indirect anodic oxidation	17
2.8. Electrode Materials	19
2.9. Hot-Filament CVD (HFCVD)	20
2.8. Review of Published Literature	22

3. MATERIALS AND METHODS 26

3.1. Power Supply and Multimeter	26
3.2. Peristaltic Pump	26
3.3. Electrochemical Reactor	26
3.4. Graphite Feed Electrodes	27
3.5. pH Meter	27
3.6. Model solution	27
3.7. UV-visible Spectrophotometer	28
3.8. Centrifuge	28
3.9. Analyzing Tests	28
3.10. Stirrer	29
3.11. Supporting Electrolyte	29
3.12. Electrode Material.....	29
3.13. Software	30
3.14. List of the Materials	30

4. EXPERIMENTS 31

4.1. Calibration	31
4.1.1. UV-visible Spectrophotometer Calibration.....	31
4.1.2. Peristaltic Pump Calibration.....	33
4.2. Experimental Setup.....	34
4.3. Process of the Experiments.....	36

4.4. Methods of Analyzing	36
4.4.1. Total Organic Carbon Analyze (TOC)	36
4.4.2. Chemical Oxygen Demand (COD)	37
4.4.3. Toxicity Analyze	37
5. RESULTS AND DISSCUTION	37
5.1. Effect of Flow Rate	38
5.2. Effect of Supporting Electrolyte	49
5.3. Effect of Initial pH	56
5.4. Effect of Current Density	62
5.5. Effect of Initial Dye Concentration	74
5.6. Spectrum of Reactive Black 5 Dye	84
5.7. Energy Consumption	85
5.8. Toxicity Studies	87
6. CONCLUSION	88
REFERENCES	90
APPENDIX-1 Calculations of Anode Surface Area of Each Electrode and Total Surface Area of BDD Electrodes	99
APPENDIX 1.1. Calculation of Anode Surface Area	99
APPENDIX-2 Calculations for Determining Dye Concentration	100
APPENDIX 2.1. Concentration Calculations	100
APPENDIX-3 Sample Calculations.....	101
Appendix 3.1. Decolorization Efficiency (%)	101
Appendix 3.2. Energy Consumption.....	101
APPENDIX-4 Chemical Oxygen Demand Test.....	102

ORDER OF FIGURES

	<u>Page</u>
Figure 2.9.1. Schematic diagram of the hot-filament CVD apparatus.....	21
Figure 4.1.1.1. Standard operational chart for UV-visible spectrophotometer	32
Figure 4.1.2.1. Drawn chart for peristaltic pump calibration.....	34
Figure 4.2.1. Overview of the dye removing system	35
Figure 5.1.2. Effect of flow rate ($C_0=40$ mg/L RB5, $i=0.75$ mA/cm ² , I=132 A, S.E=0.02 M Na ₂ SO ₄ , Q=50 mL/min, rpm=18.6, Natural pH)	46
Figure 5.1.3. Effect of flow rate ($C_0=40$ mg/L RB5, $i=0.75$ mA/cm ² , I=132 A, S.E=0.02 M Na ₂ SO ₄ , Q=75 mL/min, rpm=27.8, Natural pH)	47
Figure 5.1.4. Effect of flow rate ($C_0=40$ mg/L RB5, $i=0.75$ mA/cm ² , I=132 A, S.E=0.02 M Na ₂ SO ₄ , Q=100 mL/min, rpm=37.1, Natural pH)	47
Figure 5.1.5. Effect of flow rate ($C_0=40$ mg/L RB5, $i=0.75$ mA/cm ² , I=132 A, S.E=0.02 M Na ₂ SO ₄ , Q=150 mL/min, rpm=55.7, Natural pH)	48
Figure 5.1.6. Effect of flow rate ($C_0=40$ mg/L RB5, $i=0.75$ mA/cm ² , I=132 A, S.E=0.02 M Na ₂ SO ₄ , Q=200 mL/min, rpm=74.3, Natural pH)	48
Figure 5.1.7. Comparison chart for Effect of flow rate ($C_0=40$ mg/L RB5, $i=0.75$ mA/cm ² , I=132 A, S.E=0.02 M Na ₂ SO ₄ , Natural pH).....	49
Figure 5.2.1. Effect of supporting electrolyte ($C_0=40$ mg/L RB5, $i=0.75$ mA/cm ² , I=132 A, S.E=0.02 M Na ₂ SO ₄ , Q=100 mL/min, rpm=37.1, Natural pH)	54
Figure 5.2.2. Effect of supporting electrolyte ($C_0=40$ mg/L RB5, $i=0.75$ mA/cm ² , I=132 A, S.E=0.03 M Na ₂ SO ₄ , Q=100 mL/min, rpm=37.1, Natural pH)	54

Figure 5.2.3. Effect of supporting electrolyte (Co=40 mg/L RB5, i=0.75 mA/cm ² , I=132 A, S.E=0.05 M Na ₂ SO ₄ , Q=100 mL/min, rpm=37.1, Natural pH)	55
Figure 5.2.4. Comparison chart for effect of supporting electrolyte (Co=40 mg/L RB5, i=0.75 mA/cm ² , I=132 A, Q=100 mL/min, rpm=37.1, Natural pH)	55
Figure 5.3.1. Effect of Initial pH (Co=40 mg/L RB5, i=0.75 mA/cm ² , I=132 A, S.E=0.02 M Na ₂ SO ₄ , Q=100 mL/min, rpm=37.1, Natural pH)	60
Figure 5.3.2. Effect of Initial pH (Co=40 mg/L RB5, i=0.75 mA/cm ² , I=132 A, S.E=0.02 M Na ₂ SO ₄ , Q=100 mL/min, rpm=37.1, pH=3.52)	60
Figure 5.3.3. Effect of Initial pH (Co=40 mg/L RB5, i=0.75 mA/cm ² , I=132 A, S.E=0.02 M Na ₂ SO ₄ , Q=100 mL/min, rpm=37.1, pH=10.17)	61
Figure 5.3.4. Comparison chart for effect of Initial pH (Co=40 mg/L RB5, i=0.75 mA/cm ² , I=132 A, S.E=0.02 M Na ₂ SO ₄ , Q=100 mL/min, rpm=37.1)	61
Figure 5.4.1. Effect of current density (Co=40 mg/L RB5, i=0.5 mA/cm ² , I=88 A, S.E=0.02 M Na ₂ SO ₄ , Q=100 mL/min, rpm=37.1, Natural pH)	70
Figure 5.4.2. Effect of current density (Co=40 mg/L RB5, i=0.625 mA/cm ² , I=110 A, S.E=0.02 M Na ₂ SO ₄ , Q=100 mL/min, rpm=37.1, Natural pH)	70
Figure 5.4.3. Effect of current density (Co=40 mg/L RB5, i=0.75 mA/cm ² , I=132 A, S.E=0.02 M Na ₂ SO ₄ , Q=100 mL/min, rpm=37.1, Natural pH)	71
Figure 5.4.4. Effect of current density (Co=40 mg/L RB5, i=0.875 mA/cm ² , I=154 A, S.E=0.02 M Na ₂ SO ₄ , Q=100 mL/min, rpm=37.1, Natural pH)	71

Figure 5.4.5. Effect of current density ($C_0=40$ mg/L RB5, $i=1$ mA/cm ² , $I=176$ A, S.E= 0.02 M Na ₂ SO ₄ , $Q=100$ mL/min, rpm= 37.1 , Natural pH)	72
Figure 5.4.6. Effect of current density ($C_0=40$ mg/L RB5, $i=1.125$ mA/cm ² , $I=198$ A, S.E= 0.02 M Na ₂ SO ₄ , $Q=100$ mL/min, rpm= 37.1 , Natural pH)	72
Figure 5.4.7. Effect of current density ($C_0=40$ mg/L RB5, $i=1.25$ mA/cm ² , $I=220$ A, S.E= 0.02 M Na ₂ SO ₄ , $Q=100$ mL/min, rpm= 37.1 , Natural pH)	73
Figure 5.4.8. Comparison chart for effect of current density ($C_0=40$ mg/L RB5, S.E= 0.02 M Na ₂ SO ₄ , $Q=100$ mL/min, rpm= 37.1 , Natural pH)	73
Figure 5.5.1. Effect of initial dye concentration ($C_0=20$ mg/L RB5, $i=1$ mA/cm ² , $I=176$ A, S.E= 0.02 M Na ₂ SO ₄ , $Q=100$ mL/min, rpm= 37.1 , Natural pH)	79
Figure 5.5.2. Effect of initial dye concentration ($C_0=40$ mg/L RB5, $i=1$ mA/cm ² , $I=176$ A, S.E= 0.02 M Na ₂ SO ₄ , $Q=100$ mL/min, rpm= 37.1 , Natural pH)	79
Figure 5.5.3. Effect of initial dye concentration ($C_0=60$ mg/L RB5, $i=1$ mA/cm ² , $I=176$ A, S.E= 0.02 M Na ₂ SO ₄ , $Q=100$ mL/min, rpm= 37.1 , Natural pH)	80
Figure 5.5.4. Effect of initial dye concentration ($C_0=100$ mg/L RB5, $i=1$ mA/cm ² , $I=176$ A, S.E= 0.02 M Na ₂ SO ₄ , $Q=100$ mL/min, rpm= 37.1 , Natural pH)	80
Figure 5.5.5. Comparison chart for effect of initial dye concentration ($i=1$ mA/cm ² , $I=176$ A, S.E= 0.02 M Na ₂ SO ₄ , $Q=100$ mL/min, rpm= 37.1 , Natural pH)	81
Figure 5.6.1. Spectrum of RB5 dye ($C_0=40$ mg/L RB5, $i=1$ mA/cm ² , $I=176$ A, S.E= 0.02 M Na ₂ SO ₄ , $Q=100$ mL/min, rpm= 37.1 , Natural pH)	85

Figure 5.7.1. Variation of energy consumption with current density
($C_0=40$ mg/L RB5, S.E=0.02 M Na_2SO_4 , $Q=100$ mL/min, rpm=37.1, Natural pH) 87

Figure 5.8.1. Variation of 5th min and 15th min toxicity of dye solution with time ($C_0=40$ mg/L RB5, $i=1$ mA/cm², $I=176$ A, S.E=0.02 M Na_2SO_4 , $Q=100$ mL/min, rpm=37.1, Natural pH) 88

ORDER OF TABLES

	<u>Page</u>
Table 2.3.1. Current technologies for the treatment of organic, inorganic, and microorganism pollutants in air, water, and soil	8
Table 3.6.1. Properties and chemical structure of Reactive Black 5 dye	27
Table 4.1.1.1. Concentrations and their absorbance for UV-visible standard operational curve	32
Table 4.1.2.1. Peristaltic pump calibration.....	33
Table 5.1.1. Effect of flow rate ($C_o=40$ mg/L RB-5, $i=0.75$ mA/cm ² , $I=132$ A, S.E=0.02 M Na ₂ SO ₄ , $Q=25$ mL/min, rpm=9.3, Natural pH).....	39
Table 5.1.2. Effect of flow rate ($C_o=40$ mg/L RB-5, $i=0.75$ mA/cm ² , $I=132$ A, S.E=0.02 M Na ₂ SO ₄ , $Q=50$ mL/min, rpm=18.6, Natural pH).....	40
Table 5.1.3. Effect of flow rate ($C_o=40$ mg/L RB-5, $i=0.75$ mA/cm ² , $I=132$ A, S.E=0.02 M Na ₂ SO ₄ , $Q=75$ mL/min, rpm=27.8, Natural pH).....	41
Table 5.1.4. Effect of flow rate ($C_o=40$ mg/L RB-5, $i=0.75$ mA/cm ² , $I=132$ A, S.E=0.02 M Na ₂ SO ₄ , $Q=100$ mL/min, rpm=37.1, Natural pH).....	42
Table 5.1.5. Effect of flow rate ($C_o=40$ mg/L RB-5, $i=0.75$ mA/cm ² , $I=132$ A, S.E=0.02 M Na ₂ SO ₄ , $Q=150$ mL/min, rpm=55.7, Natural pH).....	43
Table 5.1.6. Effect of flow rate ($C_o=40$ mg/L RB-5, $i=0.75$ mA/cm ² , $I=132$ A, S.E=0.02 M Na ₂ SO ₄ , $Q=200$ mL/min, rpm=74.3, Natural pH).....	44
Table 5.1.7. Comparison table for Effect of flow rate ($C_o=40$ mg/L RB-5, $i=0.75$ mA/cm ² , $I=132$ A, S.E=0.02 M Na ₂ SO ₄ , Natural pH).....	45

Table 5.2.1. Effect of supporting electrolyte (Co=40 mg/L RB-5, i=0.75 mA/cm ² , I=132 A, S.E=0.02 M Na ₂ SO ₄ , Q=100 mL/min, rpm=37.1, Natural pH)	50
Table 5.2.2. Effect of supporting electrolyte (Co=40 mg/L RB-5, i=0.75 mA/cm ² , I=132 A, S.E=0.03 M Na ₂ SO ₄ , Q=100 mL/min, rpm=37.1, Natural pH)	51
Table 5.2.3. Effect of supporting electrolyte (Co=40 mg/L RB-5, i=0.75 mA/cm ² , I=132 A, S.E=0.05 M Na ₂ SO ₄ , Q=100 mL/min, rpm=37.1, Natural pH)	52
Table 5.2.4. Comparison table for Effect of supporting electrolyte (Co=40 mg/L RB-5, i=0.75 mA/cm ² , I=132 A, Q=100 mL/min, rpm=37.1, Natural pH)	53
Table 5.3.1. Effect of Initial pH (Co=40 mg/L RB-5, i=0.75 mA/cm ² , I=132 A, S.E=0.02 M Na ₂ SO ₄ , Q=100 mL/min, rpm=37.1, Natural pH)	56
Table 5.3.2. Effect of Initial pH (Co=40 mg/L RB-5, i=0.75 mA/cm ² , I=132 A, S.E=0.02 M Na ₂ SO ₄ , Q=100 mL/min, rpm=37.1, pH=3.52)	57
Table 5.3.3. Effect of Initial pH (Co=40 mg/L RB-5, i=0.75 mA/cm ² , I=132 A, S.E=0.02 M Na ₂ SO ₄ , Q=100 mL/min, rpm=37.1, pH=10.17)	58
Table 5.3.4. Comparison table for effect of Initial pH (Co=40 mg/L RB-5, i=0.75 mA/cm ² , I=132 A, S.E=0.02 M Na ₂ SO ₄ , Q=100 mL/min, rpm=37.1)	59
Table 5.4.1. Effect of current density (Co=40 mg/L RB-5, i=0.5 mA/cm ² , I=88 A, S.E=0.02 M Na ₂ SO ₄ , Q=100 mL/min, rpm=37.1, Natural pH)	62
Table 5.4.2. Effect of current density (Co=40 mg/L RB-5, i=0.625 mA/cm ² , I=110 A, S.E=0.02 M Na ₂ SO ₄ , Q=100 mL/min, rpm=37.1, Natural pH)	63

Table 5.4.3. Effect of current density ($C_o=40$ mg/L RB-5, $i=0.75$ mA/cm ² , $I=132$ A, $S.E=0.02$ M Na ₂ SO ₄ , $Q=100$ mL/min, rpm=37.1, Natural pH)	64
Table 5.4.4. Effect of current density ($C_o=40$ mg/L RB-5, $i=0.875$ mA/cm ² , $I=154$ A, $S.E=0.02$ M Na ₂ SO ₄ , $Q=100$ mL/min, rpm=37.1, Natural pH)	65
Table 5.4.5. Effect of current density ($C_o=40$ mg/L RB-5, $i=1$ mA/cm ² , $I=176$ A, $S.E=0.02$ M Na ₂ SO ₄ , $Q=100$ mL/min, rpm=37.1, Natural pH)	66
Table 5.4.6. Effect of current density ($C_o=40$ mg/L RB-5, $i=1.125$ mA/cm ² , $I=198$ A, $S.E=0.02$ M Na ₂ SO ₄ , $Q=100$ mL/min, rpm=37.1, Natural pH)	67
Table 5.4.7. Effect of current density ($C_o=40$ mg/L RB-5, $i=1.25$ mA/cm ² , $I=220$ A, $S.E=0.02$ M Na ₂ SO ₄ , $Q=100$ mL/min, rpm=37.1, Natural pH)	68
Table 5.4.8. Comparison table for effect of current density ($C_o=40$ mg/L RB-5, $S.E=0.02$ M Na ₂ SO ₄ , $Q=100$ mL/min, rpm=37.1, Natural pH)	69
Table 5.5.1. Effect of initial dye concentration ($C_o=20$ mg/L RB-5, $i=1$ mA/cm ² , $I=176$ A, $S.E=0.02$ M Na ₂ SO ₄ , $Q=100$ mL/min, rpm=37.1, Natural pH)	74
Table 5.5.2. Effect of initial dye concentration ($C_o=40$ mg/L RB-5, $i=1$ mA/cm ² , $I=176$ A, $S.E=0.02$ M Na ₂ SO ₄ , $Q=100$ mL/min, rpm=37.1, Natural pH)	75
Table 5.5.3. Effect of initial dye concentration ($C_o=60$ mg/L RB-5, $i=1$ mA/cm ² , $I=176$ A, $S.E=0.02$ M Na ₂ SO ₄ , $Q=100$ mL/min, rpm=37.1, Natural pH)	76
Table 5.5.4. Effect of initial dye concentration ($C_o=100$ mg/L RB-5, $i=1$ mA/cm ² , $I=176$ A, $S.E=0.02$ M Na ₂ SO ₄ , $Q=100$ mL/min, rpm=37.1, Natural pH)	77

Table 5.5.5. Comparison table for effect of initial dye concentration
($i=1 \text{ mA/cm}^2$, $I=176 \text{ A}$, $S.E=0.02 \text{ M Na}_2\text{SO}_4$, $Q=100$
 mL/min , $\text{rpm}=37.1$, Natural pH) 78

Table 5.7.1. Variation of energy consumption with current density
($C_o=40 \text{ mg/L RB-5}$, $S.E=0.02 \text{ M Na}_2\text{SO}_4$, $Q=100$
 mL/min , $\text{rpm}=37.1$, Natural pH)86

SYMBOLS AND ABBREVIATIONS

A	: Ampere
BDD	: Boron Doped Diamond
RB5	: Reactive Black 5
C_0	: Initial concentration
CO_2	: Carbon Dioxide
S.E	: Supporting Electrolyte
EC_{50}	: Concentration that cause 50% death
g	: Gram
H_2O_2	: Hydrogen Peroxide
I	: Current
i	: Current density
COD	: Chemical Oxygen Demand
kW	: Kilowatt
kWh	: Kilowatt hour
L	: Liter
mA	: Milliampere
mg	: Milligram
Na_2SO_4	: Sodium sulfate
nm	: Nanometer
Q	: Flow Rate
t	: Time
TOC	: Total Organic Carbon
UV	: Ultra Violet
V	: Volt

1. TITLE AND AIM OF THE STUDY

Nowadays electrochemical methods have been purpose of many researches for treatment of organic and inorganic resources. Generally, materials that are barely treated by biologic processes and enter to the flowing waters have caused a major problem for traditional wastewater treatment methods. Due to the treatment of this kind of wastewaters advanced systems are required that one of them is studied here.

Recently, nanotechnology has changed our world and goes to fulfill our dreams that one day were impossible to reach. In the wastewater treatment Nano technologically made boron doped diamond anodes are studied here.

In this study Anodic oxidation of Reactive Black 5 (RB5) dye using boron doped diamond anodes in a bipolar trickle tower reactor has been studied. BDD anodes effects on dye removal, COD and toxicity have been examined. Accordingly, other parameters that are important in dye removal processes and affect it directly like initial pH, current density, initial dye concentration and supporting electrolyte have been studied too.

At the end, after determining best experimental conditions COD, TOC and toxicity analyses have been performed.

2. INTRODUCTION

The most evident characteristics of textile wastewater are their color. Depending on the type of dye material used, wastewater color would be red, brown, blue, purple and black. Wastewater color changes every day and even due to meet the demand of customers, dye materials used in the dyeing process are changed several times in a day. Any change in the color would change the COD characteristic of the wastewater. If this kind of wastewaters that are full of different dye materials discharge without any treatment, it would cause destructive effects on the ecosystem (Lin and Peng 1994).

Textile industry is rated as one of the most polluting sector among the different human activities due to their high discharge volume and effluent composition (Orozco et al. 2008). Operations involved in this industrial activity are very water demanding and the effluents generated contain high concentrations of dyes, surfactants, suspended solids and organic matter (Bandala et al. 2008). Textile industry utilizes about 10,000 dyes and pigments (Daneshvar et al. 2005). The release of textile wastewater to the natural water courses is the main dispersion path of a wide variety of dyestuff in the environment. Dyes contained in textile effluents retain their color and structural integrity under diverse weather conditions due to their design to persist under oxidizing and reducing conditions, washing and light exposure (Bandala et al. 2008; Koparal et al. 2002; Chen et al. 2003; Koparal et al. 2007). According to Daneshvar et al. (2006), it is estimated that 1-15% of the dye is lost during dyeing and finishing processes and is released into wastewaters. Dyes show a high resistance to microbial degradation on wastewater treatment systems. These characteristics show synthetic dyes as very refractory chemicals able to generate toxicity to aquatic organisms and, in some cases, humans (Bandala et al. 2008). Thus, textile wastewater, adversely affects the ecosystem, and reduces the assimilative capacity of the environment (Koparal et al. 2007).

2.1. Classification of Dyes

In general, dyes are classified according to their chemical structure and application (Dos Santos et al. 2007). Specific groups (called chromophores) are responsible for the color of the dye, while electron withdrawing or donating substituents (called auxochromes) increase the coloring effect of the chromophores. Important chromophores include the azo ($-N=N-$), carbonyl ($-C=O$), methane ($-CH=$), nitro ($-NO_2$) and quinoid groups. Typical auxochromes include amine ($-NH_2$), carboxyl ($-COOH$), sulfonate ($-SO_3H$) and hydroxyl ($-OH$) groups. Approximately, one million tons of dyes are produced every year all around the world. The majority (about 70% by weight) is azo dyes while anthraquinone dyes constitute the second most important class of textile dyes (Panakoulias et al. 2010).

2.2. Dye Removing Processes and Techniques

There are many processes to remove dyes from colored effluents, some of which are applied in industry. These technologies have been classified into four main groups (Riera-Torres and Gutiérrez 2010):

- Oxidation techniques: electrochemical oxidation, peroxides, ozone, etc. (Koparal et al. 2002; Koparal et al. 2007; Wang et al. 2003).
- Physicochemical techniques: adsorption, ion exchange, coagulation /flocculation (Koparal et al. 2002; Davila-Jimenez et al. 2005; Wu et al. 2008).
- Membranes: nanofiltration, reverse osmosis, etc. (Al-Bastaki 2004; Petrinic' et al. 2007).
- Biological techniques: enzymatic decolorization processes (Swamy and Ramsay 1999; Garcia-Montano et al. 2008).
- Sometimes a combination of two of these techniques is used (Shu and Chang 2005; Yavuz et al. 2009).

Textile wastewater is typically treated by conventional methods. During chemical precipitation, although additives increase treatment efficiency, a sludge disposal problem is created (Koparal et al. 2002). Ozone and hypochlorite

oxidation are efficient decolorization methods, but they are not desirable due to the high investment and operational cost, and the secondary pollution arising from the residual chlorine (chen et al. 2003). The wide range of pH and elevated temperatures are also additional problems encountered when textile wastewaters are treated by conventional methods (Koparal et al. 2002). Azo dyes like RB5 are resistant to biodegradation under aerobic conditions, whereas anaerobic treatment is applied successfully. However, textile wastewater is not proper to use anaerobic process because the breakdown of azo dye leads to the formation of aromatic amines, which may be more toxic than the dye molecules themselves (Meriç et al. 2004).

Electrochemical methods are also used successfully for the treatment of toxic and bio-refractory organic effluents, covering also dyes and textile wastewaters. Electrochemical methods use electrons as the main reagent, but may also require the presence of supporting electrolytes (Koparal et al. 2007). In general, supporting electrolytes exist in the wastewater being treated because of its large salt content, but may not always be in sufficient concentrations. If the wastewater has high chloride content, the formation of chlorinated by-products should specifically be considered. These processes can operate at ambient temperature without a need of temperature control (Fernandes et al. 2004). The degradation products in the electrochemical oxidation of azo dyes are typically carbon dioxide, nitrate and sulfate, with the possible formation of aromatic esters, phenols, aromatic carboxylic acids, cyclic and aliphatic hydrocarbons, etc., as intermediates. Usually, the oxidation of azo group occurs, followed by the oxidation of the decomposition products (Fernandes et al. 2004).

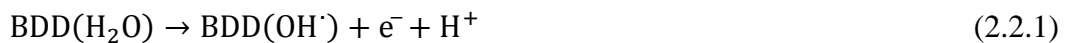
Electrochemical methods used for dye removal can be classified as electrocoagulation, electrochemical reduction, electrochemical oxidation (using metal oxide anodes, Pt anodes, boron-doped diamond (BDD) anodes), indirect electro-oxidation with strong oxidants (electro-oxidation with active chlorine, electro-Fenton), and photoassisted electrochemical methods (photoelectro-Fenton, photoelectrocatalysis) (Martínez-Huitle and Brillas 2009).

There are few published studies using bipolar trickle tower (BTT) reactor for environmental applications (Koparal et al. 2002; Yavuz et al. 2008; Yavuz et al. 2011). The conductivity of the working solution has to be considered in electrochemical treatment, and these studies show that BTT reactors have

important advantages because they can be operated successfully for the electrochemical treatment of solutions/waste-waters having relatively low conductivity.

The electrode material can also influence the mechanism and consequently the products of anodic reaction, and is the most important parameter in the electrochemical oxidation of organics. Several types of anodes for the electrochemical oxidation of dyes have been recently reviewed by Martínez-Huitle and Brillas (Martínez-Huitle and Brillas 2009). Typical examples of widely used anodes include Fe, steel, Al, Dimensionally Stable Anodes (DSA) composed of mixtures of Ti, Ir, Ru, Sn, Pb and/or Sb oxides, Pt or Ti supported Pt, granular activated carbon, activated carbon fiber (ACF), glassy carbon, graphite, polypyrrole, and BDD deposited mainly on Si, Ti or Nb substrates. These electrodes could be used either for direct (occurring at the surface of the anode) or for indirect oxidation processes such as the homogeneous reaction of organic pollutants with strong oxidants (like active chlorine, or hydroxyl radicals via Fenton's reaction) (Panakoulias et al. 2010).

BDD has great potential in electrochemical applications, especially for the treatment of waste-water and drinking water because the extraordinary chemical inertness offers the opportunity to use such electrodes (anodes as well as cathodes) in very aggressive media (Koparal et al. 2007). BDD anodes allow direct production of hydroxyl radicals (OH^\cdot) from the electrolysis of water with very high current efficiencies as shown by its dominant degradation mechanism in phenol oxidation (Kraft et al. 2003). Hydroxyl radicals also play a major role in the degradation of dye molecules. So, this technique is based on the generation of adsorbed hydroxyl radical (OH^\cdot) at the surface of BDD, a high O_2 -overvoltage anode, from oxidation of water in acid and neutral media (Flox et al. 2006; Panizza and Cerisola 2005):



or hydroxide ion at $\text{pH} \geq 10$:



Besides hydroxyl radicals and hydrogen peroxide directly produced from water, the presence of chlorides, sulfates and carbonates induces a very efficient generation of free chlorine, peroxodisulfate and percarbonates respectively (Panizza et al. 2001). Depending on electrolyte composition, the pollutants can be oxidized both on the electrode surface by reaction with hydroxyl radicals and in the bulk of the solution by inorganic oxidants electrogenerated on the BDD anodes (Panizza and Cerisola 2005). It has been proved by earlier investigators (Muruganathan et al. 2007; Flox et al. 2009; Li et al. 2010) that oxidation reaction is influenced by mediated oxidants such as peroxodisulfate ($S_2O_8^{2-}$), H_2O_2 , and O_3 according to the following reactions:



These mediated oxidants can be greatly enhanced with increasing current density (Muruganathan et al. 2007; Bechtold et al. 2006). It has also been proved that the OH^\cdot are involved in the oxidation of sulfate to form peroxodisulfate according to reaction (2.2.6).



According to reaction (2.2.6), part of OH^\cdot produced on the BDD surface is trapped by an oxidizable species like sulfate to form the corresponding peroxides. In fact, this peroxide formation indirectly helps to avoid the side reaction of oxygen evolution thus can act as mediator in the degradation of pollutants.

2.3. Current Methods for Pollutant Treatment

Table 2.3.1 lists current methods for the treatment of organic, inorganic, and microbiological pollutants in air, water, and soil.

Note that electrochemical treatment has been traditionally applied "in the field" only for the treatment of inorganic (mainly metallic) pollutants. However, there are many manufacturers of electrochemical equipment for pollution control at present. Electrochemical methods for the treatment of organics and to a lesser extent, microorganisms are reasonably well developed and appear to be poised for more widespread adoption. A similar situation holds for photoelectrochemical methods. In a limited number of instances, electrochemical technologies have been compared with the other alternatives in Table 2.3.1 in terms of performance and cost.

Another approach to a discussion of the current methods for pollutant treatment revolves around the host phase of the pollutant; namely, solid (soil), air, or liquid. However, a difficulty with this approach is that some wastes such as sludge from a wastewater treatment plant are semi-liquids (much like mud) with solids content ranging from 0.5-5%. Primary treatment of industrial wastes involves physicochemical techniques such as screening, coagulation, flocculation, and sedimentation. The BOD is reduced at this stage. Secondary treatment involves aerobic oxidation, which removes the residual BOD. Concurrently, additional solids are removed by filtration or sedimentation. Large quantities of sludge are thus generated at both these stages of waste treatment. There are four principal alternatives for disposal of the sludge: dumping in the sea or rivers, disposal at landfill sites, incineration, and application to agricultural land as fertilizer. The landfill option will be severely limited in the future by land availability and stringent legislation. Some legislative control will also constrain the dumping and agricultural options, with the result that incineration or thermal destruction becomes the most viable disposal route in many scenarios (Rajeshwar and Ibanez 1997).

Table 2.3.1. Current technologies for the treatment of organic, inorganic, and microorganism pollutants in air, water, and soil

Organics	Inorganics	Microorganisms
Incineration and pyrolysis	Precipitation/coagulation	Incineration
Air stripping	Membrane separation	High-energy (γ)-irradiation
Carbon adsorption	Distillation	Filtration
Microbial treatment	Chemical treatment	Carbon adsorption
	Electrochemical treatment	Direct UV irradiation
	Microbial treatment	Ozonation
		Chlorination

2.3.1. Incineration and pyrolysis

Combustion of oxidizable material is an effective way for reducing the mass and volume of hazardous wastes. An important side benefit of this technology is the resultant heat of combustion, which can be utilized to generate process steam. Thus the concept of using municipal refuse as part of the fuel and energy supply for a nearby electric power utility has found favor. The cement industry is another potential big user of hazardous waste; cement kilns can burn appreciable amounts of waste as part of their fuel mix. Unfortunately, however, incineration also can generate appreciable amounts of air pollution, particularly toxic degradation products and particulate matter. The public outcry to widespread adoption of this technology consequently has been vehement, and many incineration units have been forced to either shut down or significantly upgrade the quality of their output.

Three types of incinerator designs have been in use: rotary kiln, fixed or moving hearth furnaces, and fluidized bed. Of these, the use of the rotary kiln design has dominated incineration applications. A crucial parameter is the combustion temperature in all three cases. Ideally, the temperature must be high enough to ensure complete combustion (typically in the range 1050-1250 K) but not too high that slag formation occurs (Rajeshwar and Ibanez 1997).

2.3.2. Air stripping

Organics may be removed from water by packed-tower aeration, in which air is used to "strip" the organics from the aqueous phase. This methodology depends on the Henry's law of partitioning of solutes between the aqueous and gas phases; and obviously works only for volatile organic compounds. After partitioning into the gas phase, the VOCs may be subsequently destroyed either by combustion or pyrolysis followed by scrubbing of the outgases. Aside from wet scrubbers (to remove HCl, for example), electrostatic precipitators may also be added as auxiliary equipment for controlling particulate and metals emissions. A venturi-type scrubber is most commonly employed, and a quench section may precede the venturi to precool the exhaust gases. The effectiveness of the total unit is rated in terms of the total hydrocarbon (THC) emissions from it (Rajeshwar and Ibanez 1997).

2.3.3. Microbial treatment

Microorganisms-bacteria, fungi, and algae-are living catalysts that enable a vast number of chemical processes to occur in water and soil. In microbial remediation procedures, these processes are induced to the place via either the micro-organisms naturally present in the contaminated medium or those suitably inoculated into it. As an example of the first type, much of the organic matter in a sanitary landfill undergoes anaerobic decomposition catalyzed by the enzymes present in the soil bacteria. Microbial treatment is commonly done in (above-ground) bioreactors, pits, lagoons, and using soil biofilters, although in situ (subsurface) bioremediation of groundwater is emerging as a primary technology (Thomas and Ward 1989). An important aspect of microbial treatment is that the contaminants are partially or even completely destroyed with minimal impact on the environment. This is in stark contrast to many remedial techniques that simply transfer the pollutant from one part of the environment to another. Perhaps the most widespread application of bioremediation has been in the treatment of oil spills, where marine bacteria and filamentous fungi, which thrive on petroleum, are used.

2.3.4. Precipitation and coagulation

This approach has been classically used in the primary treatment of wastewater. Hence, lime is added after aeration to raise the pH and to precipitate the "water hardness" ions, Ca^{2+} and Mg^{2+} . Additional coagulants such as aluminum are added to remove the colloidal matter as gelatinous hydroxides. Activated silica or polyelectrolytes may also be added to stimulate coagulation and flocculation.

Pollutants such as Cr (VI) are also removed via hydroxide formation after first reducing them to a lower oxidation state, such as Cr (III). The commonly used reagent for this purpose is ammonium metabisulfite. Arsenic exists in natural waters primarily as arsenite (As (III)) and arsenate (As (V)) species. Conventional coagulation with iron or aluminum salt is effective in removing 80-90% As (V) from an initial concentration of ~0.1 ppm at pH 7 or below. Lime softening removes 95% As (V) at pH above 10.5. Reduction of As (V) to lower oxidation states is sometimes done (via the addition of iron salts or sulfides) prior to precipitation (Harper and Kingham 1992). On the other hand, increased removal of As (III) has been reported as well by prior oxidation, using agents such as ozone, chlorine, or permanganate.

2.3.5. Chemical treatment

Classical organic reaction routes can be employed for waste treatment. These include nucleophilic substitution, whereby hydroxyl ion substitution is induced in aryl chlorides (e.g., PCBs). Usually KOH is used as the OH⁻ source and polyethylene glycol is additionally employed for solubilizing the KOH in an aprotic medium (Brune et al. 1985). Reductive dechlorination (hydrogenolysis) has also been effected at low temperatures (e.g., 100°C) using a mixed oxide catalyst.

2.3.6. Adsorption

Another standard water treatment method consists of adsorption on activated carbon, a product obtained from a variety of carbonaceous materials including wood, peat, and lignite. Activated carbon comes in two types: granular activated carbon (GAC), consisting of particles 0.1-1 mm in diameter, and powdered activated carbon, in which the particles are predominantly in the 50-100 µm size range. The former is more commonly used, and in a water treatment system, a fixed GAC bed is employed through which the water flows downward. Accumulation of particulate matter requires periodic backwashing. A parameter for defining the adsorptive capacity of GAC is the phenol value. This is defined as the amount of carbon (in mg) required to reduce by 90% the phenol content of a 100 ppb solution. Over and above simple adsorption, bacterial growth on the carbon can provide an additional route to organics removal. Economics requires the spent carbon to be regenerated. This is normally done by heating to 950°C in a steam-air atmosphere, where the accumulated organics are burned off (Rajeshwar and Ibanez 1997).

2.3.7. Membrane processes

These include electrodialysis, reverse osmosis, and ion exchange. The common denominator here is the membrane (usually a polymer) phase. Water desalination and softening form the bulk in terms of technology applications, (Michaels 1990) although these methods are now being considered for industrial wastewater treatment.

Electrodialysis consists of applying an electric field across water layers alternately separated by cation- and anion-selective membranes. Membrane fouling is remedied by periodic reverse flushing. Generally, electrodialysis can remove up to 40-50% dissolved inorganics.

2.3.8. Distillation

An obvious method for removing inorganics from water is by distilling it. Unfortunately, this process is not energy efficient enough to be economically attractive, especially for large-scale applications. Further, volatile pollutants and odorous compounds (especially organics) are carried over to a large extent in the distillation process unless special precautions are taken.

Freezing is another related method for producing very pure water. Freeze-pump-thaw (FPT) cycles, for example, are commonly used for purifying solvents. Again this approach to water treatment does not appear to be economically attractive at present (Rajeshwar and Ibanez 1997).

2.4. Advanced Oxidation Processes

Advanced oxidation processes (or AOP) can be grouped in the same category. The AOP technologies almost all rely on the generation of very reactive free radicals, such as the hydroxyl radical ($\cdot\text{OH}$), to function as pollutant-killing agents. Four major approaches to AOP are under development at present: (Bolton and Cater 1994)

1. Homogeneous photolysis (UV/H₂O₂ and UV/O₃): These processes employ UV photolysis of H₂O₂ and/or O₃ and other additives in homogeneous solution to generate OH \cdot and other free radicals.

2. Radiolysis: A source of high-energy radiation (γ -rays) is used to irradiate the waste water. A variety of species, such as OH^\cdot , H^\cdot , $\sim e_{\text{aq}}$ (hydrated electrons) are created under these conditions.
3. Dark oxidation processes: These obviously do not employ UV light but instead the radicals are generated by other means-Fenton's reaction, ozone at high pH and O_3 /peroxide.
4. Heterogeneous photolysis or photocatalysis: This uses a semiconductor catalyst and a light source to induce photoelectrochemical reactions at or near the catalyst particle surface.

2.5. Electrochemical Technologies for Wastewater Treatment

Electrochemical technologies have recuperated their importance in the world during the past two decades. There are different companies supplying facilities for metal recoveries, treating drinking water or process water, treating various wastewaters resulting from tannery, electroplating, dairy, textile processing, oil and oil-in-water emulsion, etc. At the present time, electrochemical technologies have reached such a state that they are not only comparable with other technologies in terms of cost, but also more efficient and compact. The development, design and application of electrochemical technologies in water and wastewater treatment have been focused particularly to some technologies such as electrodeposition, electrocoagulation, electroflocculation and electrooxidation.

2.5.1. Electrodeposition

The electrochemical recovery of metals has been used in form of electrometallurgy since long time ago (Dubpernel 1978). The first recorded example of electrometallurgy was in mid-17th century in Europe (Fleet 1989). It involved the recovery of copper from cupriferous mine water, electrochemically. During the past two and half centuries, electrochemical technologies have grown into areas as energy storage, chemical synthesis, metal production, surface treatment, etc. (Leddy, 1989).

The electrochemical recovery of metals can be used in the metal surface finishing industry. It has to bear in mind that it is unable to provide a complete

solution to the industry's waste management problems because it cannot treat all the metals either technically or economically. The electrolytic recovery of metals involves two steps: collection of heavy metals and stripping of the collected metals. The first step involves plating and the stripping can be accomplished chemically or electrochemically. Actually, metals powders can be formed on the surface of carbon electrodes and a physical separation is sufficient for quite high purity metal recuperation.

Another application is in the printed circuit board manufacturing industry for treating dilute effluent, an ion-exchange can be used, while high concentration streams can be treated directly, using a recovery system as in metal surface finishing industry.

2.5.2. Electrocoagulation

This process involves the generation of coagulants in situ, by dissolving electrically either aluminum or iron ions from aluminum or iron electrodes, respectively. The metal ions generation takes place at the anode; hydrogen gas is released from the cathode. This gas would also help to float the flocculated particles out of the water. Electrodes can be arranged in a mono-polar or bi-polar mode. The materials can be aluminum or iron in plate form or packed form of scraps. The advantages of electrocoagulation include high particle removal efficiency, compact treatment facility, relatively low cost and possibility of complete automation.

This electrochemical technology is efficient in removing suspended solids as well as oil and greases. It has been proven to be effective in water treatment such as drinking water supply for small or medium sized community. Electrocoagulation is effective in removing the colloids found in natural water so that both the turbidity and color are reduced. Also, it is used in removal or destruction of algae or microorganisms; it can be also used to remove irons, silicates, humus, dissolved oxygen, etc. (Kul'skii et al. 1978).

Electrocoagulation was particularly employed in wastewater treatment. It has been employed in treating wastewaters from textile, catering, petroleum, carpet wastewater, municipal sewage, chemical fiber wastewater, oil-water

emulsions, oily wastewater, clay suspension, nitrite and dyestuff from wastewater. Also, copper reduction, coagulation and separation were effective.

2.5.3. Electroflotation

Electroflotation is a simple process that floats pollutants to the surface of a water body by tiny bubbles of hydrogen and oxygen gases generated from water electrolysis (Raju and Khangaonkar 1984). The pollutant removal efficiency is dependent on the size of the bubbles formed. The power consumption is related to cell design, electrode materials as well as the operation conditions.

Mineral recovery remains the major user of electroflotation. In water and wastewater treatment, flotation is the most effective process for the separation of oil and low-density suspended solids. Electroflotation is effective in treating palm oil mill effluent, oily wastewater or oil-water emulsion, spent cooling lubricant, wastewater from coke-production, mining wastewater, groundwater, food processing wastewater, fat-containing solutions, restaurant wastewater, or food industry effluents , dairy wastewater, urban sewage, pit waters, colloidal particles , heavy metals containing effluents, gold and silver recover from cyanide solution and many other water and wastewaters.

2.6. Positive Features of Electrochemical Approaches to Pollution Control

Electrochemical techniques offer many distinctive advantages relative to the other technologies:

- Environmental compatibility: The main reagent used is the electron, which is a clean reagent, and usually there is no need for adding extra chemicals.
- Versatility: Electrochemical processes involving direct or indirect oxidation and reduction can generate neutral, positively, or negatively charged inorganic, organic, or biochemical species. They can also deal with solid, liquid, or gaseous pollutants and can induce the production of precipitates, gaseous species, pH changes, or charge neutralization. The products from the electrolysis of pollutants often are even useful. In addition, a plethora of reactor and electrode materials, shapes and configurations can be utilized. Frequently, the same reactor can be used for

different electrochemical reactions with only minor changes. In addition, point-of-use production of chemicals is facilitated by electrochemical techniques (e.g., for water disinfection). Last, volumes of fluid from microliters to millions of liters can be treated.

- Energy efficiency: Electrochemical processes often have lower temperature and pressure requirements than those of equivalent nonelectrochemical counterparts (e.g., incineration, supercritical oxidation). The applied potentials can be controlled and electrodes and cells can be designed to minimize power losses due to poor current distribution and voltage drops (Rajeshwar and Ibanez 1997).

2.7. Electrochemical Oxidation: An Alternative in Wastewater Treatment

Studies on the electrochemical oxidation for wastewater treatment go back to the 19th century, when the electrochemical decomposition of cyanide was investigated. Extensive investigation of this technology commenced since late of 1970s. During the last two decades, research works have been focused on the efficiency in oxidizing various pollutants on different electrodes, improvement of the electrocatalytic activity and electrochemical stability of the electrode materials, investigation of factors affecting the process performance and the exploration of the mechanisms and kinetics of the pollutant degradation. Experimental investigations, focused mostly on the behavior of anodic materials, have been realized by different research groups. Attempts for an electrochemical oxidation/incineration treatment for waste or wastewater can be subdivided in two important categories (Jüttner et al. 2000):

- Direct oxidation at the anode
- Indirect oxidation using appropriate, anodically-formed oxidants

2.7.1. Direct anodic oxidation

Electrochemical oxidation of pollutants can occur directly at anodes through the generation of physically adsorbed “active oxygen” (adsorbed hydroxyl radicals, $\cdot\text{OH}$) or chemisorbed “active oxygen” (oxygen in the oxide

lattice, MO_{x+1}). This process is usually called “anodic oxidation” or “direct oxidation” and the course for the anodic oxidation has been described by Comninellis (1994); The electrochemical conversion transforms only the toxic non-biocompatible pollutants into biocompatible organics, so that a biological treatment is still required after the electrochemical oxidation. In contrast, the electrochemical combustion yields water and CO_2 and no further purification is necessary. Nevertheless, the feasibility of this process depends on three parameters:

1. The generation of chemically or physically adsorbed hydroxyl radicals
2. The nature of the anodic material
3. The process competition with the oxygen evolution reaction

The anodic oxidation does not require the addition of large amounts of chemicals to wastewater or to feed O_2 to cathodes; moreover, there is no tendency of producing secondary pollution and fewer accessories are required. These advantages make the anodic oxidation more attractive than the other oxidation processes. As previously commented, the most important parameter in this process is obviously the anode material. Among the investigated anode materials, the following can be mentioned: glassy carbon, Ti/RuO_2 , $Ti/Pt-Ir$, carbon fibers, MnO_2 , Pt carbon black, porous carbon felt, stainless steel and reticulated vitreous carbon. Unfortunately, none of them has sufficient activity and, at the same time, satisfactory stability. Pt, PbO_2 , IrO_2 , SnO_2 , and conductive diamond films are the most extensively studied anodes.

2.7.2. Indirect anodic oxidation

The electrooxidation of pollutants can be performed through different ways. Concerning the indirect oxidation, the most used electrochemical oxidant is probably chlorine, or hypochlorite. In addition, peroxide, Fenton’s reagent, peroxodisulphate and ozone are prominent oxidants that can be also electrochemically produced (Jüttner et al. 2000). Anodically generated chlorine and hypochlorite can be used to destroy oxidizable pollutants; in most cases, both inorganic and organic pollutants can be eliminated in the presence of a high

chloride concentration, typically larger than 3 g/L. However, the possible formation of chlorinated organic intermediates or final products hinders a wide application of this technique. As another drawback, if the chloride content in the raw wastewater is low, a large amount of salt must be added to increase the process efficiency. Pollutants can also be degraded by the electrochemically generated hydrogen peroxide. The electrically generated ozone is also reported for wastewater treatment. Farmer et al. proposed another kind of mediated electrooxidation for the treatment of mixed and hazardous wastes; in this case, metal ions, usually called mediators, are oxidized at an anode from a stable, low-valence state to a reactive, high-valence state, which can directly attack organic pollutants. The reaction may also produce free hydroxyl radicals, which are useful for the destruction of the organic pollutants. Subsequently, the mediators are regenerated at the anode, thus forming a closed cycle. Typical mediators are Ag^{2+} , Co^{3+} , Fe^{3+} , Ce^{4+} and Ni^{2+} (Farmer et al. 1992). The mediated electrooxidation usually needs to operate in highly acidic media; unfortunately, the resultant pollution from the added heavy metals limits its application.

2.8. Electrode Materials

The selection of electrodes for the direct anodic oxidation of organic and inorganic pollutants has to take into account the composition and nature of the solution to be treated as well as the stability of the electrode material, its cost, selectivity, and environmental compatibility. Since many organic and inorganic substances require rather high potentials for their oxidation (often higher than that for the oxidation of water), the nature of the electrode must be such that it will not corrode under the application of such potentials. This can be predicted to a certain degree in aqueous solutions with the aid of the corresponding Pourbaix diagram. Such predictions, however, may be complicated by the presence of reactive components in the solution other than the pollutant (e.g., complexing agents, dissolved gases, salts). Generally, oxidized noble metal surfaces (e.g., Pt, Ir, Ru) will be suitable for the oxidation of organic substances, although their cost poses a major restriction for their widespread use. On the other hand, cheaper substitutes such as oxidized nickel and lead can be used in aqueous media. Three-dimensional electrodes are known to offer a high surface area per unit volume. In addition, the passage of the solution through these electrodes produces local turbulence; this salutary effect facilitates mass-transfer processes. Commercially available high surface area anodes include graphite, reticulated vitreous carbon, titanium, stainless steel, nickel, and Ebonex (a Ti-based ceramic).

Care has to be taken in proper selection, since most electrodes (e.g., nickel and stainless steel) are useful in only a limited range of potential and pH (Rajeshwar and Ibanez 1997).

Another consideration in choosing the electrode materials is the influence of the cathodic reaction on the overall efficiency. For example, during the oxidation of phenol, benzoquinone is produced as an intermediate that can be reduced at the cathode, producing the corresponding hydroquinone that can, in turn, be reoxidized at the anode, thereby decreasing the efficiency of the process of interest and requiring a separator between anode and cathode. On the other hand, the high overpotential used at the SnO₂ anode yields essentially irreversible oxidations, where the products cannot be normally reduced at the cathode; therefore, higher yields are to be expected.

Carbonaceous materials (carbon felt, reticulated vitreous carbon, glassy

carbon) are known to have surface oxygenated functional groups that facilitate electron exchange with organic substances and are safe from an environmental point of view. However, noble metals and oxide-covered Pb and Ti substrates are more commonly used for these applications, due in part to their high resistance to severe conditions and the high O₂ evolution overpotentials of the oxide covered materials. An interesting approach involves the modification of metal electrodes with organic ligands to facilitate the effect just discussed.

The potential at the auxiliary electrode is also a key factor in achieving high current efficiencies. Unfortunately, the reactions normally occur in a rather unselective manner and most of the energy from the power source is spent on side reactions and heat generation. An approach that diminishes this problem consists of the use of electrocatalytic materials on the auxiliary electrode surface. This approach has been reported to afford high selectivity (Walsh and Morris 1987). Furthermore, application of an alternating current facilitates electrochemical reactions at the average electrochemical potentials set by the equilibrium between surface groups and the electrolytic solution. In addition, a self-cleaning effect occurs due to the periodic reversal of current, which changes the nature of the substances produced at each electrode, thus preventing deposits and other undesired cumulative effects (Walsh and Morris 1987).

2.9. Hot-Filament CVD (HFCVD)

Boron doped diamond electrodes were prepared by hot filament chemical vapor deposition method that is explained below.

The schematic diagram of a hot-filament CVD apparatus is shown in Figure 2.9.1. This technique was first reported by Matsumoto et al. (1982). One or multiple filaments, such as W, Ta, and Re, are mounted near the substrate and electrically heated to over 2000°C, where the simultaneous production of atomic hydrogen during the hydrocarbon pyrolysis will promote the growth of diamond film. Therefore, the filament temperature plays an important role in the diamond deposition process in HFCVD. The substrate temperature is measured by a thermocouple placed under the substrate and controlled to between 700 and 1100°C. The gas source usually is the mixture of 99% hydrogen and 1% methane. Diamond films are formed at chamber pressures between 10 and 100 Torr.

Depending on the deposition conditions, such as the properties of the substrate surface, methane concentration, filament or substrate temperature, the growth rate of diamond films is from 0.5 $\mu\text{m/hr}$ to several $\mu\text{m/hr}$ and the surface morphology and the quality of diamond films also vary.

In the case of HFCVD design, a modification has been developed. A moderately positive voltage and negative voltage are put to the substrate and to the filament, respectively. This is the so-called electron-enhanced HFCVD technique.

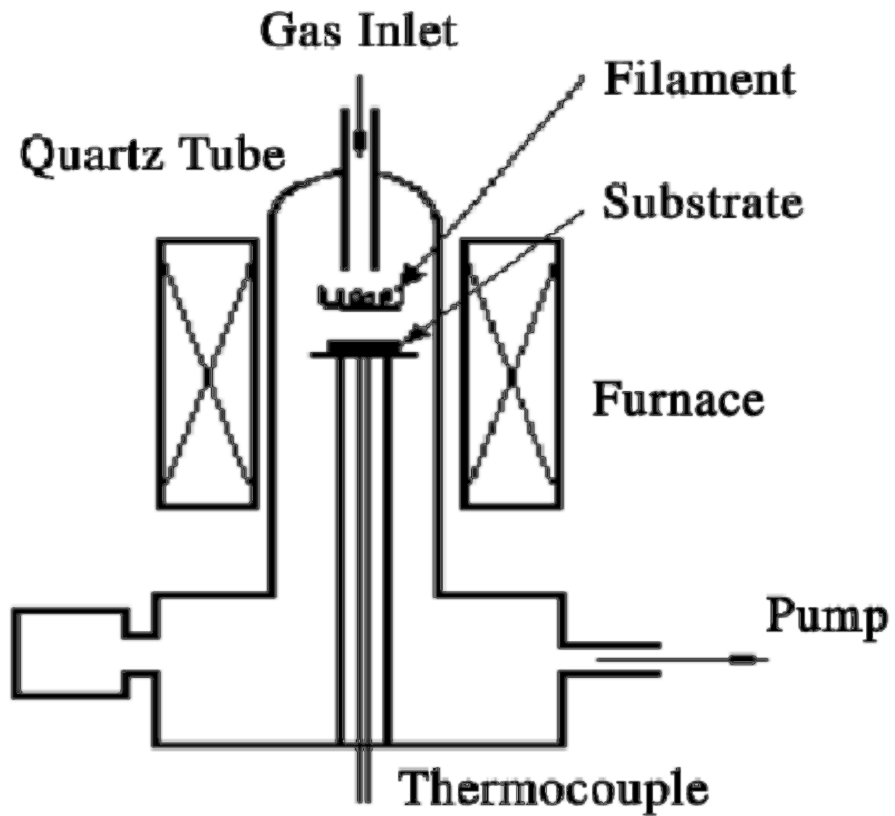


Figure 2.9.1. Schematic diagram of the hot-filament CVD apparatus (Chang et al. 2008)

The application of DC bias results in electron or ion bombardment to gas species that promote the decomposing reaction of the gas species. In addition, electron or ion bombardment to the substrate also enhances the desorption of the surface hydrogen and the diffusion of carbon-containing species on the substrate surface.

HFCVD technique is a simple method compared to others used in the growth of diamond film under low pressures. Large areas of deposition of diamond films (~30 cm in diameter) and highly-oriented diamond films have been realized by this technique. Therefore, it is also the most popular method for the growth of CVD diamond film. However, a series of problems including carbonization and distortion of the filament at high temperature and contamination of the metal filament onto the deposited diamond film were discovered. Hence, the carbideforming pretreatment of refractory metal filaments is necessary for the deposition of diamond film. (Chang et al. 2008)

2.8. Review of Published Literature

There are few studies that have used BDD electrodes in electrochemical oxidation of dyes but relevant studies are listed below.

Vlyssides et al. (1999) have studied textile dye wastewater (TDW) from a reactive azo dyeing process by an electrochemical oxidation method using Ti/Pt as anode and stainless steel 304 as cathode. Due to the strong oxidizing potential of the chemicals produced (chlorine, oxygen, hydroxyl radicals and other oxidants) when the wastewater passes through the electrolytic cell the organic pollutants oxidize to carbon dioxide and water. A number of experiments have been done in a batch, laboratory-scale, pilot-plant, and the results are reported here according to residence time and initial addition of HCl in raw wastewater. When of 2 ml of HCl 36% is added and after 18 min of electrolysis at 0.89 A/cm², chemical oxygen demand (COD) is reduced by 86%, biochemical oxygen demand (BOD₅) is reduced by 71%, ADMI color units is reduced by 100%, and TKN is reduced by 35%. The biodegradability of the wastewater is improved because the COD/BOD ratio decreases from 2.16 to 1.52.

Kim et al. (2002) have studied the performance of pilot scale combined process of fluidized biofilm process, chemical coagulation and electrochemical oxidation for textile wastewater treatment. In order to enhance biological treatment efficiency, two species of microbes, which can degrade textile wastewater pollutants efficiently, have been isolated and applied to the system with supporting media. FeCl₃.6H₂O, pH 6 and 3.25×10⁻³ mol/l were determined as optimal chemical coagulation condition and 25mM NaCl of electrolyte

concentration, 2.1 mA/cm² of current density and 0.7 l/min of flow rate were chosen for the most efficient electrochemical oxidation at pilot scale treatment. The fluidized biofilm process has showed 68.8% of chemical oxygen demand (COD) and 54.5% of color removal efficiency, even though using relatively low MLSS concentration and short sludge retention time. COD and color removals of 95.4% and 98.5% were achieved by overall combined process.

Fernandes et al. (2004) have studied the electrochemical oxidation of C.I. Acid Orange 7 (AO7) on a boron doped diamond electrode (BDD). Bulk electrolysis was studied using two different supporting electrolytes KCl and Na₂SO₄. The influence of electrolyte concentration, initial dye concentration and current density on the degradation rates has been investigated. Samples were collected at pre-selected intervals and absorbance measurements and chemical oxygen demand (COD) tests were performed, to compare the rates of colour and COD removal in each case. From the COD measurements over the time of electrolysis mass transfer coefficients were determined, and the current efficiency was estimated using a theoretical model. Results have shown an almost complete colour removal and COD removal, higher than 90%. A preliminary electro degradation study of an effluent from an UASB reactor, used on the biodegradation of a textile wastewater containing AO7, was also performed with colour and COD removals of 98% and 77%, respectively.

Grimau and Gutiérrez (2006) have studied optimisation of the electrochemical decolourisation of textile effluents containing reactive dyes with the aim of making feasible-technically and economically-this method at industrial scale. Coloured waters were treated in continuous at low current density, to reduce the electrical consumption. Ti/PtO_x electrodes were used to oxidize simulated dyebaths prepared with an azo/dichlorotriazine reactive dye (C.I. Reactive Orange 4). The decolourisation yield was dependent on the dyeing electrolyte (NaCl or Na₂SO₄). Dyeing effluents which contained from 0.5 to 20 g l⁻¹ of NaCl reached a high decolourisation yield, depending on the current density, immediately after the electrochemical process. These results were improved when the effluents were stored for several hours under solar light. After the electrochemical treatment the effluents were stored in a tank and exposed under different lighting conditions: UV light, solar light and darkness. The evolution of the decolourisation versus the

time of storage was reported and kinetic constants were calculated. The time of storage was significantly reduced by the application of UV light.

A dye mineralization study was also carried out on a concentrated dyebath. A TOC removal of 81% was obtained when high current density was applied for a prolonged treatment with recirculation. This treatment required a high electrical consumption.

Awad and Galwa (2005) have studied Electrocatalytic degradation of Acid Blue and Basic Brown dyes from simulated wastewater on lead dioxide anode in different conductive electrolytes. It was shown that complete degradation of these dyes is dependent primarily on type and concentration of the conductive electrolyte. The highest electrocatalytic activity was achieved in the presence of NaCl (2 g/l) and could be attributed to indirect oxidation of the investigated dyes by the electrogenerated hypochlorite ions formed from the chloride oxidation. In addition, contribution from direct oxidation could also be possible via reaction of these organic compounds with the electrogenerated hydroxyl radicals adsorbed on the lead dioxide surface. In the presence of NaOH, the electrocatalytic activity of the employed anode was not comparable to that in NaCl due primarily to the absence of chloride. This indicates that dyes degradation in NaOH occurs exclusively via direct electrochemical process. However, in H₂SO₄, the electrode performance was poor due partially to the absence of chloride from the conductive solution. The possibility of electrode poisoning as a result of growth of adherent film on the anode surface or production of stable intermediates not easily further oxidized by direct electrolysis in H₂SO₄ might also be accountable for the poor performance observed in this conductive electrolyte. Optimizing the conditions that ensure effective electrochemical degradation of Acid Blue and Basic Brown dyes on lead dioxide electrode necessitates the control of all the operating factors.

Panizza and Cerisola (2008) have studied electrochemical oxidation of synthetic wastewater containing acid blue 22 on a boron-doped diamond electrode (BDD) using cyclic voltammetry and bulk electrolysis. The influence of current density, dye concentration, flow rate, and temperature was investigated, in order to find the best conditions for COD and colour removal. It was found that, during oxidation, a polymeric film, causing BDD deactivation, was formed in the potential region of water stability, and that it was removed by anodic polarization at high potentials in the region of O₂ evolution. Bulk electrolysis results have

showed that the electrochemical process was suitable for completely removing COD and effectively decolourising wastewaters, due to the production of hydroxyl radicals on the diamond surface. In particular, under optimal experimental conditions of flow rates (i.e. $300 \text{ dm}^3 \text{ h}^{-1}$) and current density (i.e. 20 mA cm^{-2}), 97% of COD was removed in 12 h electrolysis, with 70 kWhm^{-3} energy consumption.

Petrucci and Montanaro (2011) have studied electrochemical oxidation using a boron-doped diamond electrode for the treatment of solutions miming a real wastewater, containing the Reactive Blue 19 dye, taken after the rinse and softening bath from a typical reactive dyes process. This effluent is a complex mixture of dyes, electrolytes at high concentration, mainly chlorides or sulphates and carbonates together with dyeing auxiliaries.

Electrolyses were conducted in an undivided electrolytic cell under galvanostatic conditions. The effect of carbonate has been extensively investigated as well as pH, temperature and current density. The efficiency of the process has been evaluated in terms of colour, chemical oxygen demand (COD) and total organic carbon (TOC) removal. Results show that colour removal was negatively affected by carbonates and favoured by both chlorides and additives while complete mineralisation was found to mainly depend only on temperature. The study of current density effect supports the hypothesis that discoloration mainly occurs via indirect oxidation mediated by electrogenerated active chlorine while COD and TOC removal is carried out by direct oxidation by means of hydroxyl radicals produced at BDD surface.

3. MATERIALS AND METHODS

3.1. Power Supply and Multimeter

For anodic oxidation of Reactive Black 5 dye some parts are needed and these parts have to be attached together to start the experiments (all the parts with their characteristics are mentioned at the end of this section). One of the important parts is power supply, because these experiments are based on electrochemical oxidation (Anodic oxidation) and need electricity. Power supply enables to change the current density and see the effect, on the amount of dye removal. Multimeter has to be used to apply the current density precisely, because digital screen of the power supply just has one decimal place.

3.2. Peristaltic Pump

Experiments have been done in a recirculated batch mode and in order to have this mode using a peristaltic pump is a necessity. Flow rate is another important parameter of the experiment and there are different flow rates on the peristaltic pump that enables to probe the effect of flow rates on the experiments.

3.3. Electrochemical Reactor

Another part that is used especially in this study is the electrochemical reactor (also called trickle tower). This reactor contains a cooling and heating jacket that cold or hot water can be circulated into it. It has two input for electric poles to be attached and two input and output part for solution to be circulated. The thermostated BTT reactor used in the study had a volume of 125 mL and consisted of two concentric glass pipes with inner diameters of 4 and 2.5 cm.

3.4. Graphite Feed Electrodes

Electrical poles have to be inert and have no influence on the experiments. Because of that graphite feed electrodes have been used and the distance between the graphite feed electrodes was about 22.5 cm.

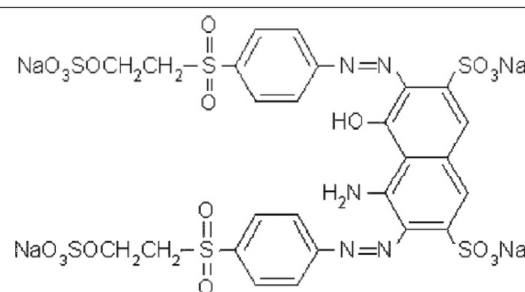
3.5. pH Meter

pH is another important factor in these kind of studies and pH meter is used to adjust the pH initially or periodically during the experiment.

3.6. Model solution

These kinds of experiments can be done on the wastewater or model solutions that here in this study model solution of Reactive Black 5 dye is chosen to be decolorized. Different initial dye concentrations have been prepared and used along the experiments and initial dye concentration is one of the parameters that have been studied. Reactive Black 5 dye's properties and chemical structure are shown in table 3.6.1.

Table 3.6.1. Properties and chemical structure of Reactive Black 5 dye

Chemical structure	
Molecular formula	$C_{20}H_{25}N_3O_{19}S_6 \cdot 4Na$
Synonyms	Remazol Black B, Begazol Black B
MW (g/mol)	991.82
C.I. number	C.I. 20505
λ_{max} (nm)	596
CAS	17095-24-8
Source	Aldrich

3.7. UV-visible Spectrophotometer

UV-visible Spectrophotometer is used to determine the absorbance. After reading the absorbance, amount of remaining dye concentration and decolorization efficiency can be obtained by some formulas. UV-visible is used at the first step of experiment to prepare standard operational curve. From this standard operational curve, formulas for calculating amount of remaining dye and decolorization efficiency can be obtained. Also, after determining optimum parameters of the experiment, spectrum of the all samples have been taken by using UV-visible Spectrophotometer.

3.8. Centrifuge

During the experiment sampling has been done. Sampling volume has been 10 ml for each time interval. But samples contain some particles that affect the UV-visible Spectrophotometer absorbance, because of that a centrifuge has been used and samples have been centrifuged at the end of the experiment at 7000 rpm/min.

3.9. Analyzing Tests

In treatment of Reactive Black 5 dye, only decolorization of water is not enough but, measuring total organic carbon (TOC), toxicity and chemical oxygen demand of the decolorized water are needed. For total organic carbon tests TOC analyzer, for toxicity tests Microtox analyzer and for chemical oxygen demand tests COD reactor has been used. All COD and TOC analyses were carried out in duplicate and average values have been reported.

3.10. Stirrer

Magnetic stirrer was used during the sampling to take homogenous samples. Because system was recirculating over and over, and without stirrer samples taken in different time intervals wouldn't have equal conditions.

3.11. Supporting Electrolyte

As mentioned above one of the analyzed parameters of this study is current density. Different current densities have been applied to the system in the order of 0.5, 1, 1.5 and 2 ampere. Electrical conductivity of Reactive Black 5 dye solution is low and more than one ampere can't be applied to the system, since voltage values increase and power supply can not supply energy more than 60 volt. Energy values are important and have to be in a range affordable to use this method of treatment. Supporting electrolyte has been used to increase the electrical conductivity of dye solution. Different types of supporting electrolytes exist like, Na_2SO_4 , NaNO_3 , etc. In this study Na_2SO_4 has been used as a supporting electrolyte and its effect on amount of dye removal has been examined as one of the parameters. Very sensitive scale was used to weight supporting electrolyte amount for the test.

3.12. Electrode Material

Chief part of the study is its electrode material that makes this study special and unique. Boron doped diamond electrodes have been in raschig ring shape and BDD electrodes consisted of thin (2–7 μm), highly conductive ($<0.1 \Omega \text{ cm}$) BDD films, deposited on niobium substrates by a hot filament chemical vapor deposition technique (HF CVD) from a gaseous feed of methane and a boron doping agent in dihydrogen. BDD Raschig rings were used as working electrodes and placed in the inner glass pipe in a bipolar electrode configuration. (Yavuz and Shahbazi 2012)

3.13. Software

For all of the calculations and drawing curves, Microsoft Excel 2010 software has been used. Obtained results have been entered to the program and charts were drawn. About toxicity tests Microtox software was used to calculate the EC₅₀% values.

3.14. List of the Materials

All the materials used in this study are listed below:

- RB5 (Aldrich, USA) was used to prepare the model solution.
- Na₂SO₄ (Merck, Germany) was used as a supporting electrolyte.
- H₂SO₄ (Merck, Germany) and NaOH (Merck, Germany) were used to adjust the pH to the desired initial value. All chemicals used were reagent grade and were used without further purification.
- COD reactor (Hach, USA).
- TOC analyzer (Elementar, LiquiTOC, Germany)
- 500 Toxicity Analyzer (AZUR Environmental)
- Statron 3234.9 model power supply
- Fluke 26 III True-rms multimeter (USA)
- Cole Parmer Masterflex L/S model peristaltic pump (USA)
- Heidolph MR3001 magnetic stirrer (Germany)
- Orion 420 A model pH meter (USA)
- Shimadzu UV-2550 model spectrophotometer (Japan).
- BDD electrodes were purchased from Magneto Special Anodes B.V. (Schiedam, The Netherlands) and were shaped as Raschig rings.
- Thermo jacketed BTT reactor

4. EXPERIMENTS

4.1. Calibration

4.1.1. UV-visible Spectrophotometer Calibration

Experiments were done through some steps. In the first step, the stock dye solution of 1000 mg/L Reactive Black 5 was prepared with deionized water, and experimental solutions were made by diluting the stock dye solution to the desired initial dye concentrations. Solution tank's volume was constant during all of the experiments and it was 1000 mL.

In the second step, standard operational curves for UV-visible spectrophotometer and peristaltic pump have been prepared. Due to the preparation of standard operational curve for UV-visible spectrophotometer, different concentrations of Reactive Black 5 dye (10, 15, 20, 25, 30, 40 and 50 mg/L) were prepared. After that, one of the concentrations has been chosen and spectrum of that concentration has been made. To have the spectrum dye solution has been scanned by UV-visible spectrophotometer between 200-800 nm and maximum peak (maximum absorbance) point has been found. Maximum absorbance point for Reactive Black 5 dye is 596 nm. Then prepared concentrations absorbance was measured in 596 nm. Concentrations and their absorbance are shown in Table 4.1.1.1. Afterward, values were entered to the Excel software and according X Y (scatter) chart was drawn (Figure 4.1.1.1). Through this chart, X Y equation (4.1.1.1) has been obtained.

$$y = 0.0233x \quad (4.1.1.1)$$

In this equation y, is the read absorbance and x, is the according concentration. Remaining dye concentration and decolorization efficiency were obtained from this formula. Dye concentration, removal percentage and energy consumption calculations can be found at appendix 2 and 3.

Table 4.1.1.1. Concentrations and their absorbance for UV-visible standard operational curve

Concentration mg/L	absorbance
10	0.274
15	0.384
20	0.485
25	0.607
30	0.682
40	0.916
50	1.144

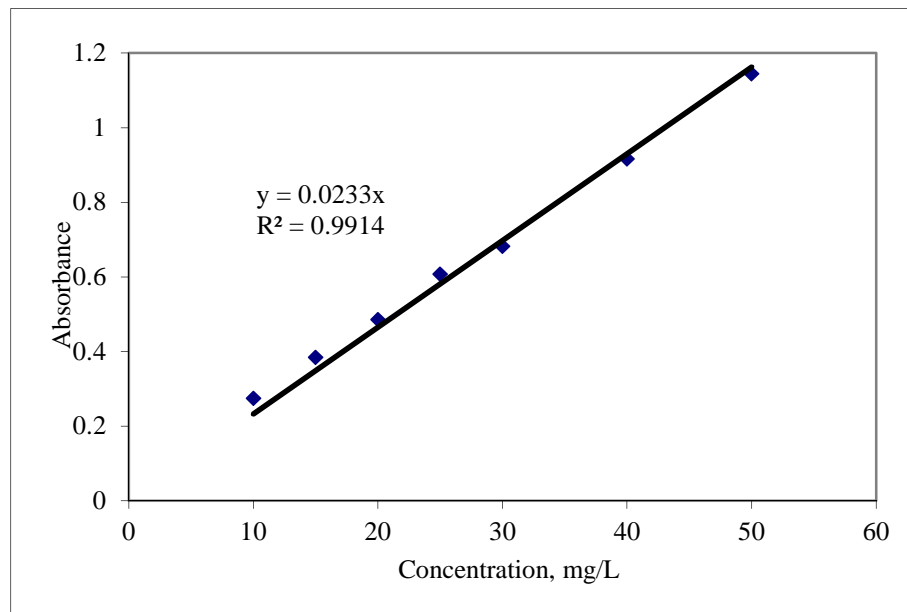


Figure 4.1.1.1. Standard operational chart for UV-visible spectrophotometer

4.1.2. Peristaltic Pump Calibration

In the third step, operational curve for peristaltic pump has been made. To do that, at different rotating speeds of peristaltic pump (5, 10, 15, 20, 30, 40, 50, 60, 70, 90, 100 rpm) the amount of flow rates in milliliter per minute (mL/min) have been gained (Table 4.1.2.1). Subsequently, values were entered to Excel software and X Y chart has been drawn. Through the acquired formula amount of flow rates as one of parameters of this study have been calculated (Figure 4.1.2.1).

$$y = 0.3713x \quad (4.1.2.1)$$

Table 4.1.2.1. Peristaltic pump calibration

mL/min	rpm
12.625	5
26.5	10
40.5	15
54	20
82.375	30
111	40
139.665	50
161.165	60
191.667	70
239	90
266	100

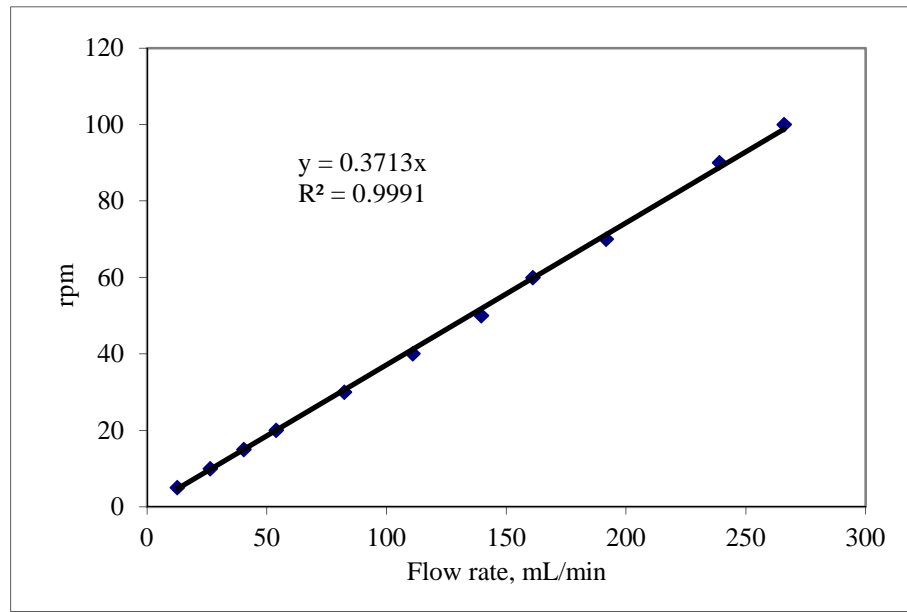


Figure 4.1.2.1. Drawn chart for peristaltic pump calibration

4.2. Experimental Setup

At the beginning, dye removing system has been established. Due to that, different parts of the system have been connected to each other. Power supplier and multimeter have been connected to each other through wires and another wires have attached to graphite feed electrodes from multimeter. Boron doped diamond electrodes that have been shaped to the raschig ring form were filled inside of thermo jacketed BTT reactor. Electrodes were placed in the inner glass pipe in a bipolar electrode configuration (Figure 4.2.1.).

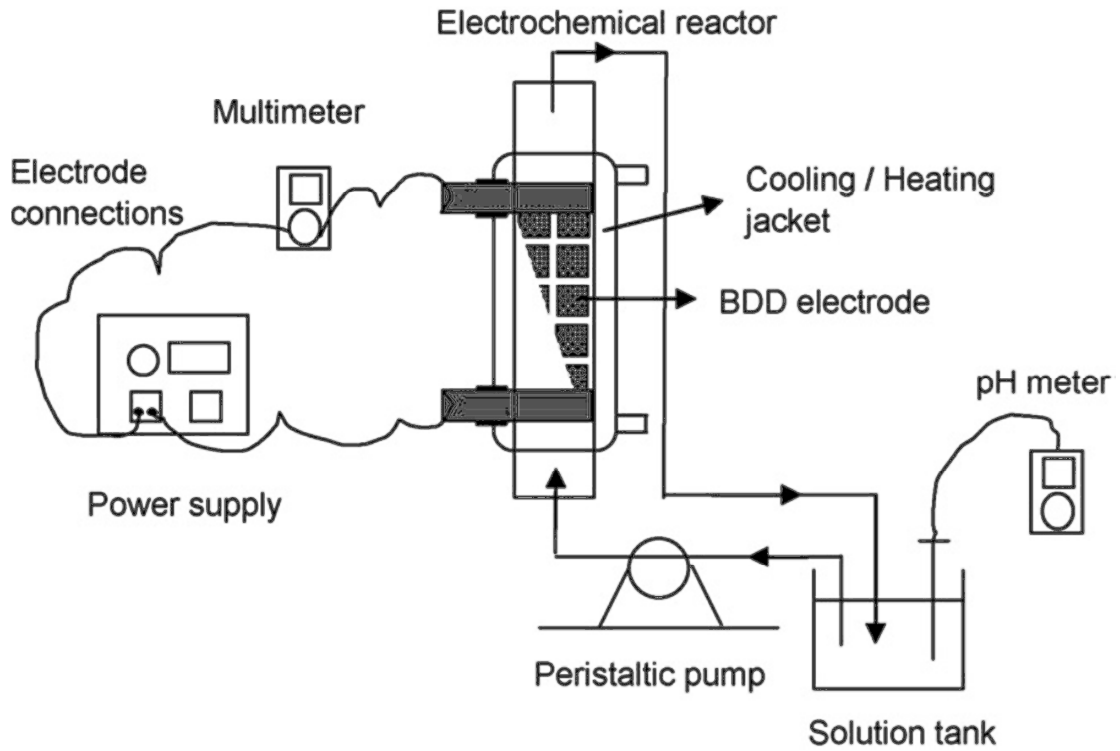


Figure 4.2.1. Overview of the dye removing system (Koparal et al. 2006)

Raschig rings employed in the reactor had a height of 8 mm, and inner and outer diameters of 6 and 8 mm, respectively. The total surface area of all BDD electrodes was 352 cm². Due to the bipolar electrode configuration one half of the total surface area (176 cm²) behaved as an anode, and the other half as a cathode. There were 26 layers in the reactor, and four electrodes in each layer. All electrode layers were isolated from each other by a dielectric material. Electrodes were placed in a way that dye solution passes over all the electrodes. Anode surface area of each electrode and total surface area of electrodes calculations can be found at appendix 1.

Water was pumped by peristaltic pump from solution tank through a hose and was poured into the reactor from top inlet of thermo jacketed BTT reactor. After passing through the reactor was poured back to the solution tank by another hose through bottom outlet.

4.3. Process of the Experiments

To start the experiment desired concentration of RB5 dye solution has been prepared from 1000 mg/L stock solution. All the parameters except initial dye concentration have been examined in 40 mg/L. After preparing the dye solution supporting electrolyte was weight and added to the solution tank and if the pH parameter was going to be examined, pH of the solution was adjusted.

In the next step flow rate was adjusted. Flow rate was 100 mL/min at all the experiments except during examining flow rate parameter.

At the end, current density has been adjusted and sampling was done. Current density was 1 mA/cm² (176 mA) at all of the experiments except experiments related to effect of current density parameter.

Samplings were done at 0, 1, 2, 3, 4, 5, 7, 10, 15, 20, 25, 30, 35, 40, 50 and 60 time intervals. 5 ml sample was taken through the bottom outlet of the reactor and its absorbance was read by UV-visible spectrophotometer. After that, it was poured back into the solution tank to keep the volume changeless (except samples taken after determining good conditions for TOC, COD, toxicity tests and UV-visible spectrum). Also, after determining good conditions at the end, before doing any analysis, samples have been centrifuged in 7000 rpm.

4.4. Methods of Analyzing

4.4.1. Total Organic Carbon Analyze (TOC)

For measuring total organic carbon amount TOC analyzer has been used. There are holes in the device that samples were replaced there. Whole of the process is fully automated and just diluting samples and programming the device is enough to start the test. Samples have been diluted 30 times. Test is comprised of Run in solution, blank, standard, and sample for each time interval. Solutions include ultra-deionized water, deionized water, TOC standard and experiment samples respectively. To have precise results each sample were tested two times. Also, to prevent result of each sample affected by the other, after each sample deionized water was put to wash the device.

4.4.2. Chemical Oxygen Demand (COD)

In environmental chemistry, the chemical oxygen demand (COD) test is commonly used to indirectly measure the amount of organic compounds in water. Most applications of COD determine the amount of organic pollutants found in surface water (e.g. lakes and rivers) or wastewater, making COD a useful measure of water quality. It is expressed in milligrams per liter (mg/L), which indicates the mass of oxygen consumed per liter of solution. The basis for the COD test is that nearly all organic compounds can be fully oxidized to carbon dioxide with a strong oxidizing agent under acidic conditions (Sawyer et al. 2003).

To have precise results two samples have been prepared for each time interval and average of them was used in calculations. Samples include two blanks, two standards and two samples for each time interval, respectively. Test has been done in related tubes. After adding substances they have replaced in the COD reactor and have been hold 2 hours in 150 centigrade. After that they were titrated by ferrous ammonium sulfate (FAS). Whole the process of the test and related calculations are given in Appendix 4.

4.4.3. Toxicity Analyze

This test certifies that water treatment system decreases toxicity of the model solution along dye removal. Base of the test is built upon percent existence of vibrio fischeri bacteria. These bacteria live in marine environments and have bioluminescent properties. After preparing samples and diluting them, microtox device measures the amount of luminescence in 0, 5 and 15 minutes. A statistical program is attached to the device and shows the result in percent dying of bacteria. Program shows the EC-50 values and if the sample is very toxic this values will be low and if it is not toxic it would be high. For example EC-50 toxicity value for 90% is less toxic than 40%.

5. RESULTS AND DISSCUTION

In this study anodic oxidation of Reactive Black 5 dye using Boron doped Diamond anodes has been studied. Experiments have been done in bipolar trickle tower reactor in recirculated batch mode. Experiments have been done on

different parameters like, effect of flow rate, current density, initial pH, initial dye concentration and supporting electrolyte.

At the all experiments Decolorization efficiency increase as the time goes on but after distinctive time it decreases and in reality there is no need to continue the experiment.

5.1. Effect of Flow Rate

Effect of flow rate has been examined in this part. Flow rates of 25, 50, 75, 100, 150 and 200 mL/min were studied. Using (4.1.2.1) formula according rpm of the peristaltic pump was adjusted. Experiments were performed in constant conditions for other parameters like, 40 mg/L RB5 concentration, 0.02 M Na₂SO₄ as supporting electrolyte, 0.75 mA/cm² (132 A) current density and just flow rate was changed. Results of experiments are included in Table 5.1.1-7 and Figure 5.1.1-7.

Table 5.1.1. Effect of flow rate (Co=40 mg/L RB5, i=0.75 mA/cm², I=132 A, S.E=0.02 M Na₂SO₄, Q=25 mL/min, rpm=9.3, Natural pH)

Time (min)	Absorbance	Voltage (V)	Concentration (mg/L)	Decolorization efficiency (%)	Energy consumption (kWhm ⁻³)
0	0.864	208	37.081	-	-
1	0.755	201	32.403	12.615	0.884
2	0.563	214	24.163	34.837	0.941
3	0.344	214	14.763	60.185	0.941
4	0.246	205	10.557	71.527	0.902
5	0.232	217	9.957	73.148	0.954
7	0.342	212	14.678	60.416	1.865
10	0.262	200	11.244	69.675	2.64
15	0.114	199	4.892	86.805	4.378
20	0.08	197	3.433	90.740	4.334
25	0.069	193	2.961	92.013	4.246
30	0.057	193	2.446	93.402	4.246
35	0.043	189	1.845	95.023	4.158
40	0.038	193	1.630	95.601	4.246
50	0.032	193	1.373	96.296	8.492

Table 5.1.2. Effect of flow rate ($C_0=40$ mg/L RB5, $i=0.75$ mA/cm², $I=132$ A, S.E=0.02 M Na₂SO₄, $Q=50$ mL/min, rpm=18.6, Natural pH)

Time (min)	Absorbance	Voltage (V)	Concentration (mg/L)	Decolorization efficiency (%)	Energy consumption (kWhm ⁻³)
0	0.864	215	37.081	-	-
1	0.661	212	28.369	23.495	0.932
2	0.52	224	22.317	39.814	0.985
3	0.418	216	17.939	51.620	0.950
4	0.416	217	17.854	51.851	0.954
5	0.402	218	17.253	53.472	0.959
7	0.328	211	14.077	62.037	1.856
10	0.305	216	13.090	64.699	2.851
15	0.202	212	8.669	76.620	4.664
20	0.122	210	5.236	85.879	4.62
25	0.084	208	3.605	90.277	4.576
30	0.055	209	2.360	93.634	4.598
35	0.037	206	1.587	95.717	4.532
40	0.028	198	1.201	96.759	4.356
50	0.025	211	1.072	97.106	9.284
60	0.024	207	1.030	97.222	9.108

Table 5.1.3. Effect of flow rate ($C_0=40$ mg/L RB5, $i=0.75$ mA/cm², $I=132$ A, S.E=0.02 M Na₂SO₄, $Q=75$ mL/min, rpm=27.8, Natural pH)

Time (min)	Absorbance	Voltage (V)	Concentration (mg/L)	Decolorization efficiency (%)	Energy consumption (kWhm ⁻³)
0	0.87	230	37.339	-	-
1	0.638	240	27.381	26.666	1.056
2	0.553	241	23.733	36.436	1.060
3	0.495	230	21.244	43.103	1.012
4	0.496	235	21.287	42.988	1.034
5	0.468	231	20.085	46.206	1.016
7	0.382	230	16.394	56.091	2.024
10	0.325	235	13.948	62.643	3.102
15	0.199	228	8.540	77.126	5.016
20	0.133	226	5.708	84.712	4.972
25	0.087	214	3.733	90.000	4.708
30	0.057	218	2.446	93.448	4.796
35	0.036	220	1.545	95.862	4.84
40	0.034	221	1.459	96.091	4.862
50	0.034	216	1.459	96.091	9.504
60	0.04	218	1.716	95.402	9.592

Table 5.1.4. Effect of flow rate ($C_0=40$ mg/L RB5, $i=0.75$ mA/cm², $I=132$ A, S.E=0.02 M Na₂SO₄, $Q=100$ mL/min, rpm=37.1, Natural pH)

Time (min)	Absorbance	Voltage (V)	Concentration (mg/L)	Decolorization efficiency (%)	Energy consumption (kWhm ⁻³)
0	0.87	205	37.339	-	-
1	0.733	211	31.459	15.747	0.928
2	0.627	227	26.909	27.931	0.998
3	0.586	228	25.150	32.643	1.003
4	0.547	229	23.476	37.126	1.007
5	0.504	223	21.630	42.068	0.981
7	0.456	223	19.570	47.586	1.962
10	0.37	222	15.879	57.471	2.930
15	0.23	219	9.871	73.563	4.818
20	0.156	212	6.695	82.068	4.664
25	0.101	216	4.334	88.390	4.752
30	0.063	210	2.703	92.758	4.62
35	0.04	209	1.716	95.402	4.598
40	0.034	208	1.459	96.091	4.576
50	0.034	215	1.459	96.091	9.46
60	0.039	209	1.673	95.517	9.196

Table 5.1.5. Effect of flow rate ($C_0=40$ mg/L RB5, $i=0.75$ mA/cm², $I=132$ A, S.E=0.02 M Na₂SO₄, $Q=150$ mL/min, rpm=55.7, Natural pH)

Time (min)	Absorbance	Voltage (V)	Concentration (mg/L)	Decolorization efficiency (%)	Energy consumption (kWhm ⁻³)
0	0.87	234	37.339	-	-
1	0.719	233	30.858	17.356	1.025
2	0.664	232	28.497	23.678	1.020
3	0.605	236	25.965	30.459	1.038
4	0.578	228	24.806	33.563	1.003
5	0.535	226	22.961	38.505	0.994
7	0.476	220	20.429	45.287	1.936
10	0.36	225	15.450	58.620	2.97
15	0.273	222	11.716	68.620	4.884
20	0.172	222	7.3819	80.229	4.884
25	0.098	226	4.206	88.735	4.972
30	0.057	218	2.446	93.448	4.796
35	0.036	214	1.545	95.862	4.708
40	0.03	214	1.287	96.551	4.708
50	0.031	212	1.330	96.436	9.328
60	0.035	206	1.502	95.977	9.064

Table 5.1.6. Effect of flow rate ($C_0=40$ mg/L RB5, $i=0.75$ mA/cm², $I=132$ A, S.E=0.02 M Na₂SO₄, $Q=200$ mL/min, rpm=74.3, Natural pH)

Time (min)	Absorbance	Voltage (V)	Concentration (mg/L)	Decolorization efficiency (%)	Energy consumption (kWhm ⁻³)
0	0.87	235	37.339	-	-
1	0.79	233	33.905	9.195	1.025
2	0.72	238	30.901	17.241	1.047
3	0.661	236	28.369	24.022	1.038
4	0.63	229	27.038	27.586	1.007
5	0.586	227	25.150	32.643	0.998
7	0.498	224	21.373	42.758	1.971
10	0.451	226	19.356	48.160	2.983
15	0.305	220	13.090	64.942	4.84
20	0.189	214	8.111	78.275	4.708
25	0.113	222	4.849	87.011	4.884
30	0.072	212	3.090	91.724	4.664
35	0.049	214	2.103	94.367	4.708
40	0.039	214	1.673	95.517	4.708
50	0.039	215	1.673	95.517	9.46
60	0.045	210	1.931	94.827	9.24

Table 5.1.7. Comparison table for Effect of flow rate (Co=40 mg/L RB5, i=0.75 mA/cm², I=132 A, S.E=0.02 M Na₂SO₄, Natural pH)

Time (min)	25 mL/min	50 mL/min	75 mL/min	100 mL/min	150 mL/min	200 mL/min
0	0	0	0	0	0	0
1	12.616	23.495	26.667	15.747	17.356	9.1954
2	34.838	39.815	36.437	27.931	23.678	17.241
3	-	51.62	43.103	32.644	30.46	24.023
4	-	51.852	42.989	37.126	33.563	27.586
5	-	53.472	46.207	42.069	38.506	32.644
7	60.417	62.037	56.092	47.586	45.287	42.759
10	69.676	64.699	62.644	57.471	58.621	48.161
15	86.806	76.62	77.126	73.563	68.621	64.943
20	90.741	85.88	84.713	82.069	80.23	78.276
25	92.014	90.278	90	88.391	88.736	87.011
30	93.403	93.634	93.448	92.759	93.448	91.724
35	95.023	95.718	95.862	95.402	95.862	94.368
40	95.602	96.759	96.092	96.092	96.552	95.517
50	96.296	97.106	96.092	96.092	96.437	95.517
60	-	97.222	95.402	95.517	95.977	94.828

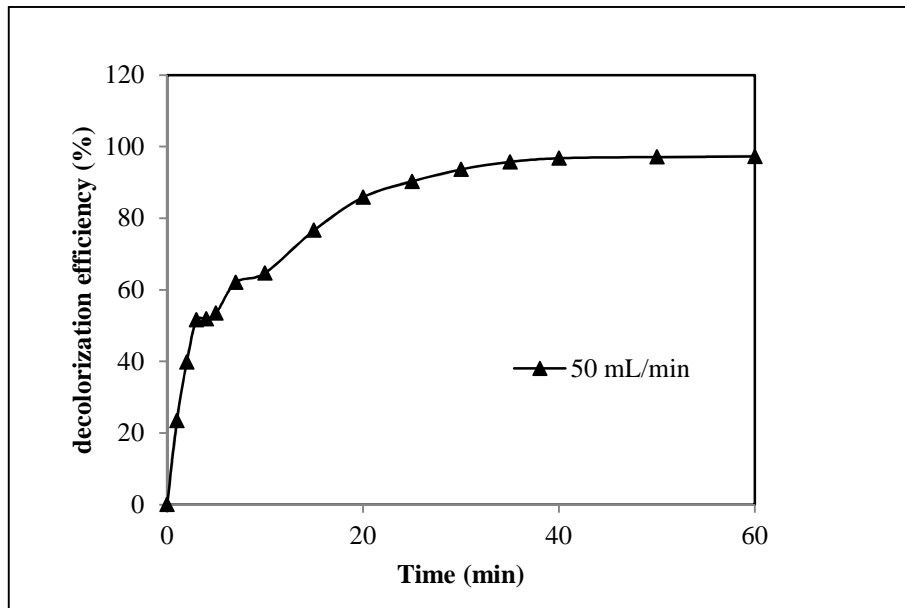
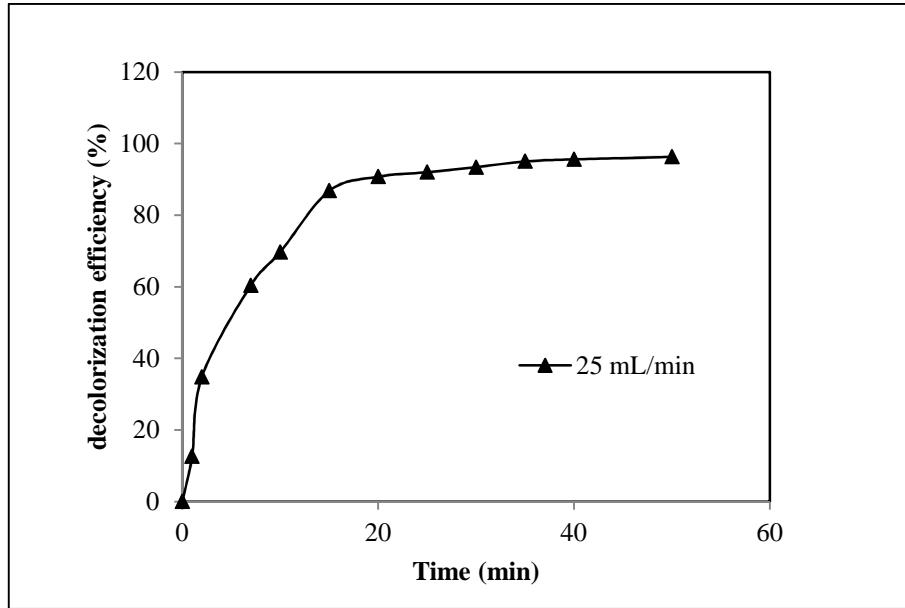


Figure 5.1.2. Effect of flow rate ($C_0=40$ mg/L RB5, $i=0.75$ mA/cm², $I=132$ A, S.E=0.02 M Na₂SO₄, $Q=50$ mL/min, rpm=18.6, Natural pH)

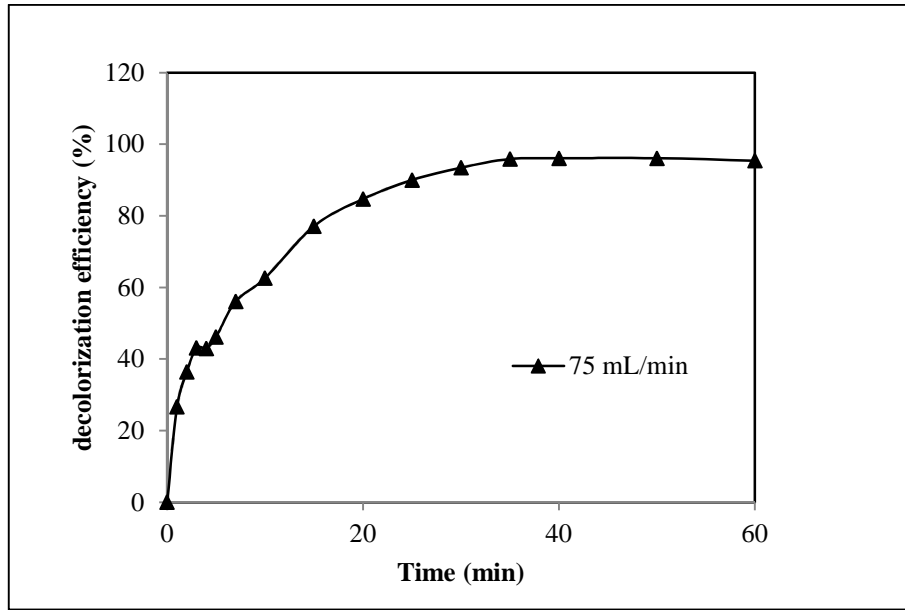


Figure 5.1.3. Effect of flow rate ($C_0=40$ mg/L RB5, $i=0.75$ mA/cm², $I=132$ A, S.E=0.02 M Na₂SO₄, $Q=75$ mL/min, rpm=27.8, Natural pH)

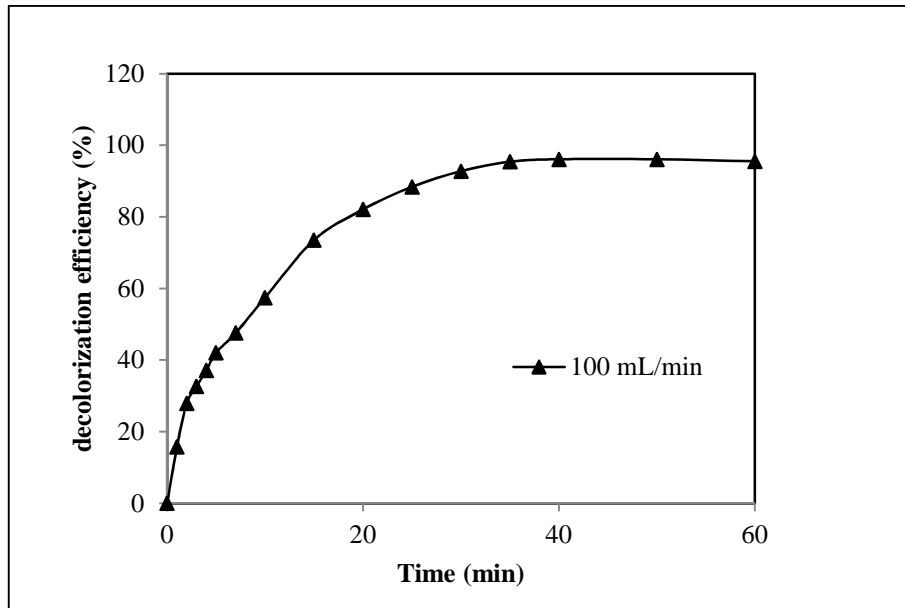


Figure 5.1.4. Effect of flow rate ($C_0=40$ mg/L RB5, $i=0.75$ mA/cm², $I=132$ A, S.E=0.02 M Na₂SO₄, $Q=100$ mL/min, rpm=37.1, Natural pH)

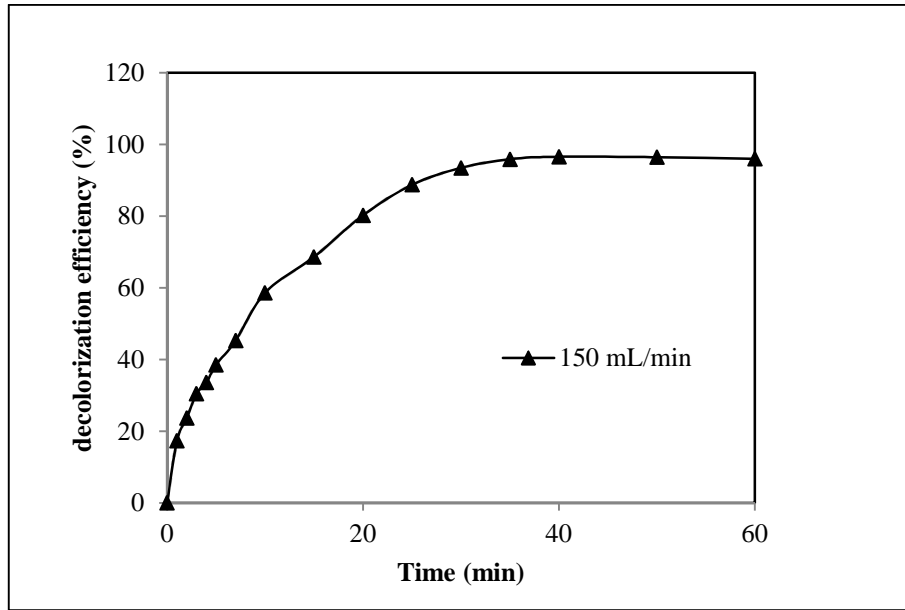


Figure 5.1.5. Effect of flow rate ($C_0=40$ mg/L RB5, $i=0.75$ mA/cm², $I=132$ A, S.E=0.02 M Na₂SO₄, $Q=150$ mL/min, rpm=55.7, Natural pH)

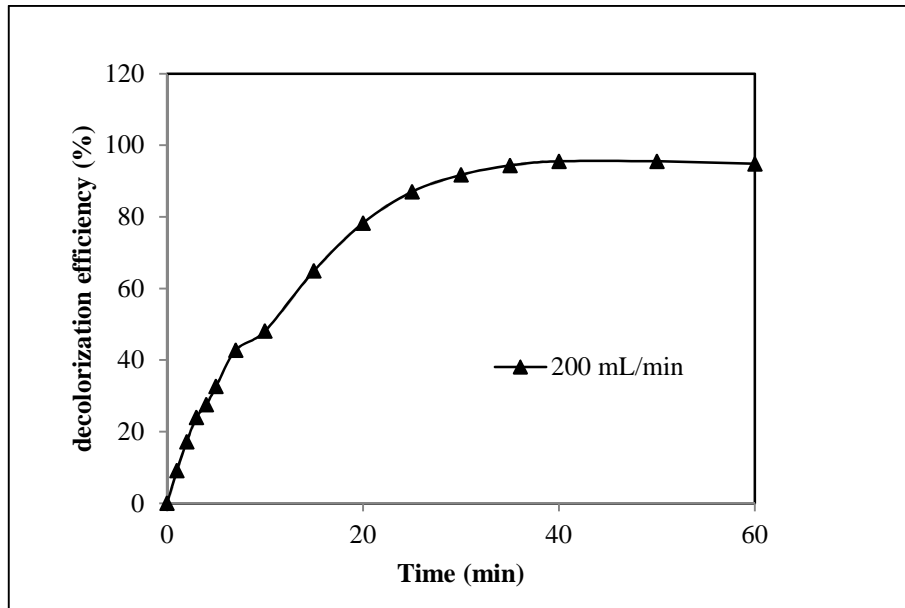


Figure 5.1.6. Effect of flow rate ($C_0=40$ mg/L RB5, $i=0.75$ mA/cm², $I=132$ A, S.E=0.02 M Na₂SO₄, $Q=200$ mL/min, rpm=74.3, Natural pH)

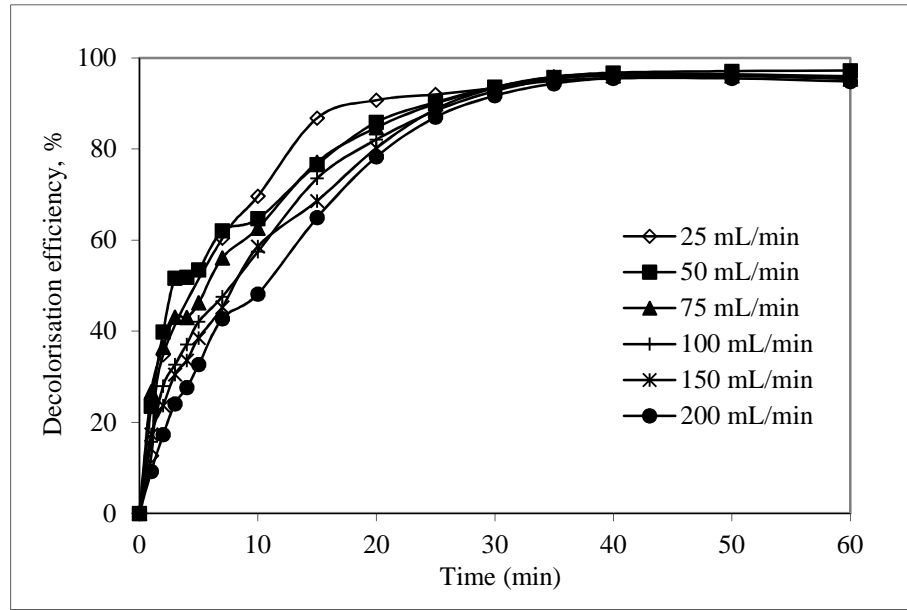


Figure 5.1.7. Comparison chart for Effect of flow rate ($C_0=40$ mg/L RB5, $i=0.75$ mA/cm², $I=132$ A, S.E=0.02 M Na₂SO₄, Natural pH)

5.2. Effect of Supporting Electrolyte

Due to the effect of supporting electrolyte on energy consumption values, decolorization efficiency and conductivity different amounts of Na₂SO₄ have been studied in this section. Other parameters of the study were constant and just supporting electrolyte amounts were varied ($C_0=40$ mg/L RB5, $i=0.75$ mA/cm², $I=132$ A, $Q=100$ mL/min, rpm=37.1, Natural pH). Results are shown in Table 5.2.1-4 and Figure 5.2.1-4.

Table 5.2.1. Effect of supporting electrolyte ($C_0=40$ mg/L RB5, $i=0.75$ mA/cm², $I=132$ A, S.E= 0.02 M Na₂SO₄, $Q=100$ mL/min, rpm= 37.1 , Natural pH)

Time (min)	Absorbance	Voltage (V)	Concentration (mg/L)	Decolorization efficiency (%)	Energy consumption (kWhm ⁻³)
0	0.87	205	37.339	-	-
1	0.733	211	31.459	15.747	0.928
2	0.627	227	26.909	27.931	0.998
3	0.586	228	25.150	32.643	1.003
4	0.547	229	23.476	37.126	1.007
5	0.504	223	21.630	42.068	0.981
7	0.456	223	19.570	47.586	1.962
10	0.37	222	15.879	57.471	2.930
15	0.23	219	9.871	73.563	4.818
20	0.156	212	6.695	82.068	4.664
25	0.101	216	4.334	88.390	4.752
30	0.063	210	2.703	92.758	4.62
35	0.04	209	1.716	95.402	4.598
40	0.034	208	1.459	96.091	4.576
50	0.034	215	1.459	96.091	9.46
60	0.039	209	1.673	95.517	9.196

Table 5.2.2. Effect of supporting electrolyte (Co=40 mg/L RB5, $i=0.75 \text{ mA/cm}^2$, $I=132 \text{ A}$, S.E=0.03 M Na_2SO_4 , $Q=100 \text{ mL/min}$, rpm=37.1, Natural pH)

Time (min)	Absorbance	Voltage (V)	Concentration (mg/L)	Decolorization efficiency (%)	Energy consumption (kWhm^{-3})
0	0.87	175	37.339	-	-
1	0.782	172	33.562	10.114	0.756
2	0.74	192	31.759	14.942	0.844
3	0.65	193	27.897	25.287	0.849
4	0.62	201	26.609	28.735	0.884
5	0.589	193	25.278	32.298	0.849
7	0.541	188	23.218	37.816	1.654
10	0.46	190	19.742	47.126	2.508
15	0.324	192	13.905	62.758	4.224
20	0.236	178	10.128	72.873	3.916
25	0.174	186	7.467	80.000	4.092
30	0.122	180	5.236	85.977	3.96
35	0.078	182	3.347	91.034	4.004
40	0.051	179	2.188	94.137	3.938
50	0.033	180	1.416	96.206	7.92
60	0.032	182	1.373	96.321	8.008

Table 5.2.3. Effect of supporting electrolyte (Co=40 mg/L RB5, $i=0.75 \text{ mA/cm}^2$, $I=132 \text{ A}$, S.E=0.05 M Na_2SO_4 , $Q=100 \text{ mL/min}$, $\text{rpm}=37.1$, Natural pH)

Time (min)	Absorbance	Voltage (V)	Concentration (mg/L)	Decolorization efficiency (%)	Energy consumption (kWhm^{-3})
0	0.87	119	37.339	-	-
1	0.83	120	35.622	4.597	0.528
2	0.828	122	35.536	4.827	0.536
3	0.813	126	34.892	6.551	0.554
4	0.81	130	34.763	6.896	0.572
5	0.796	136	34.163	8.505	0.598
7	0.76	147	32.618	12.643	1.293
10	0.67	154	28.755	22.988	2.032
15	0.563	155	24.163	35.287	3.41
20	0.476	154	20.429	45.287	3.388
25	0.37	157	15.879	57.471	3.454
30	0.301	145	12.918	65.402	3.19
35	0.245	150	10.515	71.839	3.3
40	0.183	148	7.854	78.965	3.256
50	0.109	151	4.678	87.471	6.644
60	0.072	142	3.090	91.724	6.248

Table 5.2.4. Comparison table for Effect of supporting electrolyte (Co=40 mg/L RB5, i=0.75 mA/cm², I=132 A, Q=100 mL/min, rpm=37.1, Natural pH)

Time (min)	Decolorization efficiency (%)	Decolorization efficiency (%)	Decolorization efficiency (%)
	0,02 M Na ₂ SO ₄	0,03 M Na ₂ SO ₄	0,05 M Na ₂ SO ₄
0	0	0	0
1	15.747	10.114	4.597
2	27.931	14.942	4.827
3	32.643	25.287	6.551
4	37.126	28.735	6.896
5	42.068	32.298	8.505
7	47.586	37.816	12.643
10	57.471	47.126	22.988
15	73.563	62.758	35.287
20	82.068	72.873	45.287
25	88.390	80.000	57.471
30	92.758	85.977	65.402
35	95.402	91.034	71.839
40	96.091	94.137	78.965
50	96.091	96.206	87.471
60	95.517	96.321	91.724

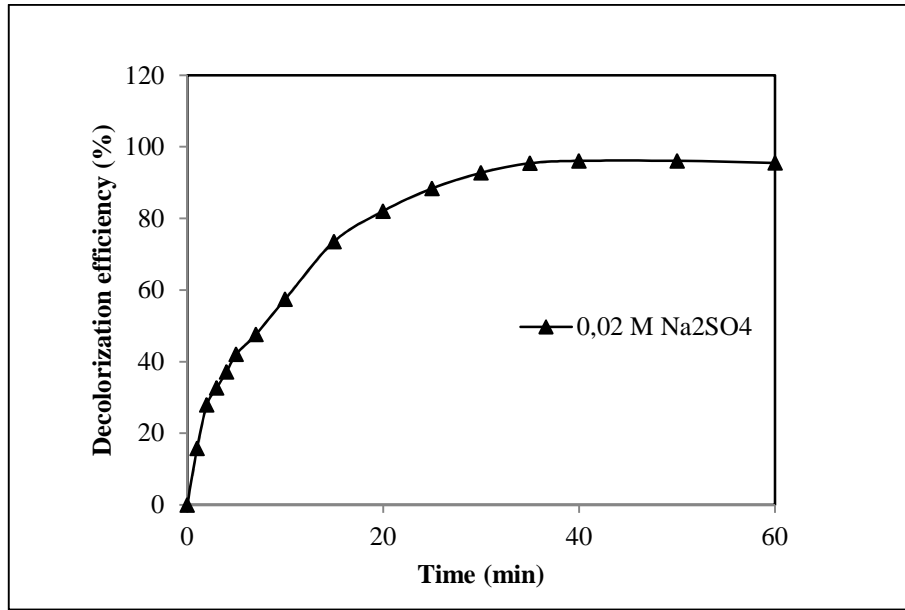


Figure 5.2.1. Effect of supporting electrolyte (Co=40 mg/L RB5, $i=0.75 \text{ mA/cm}^2$, $I=132 \text{ A}$, S.E=0.02 M Na_2SO_4 , $Q=100 \text{ mL/min}$, $\text{rpm}=37.1$, Natural pH)

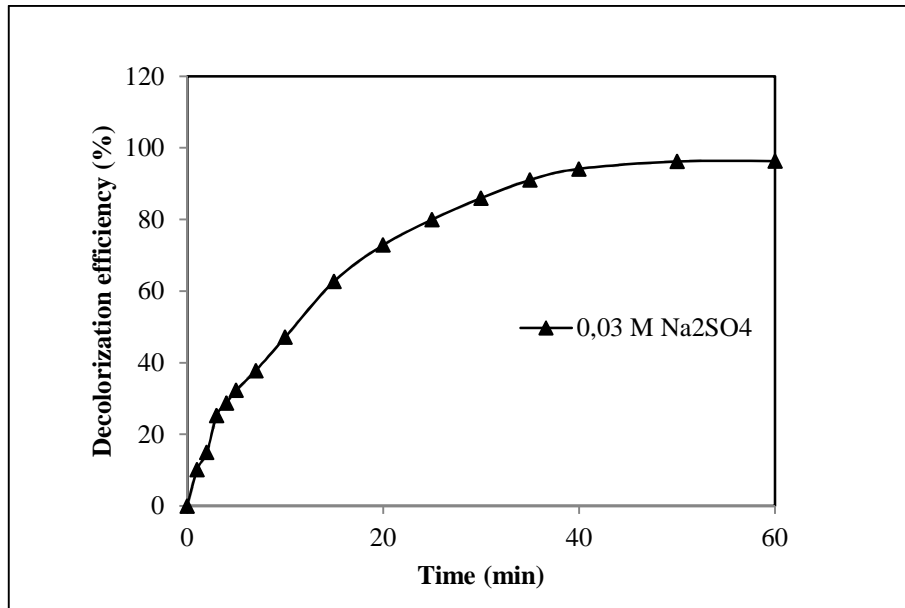


Figure 5.2.2. Effect of supporting electrolyte (Co=40 mg/L RB5, $i=0.75 \text{ mA/cm}^2$, $I=132 \text{ A}$, S.E=0.03 M Na_2SO_4 , $Q=100 \text{ mL/min}$, $\text{rpm}=37.1$, Natural pH)

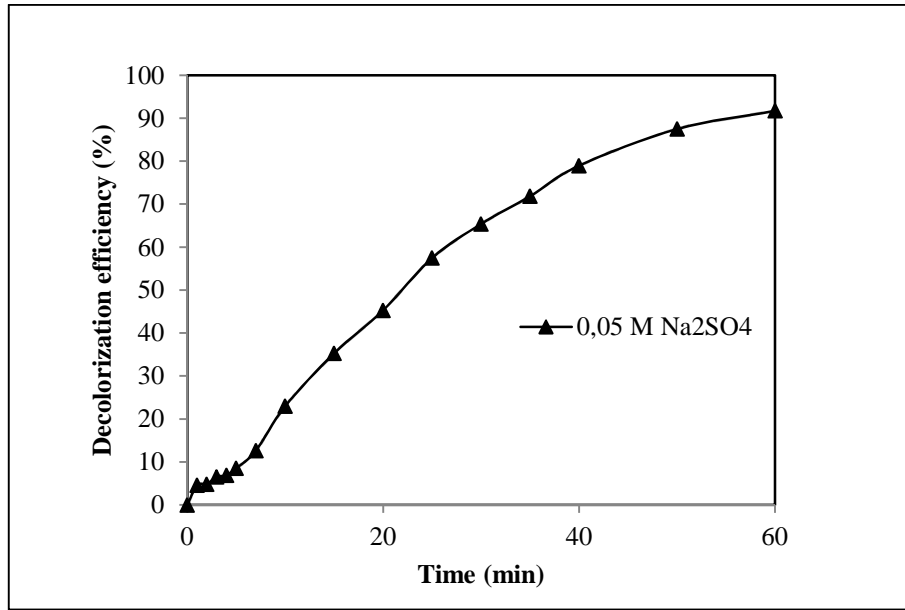


Figure 5.2.3. Effect of supporting electrolyte (Co=40 mg/L RB5, $i=0.75 \text{ mA/cm}^2$, $I=132 \text{ A}$, S.E=0.05 M Na_2SO_4 , $Q=100 \text{ mL/min}$, rpm=37.1, Natural pH)

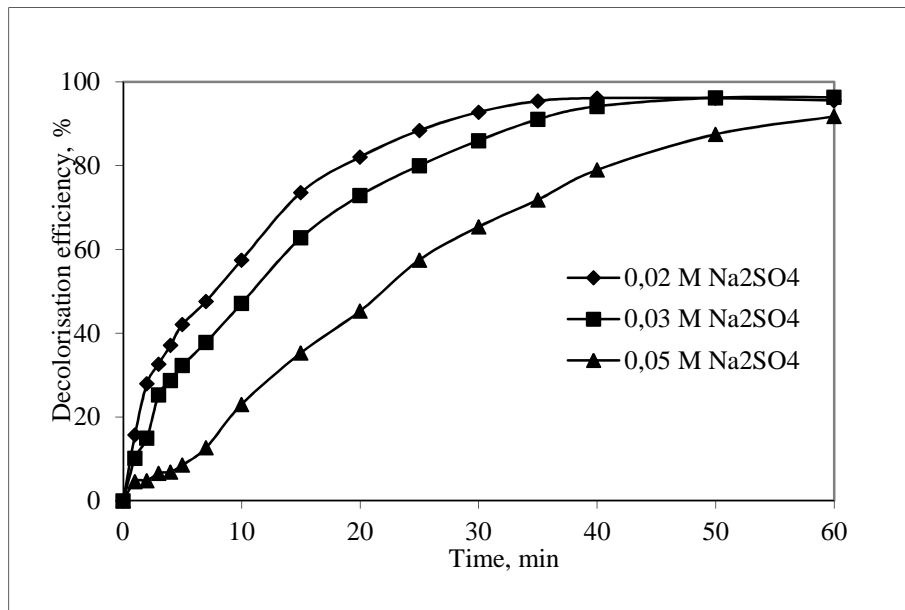


Figure 5.2.4. Comparison chart for effect of supporting electrolyte (Co=40 mg/L RB5, $i=0.75 \text{ mA/cm}^2$, $I=132 \text{ A}$, $Q=100 \text{ mL/min}$, rpm=37.1, Natural pH)

5.3. Effect of Initial pH

In anodic oxidation of Reactive Black 5 dye pH parameter doesn't have any effect on water treatment and there is no need to adjust the pH. But to prove it experiments have been done in 3 different pH values. Results are shown in Table 5.3.1-4 and Figure 5.3.1-4.

Table 5.3.1. Effect of Initial pH (Co=40 mg/L RB5, $i=0.75$ mA/cm², I=132 A, S.E=0.02 M Na₂SO₄, Q=100 mL/min, rpm=37.1, Natural pH)

Time (min)	Absorbance	Voltage (V)	Concentration (mg/L)	Decolorization efficiency (%)	Energy consumption (kWhm ⁻³)
0	0.87	205	37.339	-	-
1	0.733	211	31.459	15.747	0.928
2	0.627	227	26.909	27.931	0.998
3	0.586	228	25.150	32.643	1.003
4	0.547	229	23.476	37.126	1.007
5	0.504	223	21.630	42.068	0.981
7	0.456	223	19.570	47.586	1.962
10	0.37	222	15.879	57.471	2.930
15	0.23	219	9.871	73.563	4.818
20	0.156	212	6.695	82.068	4.664
25	0.101	216	4.334	88.390	4.752
30	0.063	210	2.703	92.758	4.62
35	0.04	209	1.716	95.402	4.598
40	0.034	208	1.459	96.091	4.576
50	0.034	215	1.459	96.091	9.46
60	0.039	209	1.673	95.517	9.196

Table 5.3.2. Effect of Initial pH (Co=40 mg/L RB5, $i=0.75 \text{ mA/cm}^2$, $I=132 \text{ A}$, $S.E=0.02 \text{ M Na}_2\text{SO}_4$, $Q=100 \text{ mL/min}$, $\text{rpm}=37.1$, $\text{pH}=3.52$)

Time (min)	Absorbance	Voltage (V)	Concentration (mg/L)	Decolorization efficiency (%)	Energy consumption (kWhm^{-3})
0	0.87	205	37.339	-	-
1	0.706	220	30.300	18.850	0.968
2	0.63	223	27.038	27.586	0.981
3	0.567	229	24.334	34.827	1.007
4	0.531	222	22.789	38.965	0.976
5	0.496	217	21.287	42.988	0.954
7	0.45	224	19.313	48.275	1.971
10	0.378	212	16.223	56.551	2.798
15	0.243	212	10.429	72.068	4.664
20	0.147	213	6.309	83.103	4.686
25	0.094	209	4.034	89.195	4.598
30	0.059	210	2.532	93.218	4.62
35	0.042	212	1.802	95.172	4.664
40	0.036	220	1.545	95.862	4.84
50	0.039	206	1.673	95.517	9.064
60	0.043	212	1.845	95.057	9.328

Table 5.3.3. Effect of Initial pH (Co=40 mg/L RB5, $i=0.75 \text{ mA/cm}^2$, $I=132 \text{ A}$, $S.E=0.02 \text{ M Na}_2\text{SO}_4$, $Q=100 \text{ mL/min}$, $\text{rpm}=37.1$, $\text{pH}=10.17$)

Time (min)	Absorbance	Voltage (V)	Concentration (mg/L)	Decolorization efficiency (%)	Energy consumption (kWhm^{-3})
0	0.87	209	37.339	-	-
1	0.722	210	30.987	17.011	0.924
2	0.67	230	28.755	22.988	1.012
3	0.592	230	25.407	31.954	1.012
4	0.527	232	22.618	39.425	1.020
5	0.498	233	21.373	42.758	1.025
7	0.422	229	18.111	51.494	2.015
10	0.33	226	14.163	62.068	2.983
15	0.212	223	9.098	75.632	4.906
20	0.132	215	5.665	84.827	4.73
25	0.078	225	3.347	91.034	4.95
30	0.051	212	2.188	94.137	4.664
35	0.04	210	1.716	95.402	4.62
40	0.036	209	1.545	95.862	4.598
50	0.042	210	1.802	95.172	9.24
60	0.049	206	2.103	94.367	9.064

Table 5.3.4. Comparison table for effect of Initial pH ($C_0=40$ mg/L RB5, $i=0.75$ mA/cm², $I=132$ A, $S.E=0.02$ M Na₂SO₄, $Q=100$ mL/min, rpm=37.1)

Time (min)	Decolorization efficiency (%)	Decolorization efficiency (%)	Decolorization efficiency (%)
	Natural pH	pH=3.52	pH=10.17
0	0	0	0
1	15.747	18.850	17.011
2	27.931	27.586	22.988
3	32.643	34.827	31.954
4	37.126	38.965	39.425
5	42.068	42.988	42.758
7	47.586	48.275	51.494
10	57.471	56.551	62.068
15	73.563	72.068	75.632
20	82.068	83.103	84.827
25	88.390	89.195	91.034
30	92.758	93.218	94.137
35	95.402	95.172	95.402
40	96.091	95.862	95.862
50	96.091	95.517	95.172
60	95.517	95.057	94.367

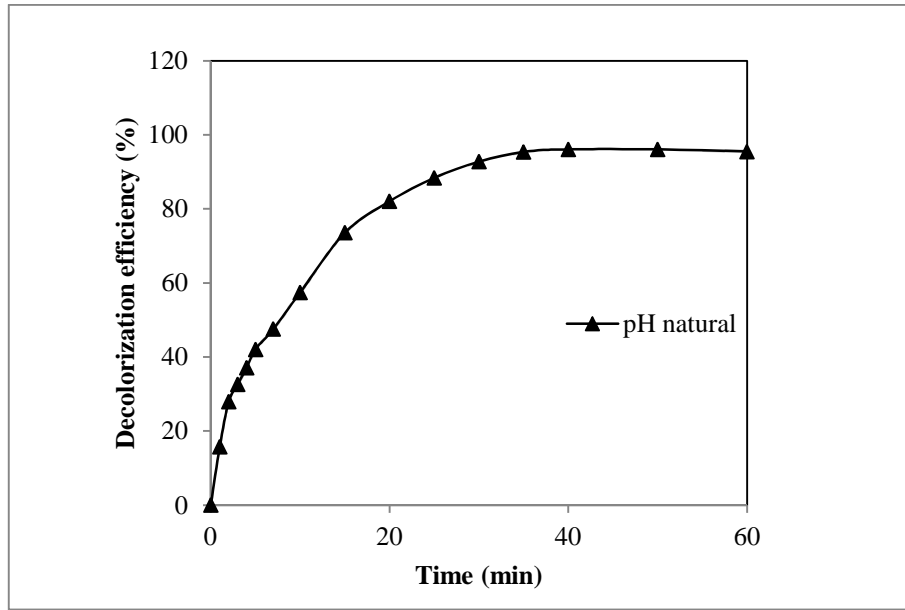


Figure 5.3.1. Effect of Initial pH ($C_0=40$ mg/L RB5, $i=0.75$ mA/cm², $I=132$ A, S.E=0.02 M Na₂SO₄, $Q=100$ mL/min, rpm=37.1, Natural pH)

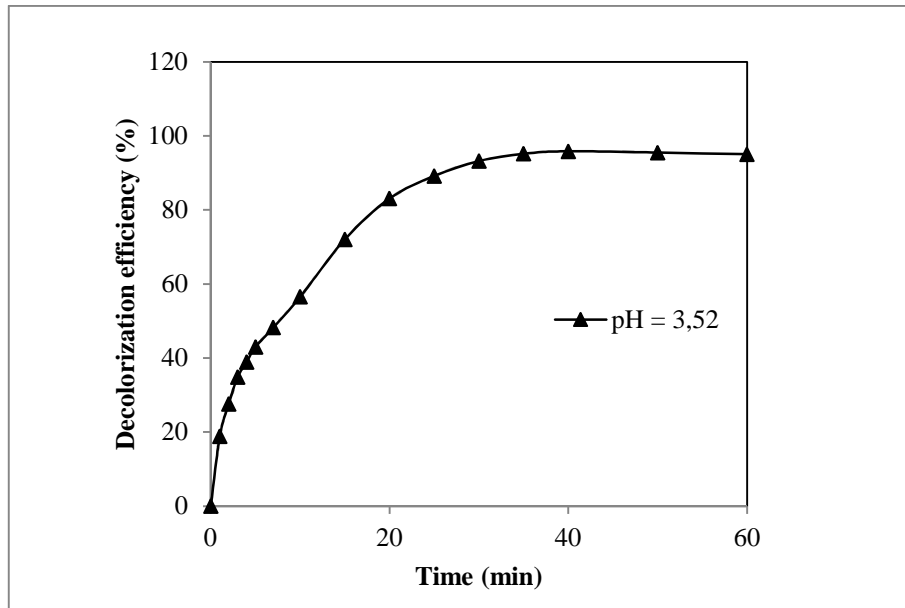


Figure 5.3.2. Effect of Initial pH ($C_0=40$ mg/L RB5, $i=0.75$ mA/cm², $I=132$ A, S.E=0.02 M Na₂SO₄, $Q=100$ mL/min, rpm=37.1, pH=3.52)

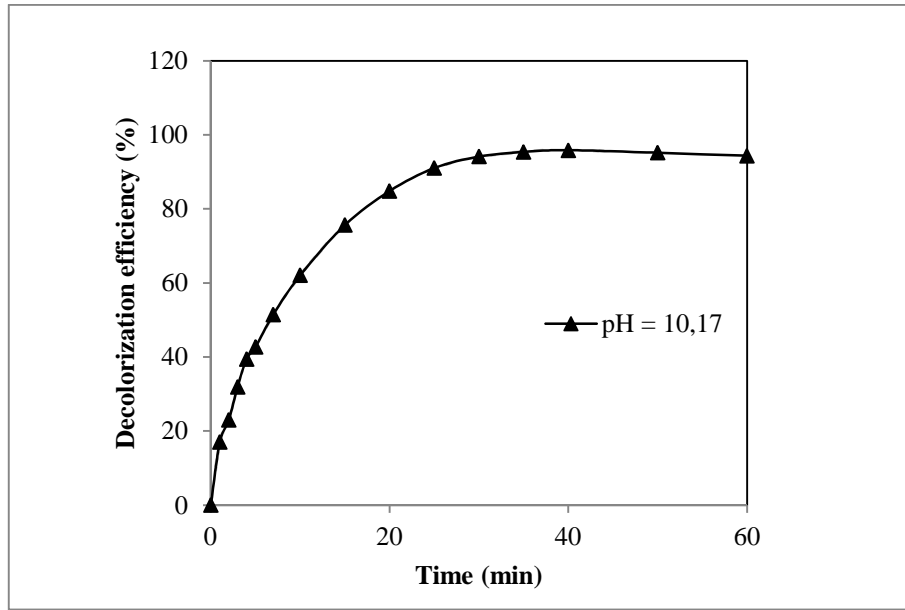


Figure 5.3.3. Effect of Initial pH ($C_0=40$ mg/L RB5, $i=0.75$ mA/cm², $I=132$ A, S.E=0.02 M Na₂SO₄, $Q=100$ mL/min, rpm=37.1, pH=10.17)

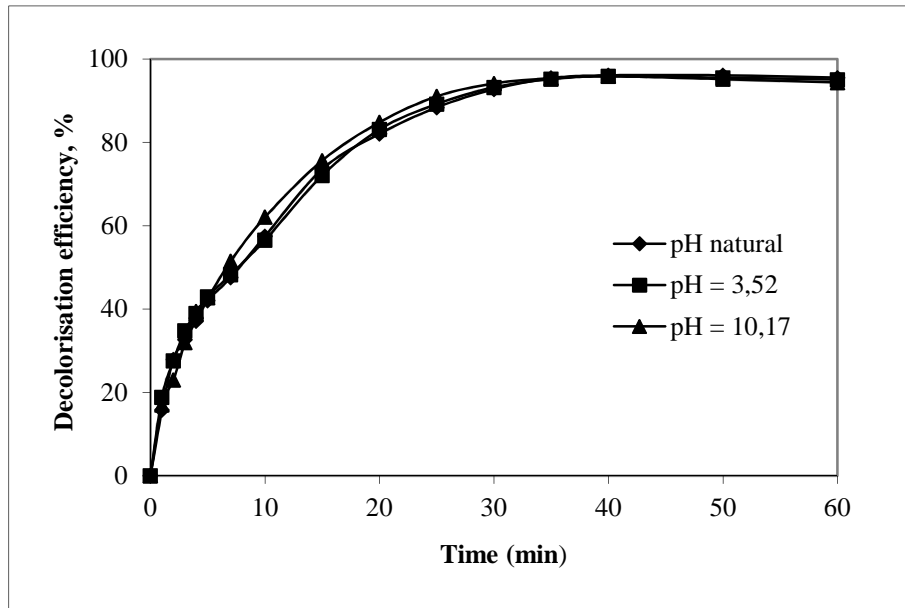


Figure 5.3.4. Comparison chart for effect of Initial pH ($C_0=40$ mg/L RB5, $i=0.75$ mA/cm², $I=132$ A, S.E=0.02 M Na₂SO₄, $Q=100$ mL/min, rpm=37.1)

5.4. Effect of Current Density

Another parameter that has been considered in this study is the effect of current density. Current density has a direct effect on decolorization of the dye stuff, in a way that any increase in the current density decreases the time of decolorization but using high current densities are not advantageous. A normal and optimum current density value has been achieved through evaluating current density effect. Results are presented in table 5.4.1-8 and figure 5.4.1-8.

Table 5.4.1. Effect of current density ($C_0=40$ mg/L RB5, $i=0.5$ mA/cm², $I=88$ A, $S.E=0.02$ M Na₂SO₄, $Q=100$ mL/min, rpm=37.1, Natural pH)

Time (min)	Absorbance	Voltage (V)	Concentration (mg/L)	Decolorization efficiency (%)	Energy consumption (kWhm ⁻³)
0	0.87	155	37.339	-	-
1	0.844	156	36.223	2.988	0.457
2	0.832	162	35.708	4.367	0.475
3	0.813	169	34.892	6.551	0.495
4	0.783	175	33.605	10	0.513
5	0.753	184	32.317	13.448	0.539
7	0.715	183	30.686	17.81	1.073
10	0.62	193	26.609	28.735	1.698
15	0.533	180	22.875	38.735	2.64
20	0.427	187	18.326	50.919	2.742
25	0.363	176	15.579	58.275	2.581
30	0.293	179	12.575	66.321	2.625
35	0.246	176	10.557	71.724	2.581
40	0.203	173	8.712	76.666	2.537
50	0.133	173	5.708	84.712	5.074
60	0.086	173	3.690	90.114	5.074

Table 5.4.2. Effect of current density ($C_0=40$ mg/L RB5, $i=0.625$ mA/cm², $I=110$ A, S.E=0.02 M Na₂SO₄, $Q=100$ mL/min, rpm=37.1, Natural pH)

Time (min)	Absorbance	Voltage (V)	Concentration (mg/L)	Decolorization efficiency (%)	Energy consumption (kWhm ⁻³)
0	0.87	199	37.339	-	-
1	0.672	200	28.841	22.758	0.733
2	0.658	203	28.240	24.367	0.744
3	0.625	205	26.824	28.160	0.751
4	0.592	201	25.407	31.954	0.737
5	0.542	216	23.261	37.701	0.792
7	0.505	210	21.673	41.954	1.54
10	0.428	203	18.369	50.804	2.233
15	0.315	200	13.519	63.793	3.666
20	0.234	196	10.042	73.103	3.593
25	0.168	194	7.210	80.689	3.556
30	0.113	198	4.849	87.011	3.63
35	0.073	198	3.133	91.609	3.63
40	0.06	200	2.575	93.103	3.666
50	0.043	193	1.845	95.057	7.076
60	0.043	194	1.845	95.057	7.113

Table 5.4.3. Effect of current density (Co=40 mg/L RB5, $i=0.75 \text{ mA/cm}^2$, $I=132 \text{ A}$, S.E=0.02 M Na_2SO_4 , $Q=100 \text{ mL/min}$, rpm=37.1, Natural pH)

Time (min)	Absorbance	Voltage (V)	Concentration (mg/L)	Decolorization efficiency (%)	Energy consumption (kWhm^{-3})
0	0.87	205	37.339	-	-
1	0.733	211	31.459	15.747	0.928
2	0.627	227	26.909	27.931	0.998
3	0.586	228	25.150	32.643	1.003
4	0.547	229	23.476	37.126	1.007
5	0.504	223	21.630	42.068	0.981
7	0.456	223	19.570	47.586	1.962
10	0.37	222	15.879	57.471	2.930
15	0.23	219	9.871	73.563	4.818
20	0.156	212	6.695	82.068	4.664
25	0.101	216	4.334	88.390	4.752
30	0.063	210	2.703	92.758	4.62
35	0.04	209	1.716	95.402	4.598
40	0.034	208	1.459	96.091	4.576
50	0.034	215	1.459	96.091	9.46
60	0.039	209	1.673	95.517	9.196

Table 5.4.4. Effect of current density ($C_0=40$ mg/L RB5, $i=0.875$ mA/cm², $I=154$ A, S.E=0.02 M Na₂SO₄, $Q=100$ mL/min, rpm=37.1, Natural pH)

Time (min)	Absorbance	Voltage (V)	Concentration (mg/L)	Decolorization efficiency (%)	Energy consumption (kWhm ⁻³)
0	0.87	242	37.339	-	-
1	0.52	243	22.317	40.229	1.247
2	0.468	244	20.085	46.206	1.252
3	0.432	249	18.540	50.344	1.278
4	0.39	246	16.738	55.172	1.262
5	0.353	255	15.150	59.425	1.309
7	0.305	240	13.090	64.942	2.464
10	0.225	234	9.656	74.137	3.603
15	0.111	245	4.763	87.241	6.288
20	0.063	225	2.703	92.758	5.775
25	0.038	222	1.630	95.632	5.698
30	0.032	233	1.373	96.321	5.980
35	0.033	230	1.416	96.206	5.903
40	0.036	218	1.545	95.862	5.595
50	0.043	233	1.845	95.057	11.960
60	0.049	220	2.103	94.367	11.293

Table 5.4.5. Effect of current density ($C_0=40$ mg/L RB5, $i=1$ mA/cm², $I=176$ A, S.E=0.02 M Na₂SO₄, $Q=100$ mL/min, rpm=37.1, Natural pH)

Time (min)	Absorbance	Voltage (V)	Concentration (mg/L)	Decolorization efficiency (%)	Energy consumption (kWhm ⁻³)
0	0.87	250	37.339	-	-
1	0.512	253	21.974	41.149	1.484
2	0.458	265	19.656	47.356	1.554
3	0.42	257	18.025	51.724	1.507
4	0.365	256	15.665	58.045	1.501
5	0.323	258	13.862	62.873	1.513
7	0.247	253	10.600	71.609	2.968
10	0.155	246	6.652	82.183	4.329
15	0.071	250	3.047	91.839	7.333
20	0.036	258	1.545	95.862	7.568
25	0.029	245	1.244	96.666	7.186
30	0.029	233	1.244	96.666	6.834
35	0.033	235	1.416	96.206	6.893
40	0.036	232	1.545	95.862	6.805
50	0.049	229	2.103	94.367	13.434
60	0.059	234	2.532	93.218	13.728

Table 5.4.6. Effect of current density ($C_0=40$ mg/L RB5, $i=1.125$ mA/cm², $I=198$ A, S.E=0.02 M Na₂SO₄, $Q=100$ mL/min, rpm=37.1, Natural pH)

Time (min)	Absorbance	Voltage (V)	Concentration (mg/L)	Decolorization efficiency (%)	Energy consumption (kWhm ⁻³)
0	0.89	270	38.197	-	-
1	0.474	278	20.343	46.741	1.834
2	0.407	272	17.467	54.269	1.795
3	0.338	263	14.506	62.022	1.735
4	0.306	270	13.133	65.617	1.782
5	0.263	272	11.287	70.449	1.795
7	0.196	262	8.412	77.977	3.458
10	0.114	261	4.892	87.191	5.167
15	0.058	251	2.489	93.483	8.283
20	0.042	250	1.802	95.280	8.25
25	0.043	257	1.845	95.168	8.481
30	0.05	245	2.145	94.382	8.085

Table 5.4.7. Effect of current density (Co=40 mg/L RB5, $i=1.25 \text{ mA/cm}^2$, $I=220 \text{ A}$, S.E=0.02 M Na_2SO_4 , $Q=100 \text{ mL/min}$, rpm=37.1, Natural pH)

Time (min)	Absorbance	Voltage (V)	Concentration (mg/L)	Decolorization efficiency (%)	Energy consumption (kWhm^{-3})
0	0.87	295	37.339	-	-
1	0.599	297	25.708	31.149	2.178
2	0.368	291	15.793	57.701	2.134
3	0.27	279	11.587	68.965	2.046
4	0.208	283	8.927	76.091	2.075
5	0.188	293	8.068	78.390	2.148
7	0.139	279	5.965	84.022	4.092
10	0.078	270	3.347	91.034	5.94
15	0.033	268	1.416	96.206	9.826
20	0.032	263	1.373	96.321	9.643
25	0.039	263	1.673	95.517	9.643

Table 5.4.8. Comparison table for effect of current density (Co=40 mg/L RB5, S.E=0.02 M Na₂SO₄, Q=100 mL/min, rpm=37.1, Natural pH)

Time (min)	0,5 mA/cm ²	0,625 mA/cm ²	0,75 mA/cm ²	0,875 mA/cm ²	1 mA/cm ²	1,125 mA/cm ²	1,25 mA/cm ²
0	0	0	0	0	0	0	0
1	2.989	22.759	15.747	40.23	41.149	46.742	31.149
2	4.368	24.368	27.931	46.207	47.356	54.27	57.701
3	6.552	28.161	32.644	50.345	51.724	62.022	68.966
4	10	31.954	37.126	55.172	58.046	65.618	76.092
5	13.45	37.701	42.069	59.425	62.874	70.449	78.391
7	17.82	41.954	47.586	64.943	71.609	77.978	84.023
10	28.74	50.805	57.471	74.138	82.184	87.191	91.034
15	38.74	63.793	73.563	87.241	91.839	93.483	96.207
20	50.92	73.103	82.069	92.759	95.862	95.281	96.322
25	58.28	80.69	88.391	95.632	96.667	-	-
30	66.32	87.011	92.759	96.322	96.667	-	-
35	71.72	91.609	95.402	96.207	-	-	-
40	76.67	93.103	96.092	95.862	-	-	-
50	84.71	95.057	96.092	95.057	-	-	-
60	90.11	-	-	-	-	-	-

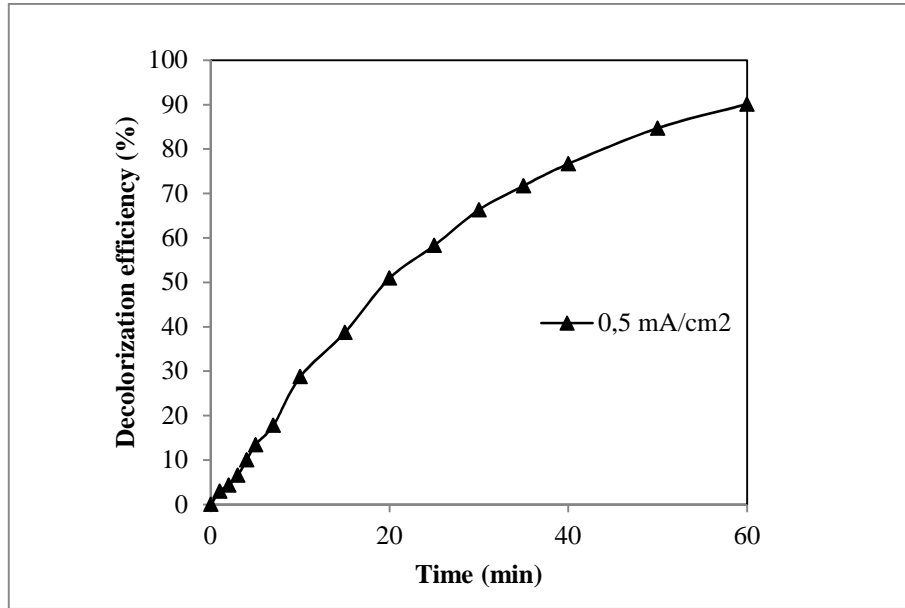


Figure 5.4.1. Effect of current density ($C_0=40$ mg/L RB5, $i=0.5$ mA/cm², $I=88$ A, S.E=0.02 M Na₂SO₄, $Q=100$ mL/min, rpm=37.1, Natural pH)

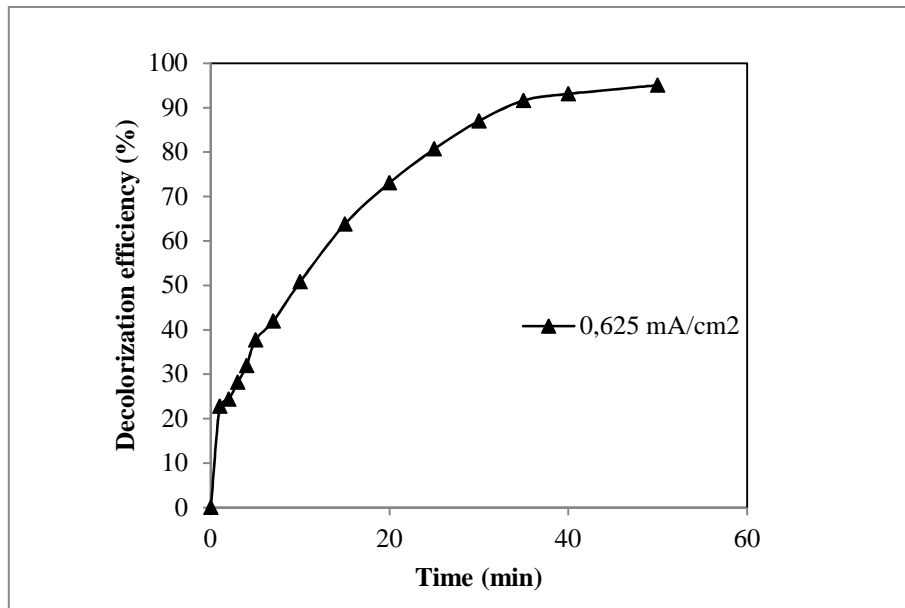


Figure 5.4.2. Effect of current density ($C_0=40$ mg/L RB5, $i=0.625$ mA/cm², $I=110$ A, S.E=0.02 M Na₂SO₄, $Q=100$ mL/min, rpm=37.1, Natural pH)

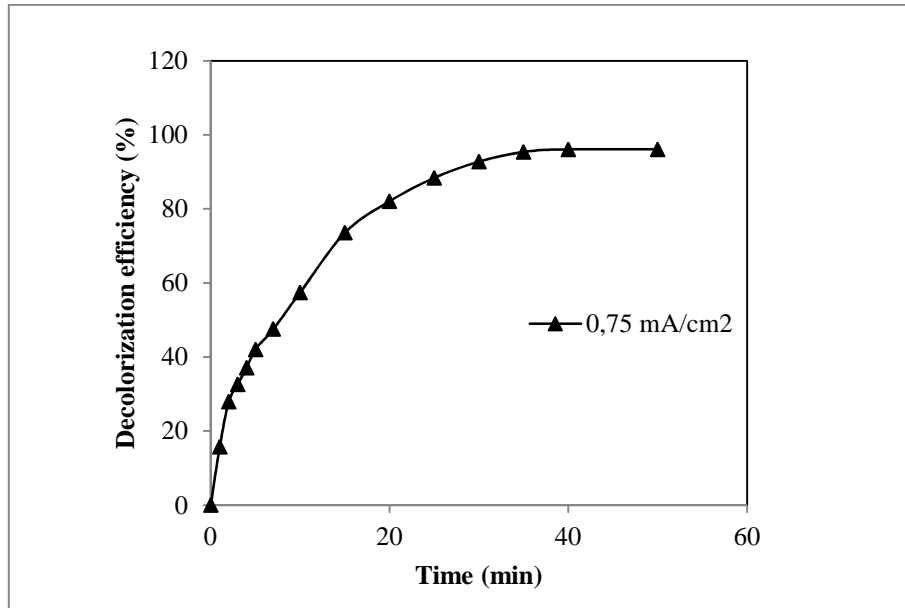


Figure 5.4.3. Effect of current density ($C_0=40$ mg/L RB5, $i=0.75$ mA/cm², $I=132$ A, S.E=0.02 M Na₂SO₄, $Q=100$ mL/min, rpm=37.1, Natural pH)

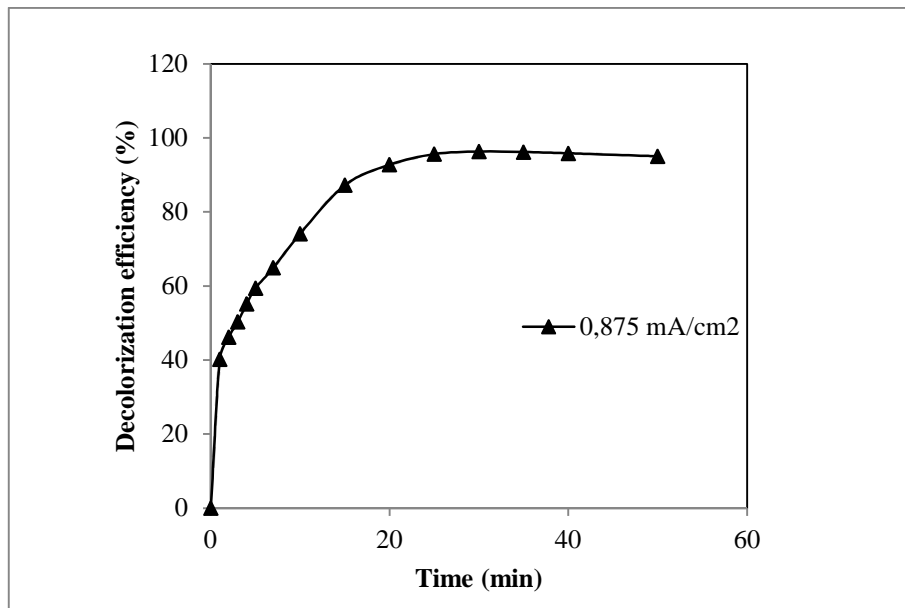


Figure 5.4.4. Effect of current density ($C_0=40$ mg/L RB5, $i=0.875$ mA/cm², $I=154$ A, S.E=0.02 M Na₂SO₄, $Q=100$ mL/min, rpm=37.1, Natural pH)

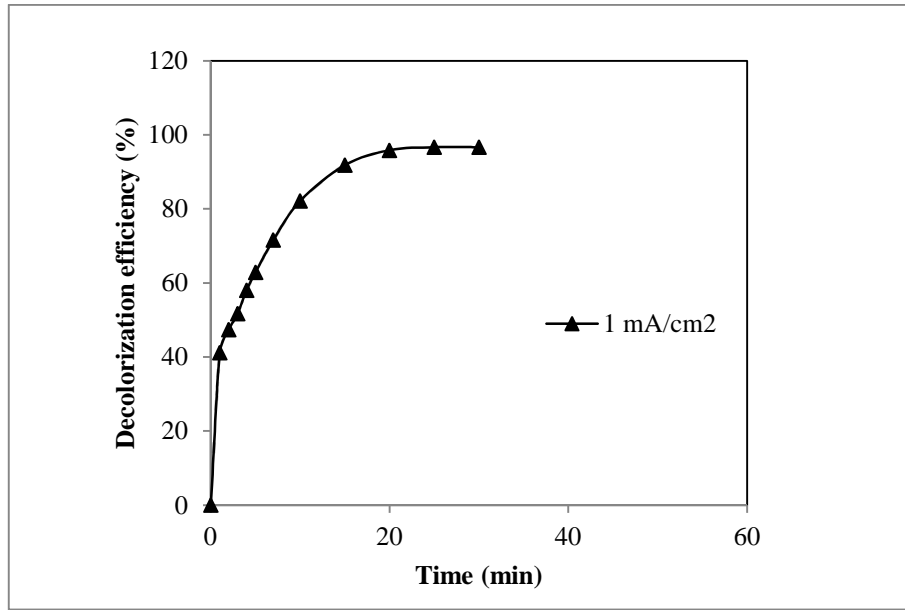


Figure 5.4.5. Effect of current density ($C_0=40$ mg/L RB5, $i=1$ mA/cm², $I=176$ A, S.E=0.02 M Na₂SO₄, $Q=100$ mL/min, rpm=37.1, Natural pH)

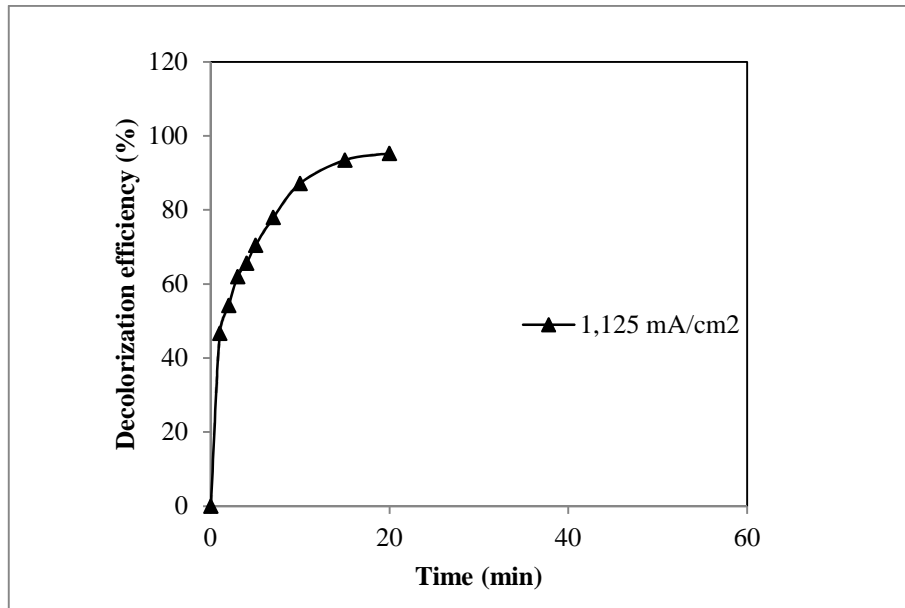


Figure 5.4.6. Effect of current density ($C_0=40$ mg/L RB5, $i=1.125$ mA/cm², $I=198$ A, S.E=0.02 M Na₂SO₄, $Q=100$ mL/min, rpm=37.1, Natural pH)

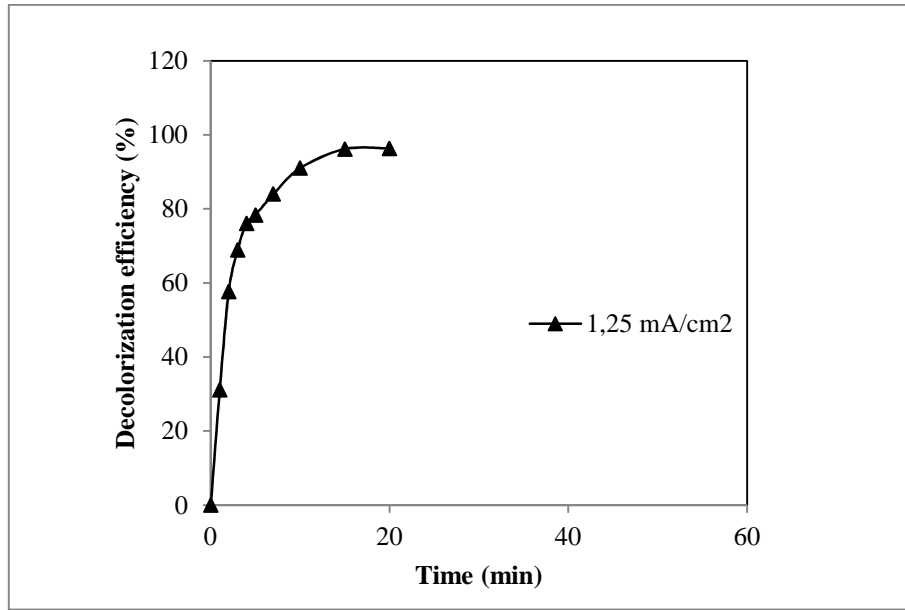


Figure 5.4.7. Effect of current density ($C_0=40$ mg/L RB5, $i=1.25$ mA/cm², $I=220$ A, S.E=0.02 M Na₂SO₄, $Q=100$ mL/min, rpm=37.1, Natural pH)

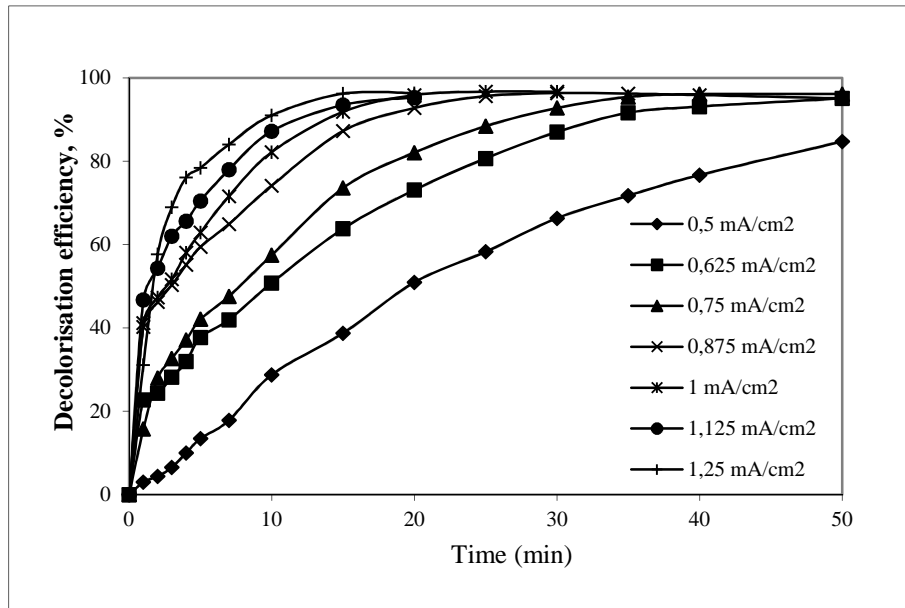


Figure 5.4.8. Comparison chart for effect of current density ($C_0=40$ mg/L RB5, S.E=0.02 M Na₂SO₄, $Q=100$ mL/min, rpm=37.1, Natural pH)

5.5. Effect of Initial Dye Concentration

Because of the dimensions of the system, it will be productive until distinctive initial dye concentration. More concentrate solutions will need more time to be decolorized. But to show the systems capability in decolorization of more concentrate dye solutions and also time difference between decolorization of different dye initial concentrations, effect of initial dye concentration has been considered in this section. Like other experiments, in this experiment all the parameters except initial dye concentration have been constant too. Results are exposed in Tables 5.5.1-5 and Figures 5.5.1-5.

Table 5.5.1. Effect of initial dye concentration ($C_0=20$ mg/L RB5, $i=1$ mA/cm², $I=176$ A, S.E=0.02 M Na₂SO₄, $Q=100$ mL/min, rpm=37.1, Natural pH)

Time (min)	Absorbance	Voltage (V)	Concentration (mg/L)	Decolorization efficiency (%)	Energy consumption (kWhm ⁻³)
0	0.448	252	19.227	-	-
1	0.226	253	9.699	49.553	1.484
2	0.143	245	6.137	68.080	1.437
3	0.117	252	5.021	73.883	1.478
4	0.1	252	4.291	77.678	1.478
5	0.076	257	3.261	83.035	1.50
7	0.048	250	2.060	89.285	2.933
10	0.031	250	1.330	93.080	4.4
15	0.025	251	1.072	94.419	7.362
20	0.026	238	1.115	94.196	6.981
25	0.03	225	1.287	93.303	6.6

Table 5.5.2. Effect of initial dye concentration ($C_0=40$ mg/L RB5, $i=1$ mA/cm², $I=176$ A, S.E= 0.02 M Na₂SO₄, $Q=100$ mL/min, rpm= 37.1 , Natural pH)

Time (min)	Absorbance	Voltage (V)	Concentration (mg/L)	Decolorization efficiency (%)	Energy consumption (kWhm ⁻³)
0	0.87	250	37.339	-	-
1	0.512	253	21.974	41.149	1.484
2	0.458	265	19.657	47.356	1.555
3	0.42	257	18.026	51.724	1.508
4	0.365	256	15.665	58.046	1.502
5	0.323	258	13.863	62.874	1.514
7	0.247	253	10.601	71.609	2.969
10	0.155	246	6.6524	82.184	4.33
15	0.071	250	3.0472	91.839	7.333
20	0.036	258	1.5451	95.862	7.568
25	0.029	245	1.2446	96.667	7.187
30	0.029	233	1.2446	96.667	6.835
35	0.033	235	1.4163	96.207	6.893
40	0.036	232	1.5451	95.862	6.805
50	0.049	229	2.103	94.368	13.43
60	0.059	234	2.5322	93.218	13.73

Table 5.5.3. Effect of initial dye concentration ($C_0=60$ mg/L RB5, $i=1$ mA/cm², $I=176$ A, S.E=0.02 M Na₂SO₄, Q=100 mL/min, rpm=37.1, Natural pH)

Time (min)	Absorbance	Voltage (V)	Concentration (mg/L)	Decolorization efficiency (%)	Energy consumption (kWhm ⁻³)
0	1.307	234	56.094	-	-
1	0.959	264	41.159	26.626	1.549
2	0.81	246	34.764	38.026	1.443
3	0.73	256	31.33	44.147	1.502
4	0.66	252	28.326	49.503	1.478
5	0.629	250	26.996	51.875	1.467
7	0.55	246	23.605	57.919	2.886
10	0.413	247	17.725	68.401	4.347
15	0.249	245	10.687	80.949	7.187
20	0.137	240	5.8798	89.518	7.04
25	0.08	242	3.4335	93.879	7.099
30	0.047	236	2.0172	96.404	6.923
35	0.039	230	1.6738	97.016	6.747
40	0.04	233	1.7167	96.94	6.835

Table 5.5.4. Effect of initial dye concentration ($C_0=100$ mg/L RB5, $i=1$ mA/cm², $I=176$ A, $S.E=0.02$ M Na₂SO₄, $Q=100$ mL/min, rpm=37.1, Natural pH)

Time (min)	Absorbance	Voltage (V)	Concentration (mg/L)	Decolorization efficiency (%)	Energy consumption (kWhm ⁻³)
0	2.165	260	92.918	-	-
1	1.765	263	75.751	18.476	1.543
2	1.63	259	69.957	24.711	1.519
3	1.555	252	66.738	28.176	1.478
4	1.427	258	61.245	34.088	1.514
5	1.358	255	58.283	37.275	1.496
7	1.262	250	54.163	41.709	2.933
10	1.086	254	46.609	49.838	4.47
15	0.81	245	34.764	62.587	7.187
20	0.57	230	24.464	73.672	6.747
25	0.414	245	17.768	80.878	7.187
30	0.273	240	11.717	87.39	7.04
35	0.186	237	7.9828	91.409	6.952
40	0.125	234	5.3648	94.226	6.864
50	0.07	235	3.0043	96.767	13.79
60	0.064	233	2.7468	97.044	13.67
70	0.072	232	3.0901	96.674	13.61

Table 5.5.5. Comparison table for effect of initial dye concentration ($i=1 \text{ mA/cm}^2$, $I=176 \text{ A}$, $S.E=0.02 \text{ M Na}_2\text{SO}_4$, $Q=100 \text{ mL/min}$, $\text{rpm}=37.1$, Natural pH)

Time (min)	Decolorization efficiency (%) 20 mg/L RB5	Decolorization efficiency (%) 40 mg/L RB5	Decolorization efficiency (%) 60 mg/L RB5	Decolorization efficiency (%) 100 mg/L RB5
0	0	0	0	0
1	49.554	41.149	26.626	18.476
2	68.08	47.356	38.026	24.711
3	73.884	51.724	44.147	28.176
4	77.679	58.046	49.503	34.088
5	83.036	62.874	51.875	37.275
7	89.286	71.609	57.919	41.709
10	93.08	82.184	68.401	49.838
15	94.42	91.839	80.949	62.587
20	95.862	95.862	89.518	73.672
25	-	96.667	93.879	80.878
30	-	96.667	96.404	87.39
35	-	-	97.016	91.409
40	-	-	97.016	94.226
50	-	-	-	96.767
60	-	-	-	97.044
70	-	-	-	97.044

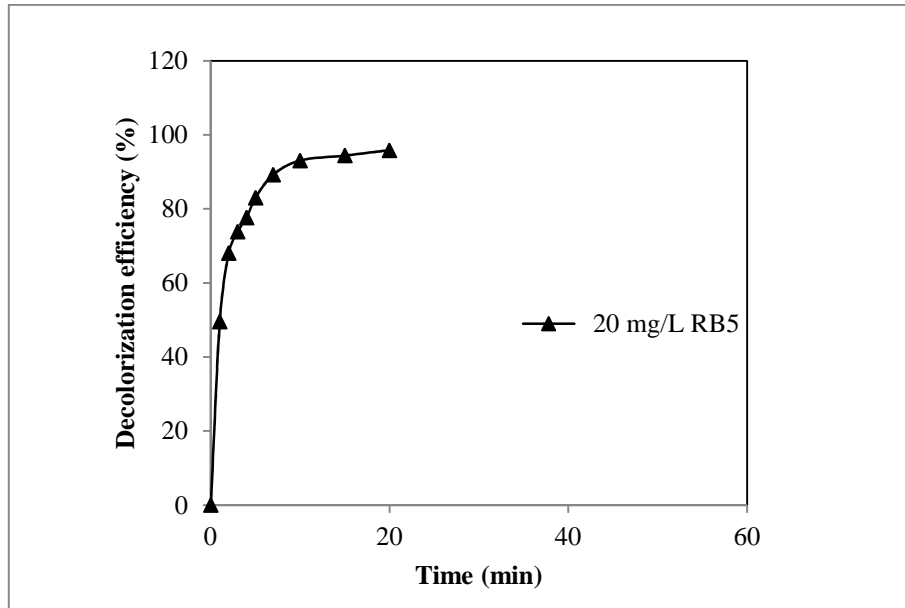


Figure 5.5.1. Effect of initial dye concentration ($C_0=20$ mg/L RB5, $i=1$ mA/cm², $I=176$ A, S.E=0.02 M Na₂SO₄, $Q=100$ mL/min, rpm=37.1, Natural pH)

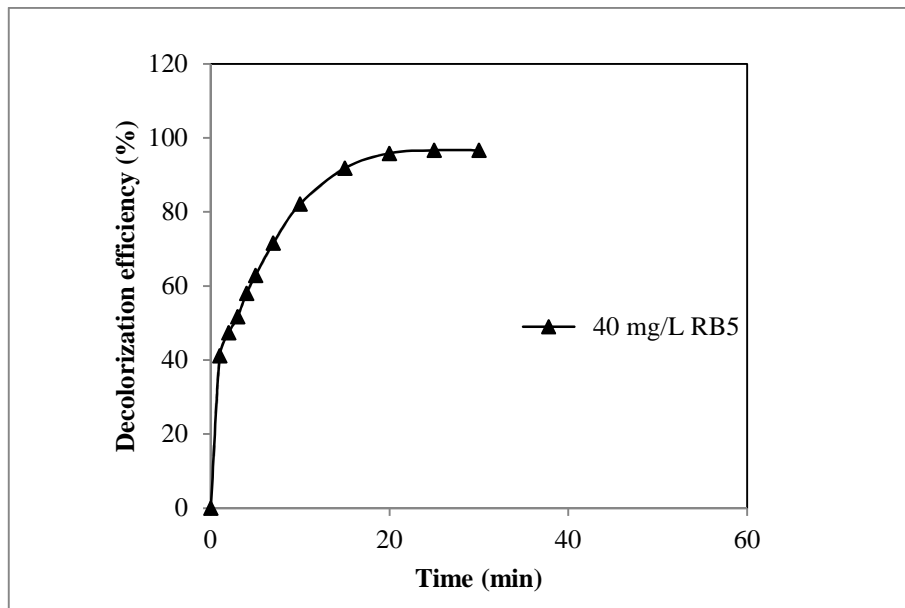


Figure 5.5.2. Effect of initial dye concentration ($C_0=40$ mg/L RB5, $i=1$ mA/cm², $I=176$ A, S.E=0.02 M Na₂SO₄, $Q=100$ mL/min, rpm=37.1, Natural pH)

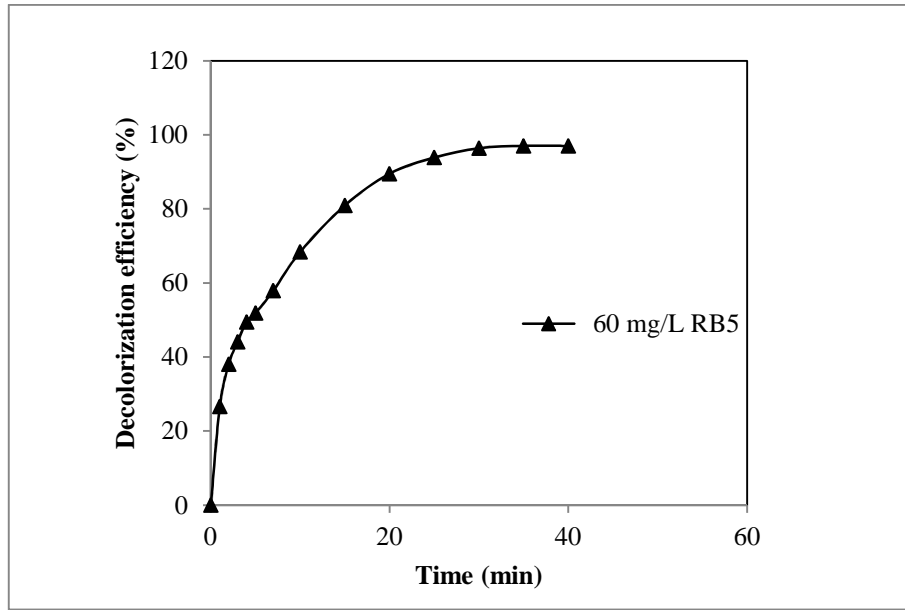


Figure 5.5.3. Effect of initial dye concentration ($C_0=60$ mg/L RB5, $i=1$ mA/cm², $I=176$ A, S.E=0.02 M Na₂SO₄, Q=100 mL/min, rpm=37.1, Natural pH)

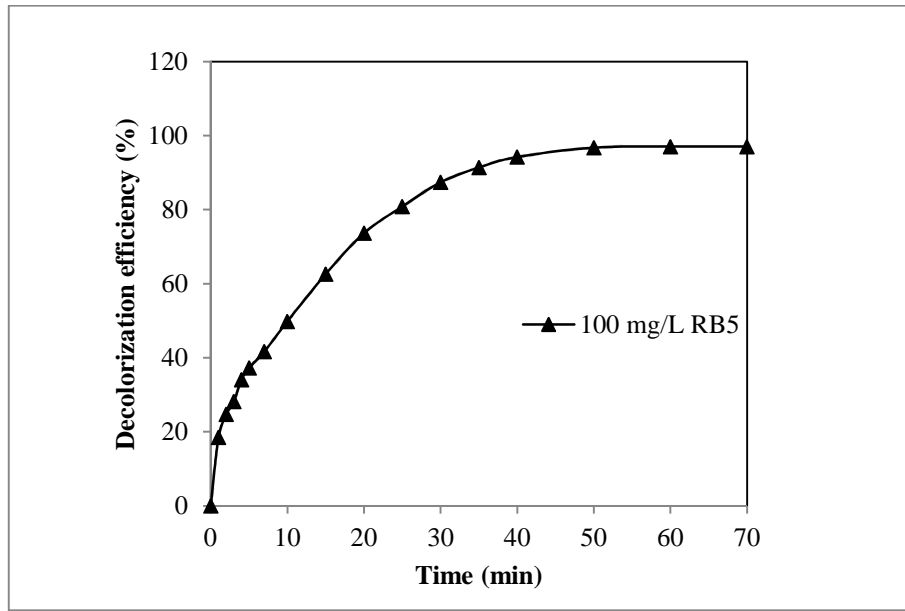


Figure 5.5.4. Effect of initial dye concentration ($C_0=100$ mg/L RB5, $i=1$ mA/cm², $I=176$ A, S.E=0.02 M Na₂SO₄, Q=100 mL/min, rpm=37.1, Natural pH)

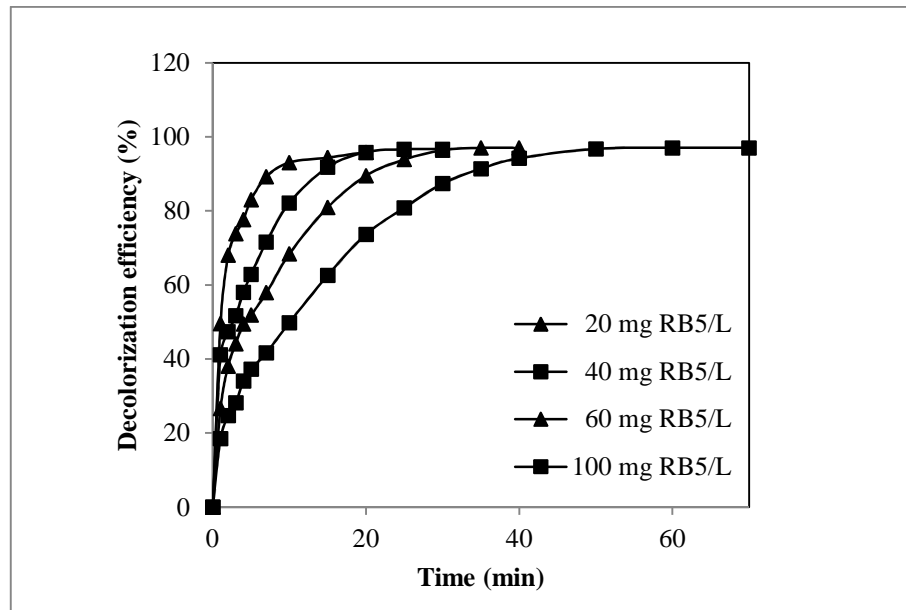


Figure 5.5.5. Comparison chart for effect of initial dye concentration ($i=1 \text{ mA/cm}^2$, $I=176 \text{ A}$, $S.E=0.02 \text{ M Na}_2\text{SO}_4$, $Q=100 \text{ mL/min}$, $\text{rpm}=37.1$, Natural pH)

Effects of flow rate, initial dye concentration, current density, supporting electrolyte, initial pH were examined in anodic oxidation of Reactive Black 5 dye using boron doped diamond anodes in a bipolar trickle tower reactor.

Flow rate of 100 mL/min was chosen as optimum flow rate. Because in low flow rates due to the gas formation, solution flows slowly and it causes the increase of temperature and even in high current densities boiling of the water. Using this value, elimination of any concentration polarization phenomena to be encountered at low flow rates was also assured. When the BTT reactor volume of 125 mL is taken into account, average flow rate of 100 mL/min is a quite high value. This means, solution content of BTT reactor changes completely almost in every 1 min . On the other hand, as a natural and inevitable process of electrochemical systems (especially in a trickle tower reactor) gas formation occurred. These gases contribute to the mixing of the solution and thus also positively affect the mass transfer (Yavuz et al. 2011). Therefore, the results concerning the effect of flow rate on the system may also be attributed to this feature of gas formation in electrochemical systems.

On the other hand, mass transfer coefficients (k_m) for this type of reactor were calculated for comparison purposes. Details about the calculation of mass transfer coefficients can be found elsewhere (Walsh 1993). Little variations in

mass transfer coefficients were observed for different flow rates as it was in decolorization efficiencies. Mass transfer coefficients calculated varied from $1.83 \times 10^{-6} \text{ms}^{-1}$ to $4.66 \times 10^{-6} \text{ms}^{-1}$ with increasing flow rate.

Sodium sulfate was used as supporting electrolyte in this study. 0.02 M Na_2SO_4 is the ideal amount to provide conductivity and dye removal. The peroxodisulfate ion ($\text{S}_2\text{O}_8^{2-}$) is expected to produce in Na_2SO_4 electrolyte when BDD anode is used (Panizza and Cerisola 2010). This ion, generated from the oxidation of SO_4^{2-} ions can also play an important role in the degradation of dye with high reaction rate (Muruganathan et al. 2007; Chen et al. 2003; Cañizares et al. 2004). Additionally, the production of peroxodisulfates is favored at higher concentrations of electrolyte under high temperature and current density conditions (Panizza et al. 2001; Muruganathan et al. 2007; Bechtold et al. 2006).

pH studies showed that there is no need to adjust the pH of the solution. Decolorization efficiencies in all pH experiments (acidic, alkali, natural pH) were near each other and because of that all the experiments were done in natural pH (6.15) without any pH adjustment. This is probably due to the degradation of dye and the electrode reactions. It is a positive result because additional chemical usage is not required and it makes the process cost effective. Final pH values were about 7.07, 7.11, and 7.97 for initial pH studies of 3.52, 6.15, and 10.17, respectively. As the discharge standards about neutral pH values are taken into consideration, these results are positive.

One of the most important parameters affecting the performance of an electrochemical system is current density (Yavuz et al. 2011). The dependence of RB5 concentration on current density can be seen in Figure 5.4.8. As shown in the figure the highest current density led to the most significant decrease in RB5 concentration. It is clear that increasing the current density accelerates dye removal. For instance, after 10 min electrolysis 28.7%, 57.5%, 82.2% and 91% dye removal values were obtained for the current densities of 0.5, 0.75, 1 and 1.25 mA/cm^2 , respectively. It took only 20 min electrolysis to reach more than 95% dye removal for the current densities of $\geq 1 \text{ mA/cm}^2$ with an energy consumption value of 29.76 kWh m^3 . However, even after 60 min electrolysis 90% dye removal at the current density of 0.5 mA/cm^2 could be obtained with an energy consumption value of 31.11 kWh m^3 . In this situation, although more current density (1 mA/cm^2 versus 0.5 mA/cm^2) is applied to the electrochemical system,

unit energy consumption as kWh per m³ wastewater treated is less in higher current density. Besides, for three higher current densities studied (1, 1.125 and 1.25 mA/cm²) performances were almost similar as shown in Figure 4.4.8. It should also be noted that decay of graphite feeder electrodes to fine particles was observed for higher current densities like 1.125 and 1.25 mA/cm². Finally, in the light of all these results achieved, the optimum current density was chosen as 1 mA/cm².

Dye removal of over 97% was reached for all initial dye concentrations and according to the figure, the smaller the concentration the higher the removal efficiencies. That is, as the concentration increased, as expected the time required to obtain the same decolorization efficiency increased. For instance, it took 20, 25, 30 and 50 min electrolysis to achieve 97% dye removal for initial dye concentrations of 20, 40, 60 and 100 mg/L RB5, respectively.

After the best experimental conditions were determined, COD and total organic carbon (TOC) analysis were performed under these conditions using an initial dye concentration of 100 mg/L. Although dye concentration was very high (100 mg/L), corresponding COD (88.5 mg/L) and TOC (140 mg/L) values were low. After 25 min electrolysis, initial COD was decreased to 43.4 mg/L, giving a removal efficiency of ~51%. Similarly, initial TOC was decreased to 99 mg/L with a removal efficiency of 29.3%. The COD and TOC removal were marginal after a given time period. COD and TOC analysis were also repeated after 50 min electrolysis extending the experimental study time. However, results didn't change. Nevertheless COD and TOC removal results for RB5 dye comply with literature (Riera-Torres and Gutiérrez 2010; Sakalis et al. 2005; Soloman et al. 2009). Riera-Torres and Gutiérrez (2010) have mentioned 15% COD reduction at the current density of 6 mA/cm² with electrochemical treatment in their studies. Sakalis et al. (2005) have reported 45% COD removal in batch mode and Soloman et al. (2009) have reported some COD removal values between 47% and 72.9% for batch reactor in recirculation mode. Literature reports state that the chromophore groups of dyes are easily destroyed by direct and indirect oxidation, and later the subsequent intermediate products and other organics undergo further anodic oxidation at a much lower rate (Naumczyk et al. 1996). In the electrochemical degradation of textile dye solutions, the rate of color removal was

higher than COD removal due to the faster azo bond degradation (Körbahti and Tanyolaç 2008).

5.6. Spectrum of Reactive Black 5 Dye

After determining the optimum conditions for the study analyzing tests have been performed, one of these analyzing tests is dye's spectra in different time intervals. UV–VIS spectra of RB5 from the start ($t = 0$) to the end ($t = 25$ min) of electrolysis under the best experimental conditions was performed. The RB5 spectra in the VIS region and the organics degradation in the UV region between 200 and 800 nm were investigated. Spectra chart shows the dye removal in different time intervals according to samples absorbance. And also shows the wavelength of the dye solution. Reactive Black 5 dye contains some organic materials that have their absorbance in UV region. Looking to the spectra it is obvious that decolorization was happened at the two wavelength point simultaneously (Figure 5.6.1). After 25 min electrolysis almost zero absorbance values were reached for dye removal in the VIS region. On the other side, peaks that responsible for organics in the UV region decreased by about 50% as complied with the COD results.

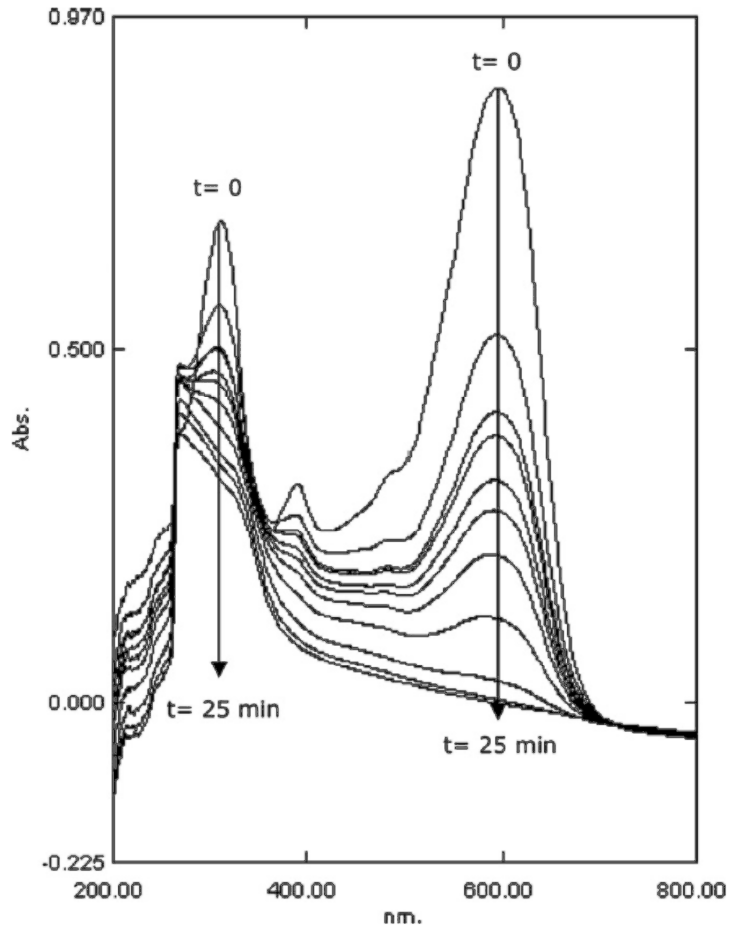


Figure 5.6.1. Spectrum of RB5 dye (Co=40 mg/L RB5, $i=1 \text{ mA/cm}^2$, $I=176 \text{ A}$, S.E=0.02 M Na_2SO_4 , $Q=100 \text{ mL/min}$, rpm=37.1, Natural pH)

5.7. Energy Consumption

Current density is closely related with the applied potential. More voltage is required to provide high current density. This situation also results in more energy consumption. Any new method in water treatment to get used, have to be affordable. Here in this section energy consumption values are shown in the table 4.7.1 and figure 5.7.1 to show how much energy this dye removal system consumes.

Table 5.7.1. Variation of energy consumption with current density (Co=40 mg/L RB5, S.E=0.02 M Na₂SO₄, Q=100 mL/min, rpm=37.1, Natural pH)

Time (min)	0,5 mA/cm ²	0,625 mA/cm ²	0,75 mA/cm ²	0,875 mA/cm ²	1 mA/cm ²	1,125 mA/cm ²	1,25 mA/cm ²
0	0	0	0	0	0	0	0
1	0.458	0.733	0.928	1.247	1.484	1.835	2.178
2	0.933	1.478	1.927	2.5	3.039	3.63	4.312
3	1.429	2.229	2.93	3.778	4.547	5.366	6.358
4	1.942	2.966	3.938	5.041	6.049	7.148	8.433
5	2.482	3.758	4.919	6.35	7.562	8.943	10.58
7	3.555	5.298	6.882	8.814	10.53	12.4	14.67
10	5.254	7.531	9.812	12.42	14.86	17.57	20.61
15	7.894	11.2	14.63	18.71	22.19	25.85	30.44
20	10.64	14.79	19.29	24.48	29.76	34.1	40.08
25	13.22	18.35	24.05	30.18	36.95	-	-
30	15.84	21.98	28.67	36.16	-	-	-
35	18.42	25.61	33.26	42.06	-	-	-
40	20.96	29.27	37.84	47.66	-	-	-
50	26.04	36.35	47.3	59.62	-	-	-
60	31.11	43.46	-	-	-	-	-

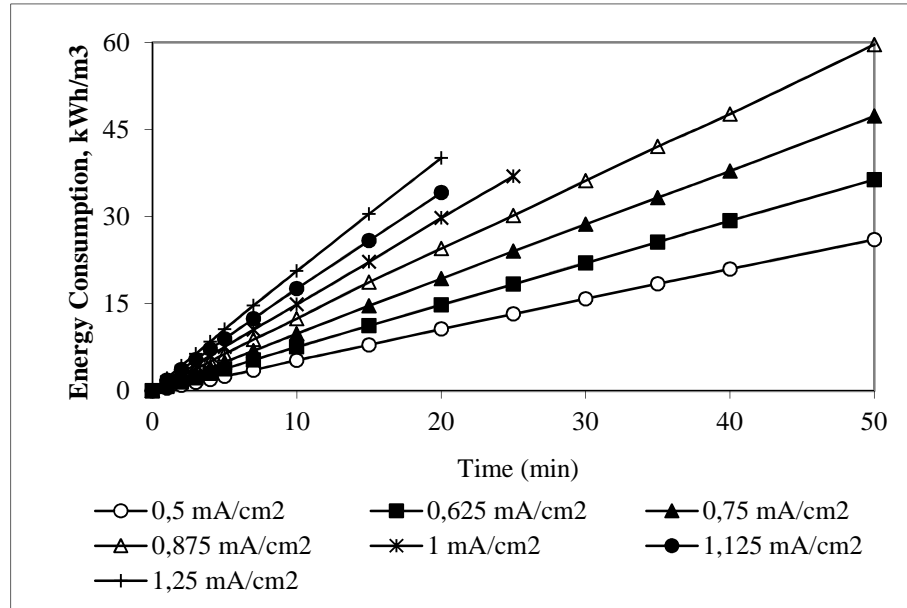


Figure 5.7.1. Variation of energy consumption with current density ($C_0=40$ mg/L RB5, $S.E=0.02$ M Na_2SO_4 , $Q=100$ mL/min, $rpm=37.1$, Natural pH)

5.8. Toxicity Studies

Microtox[®] bioassay tests were performed to measure the toxicity of model solution treated in the electrochemical reactor for given times including the time zero and under best experimental conditions. Toxicity results were given as relative toxicity index (RTI) (5.8.1) (Yavuz et al. 2006).

$$RTI = \frac{EC_{50}\% (t=0)}{EC_{50}\% (t=t)} \quad (5.8.1)$$

Where $EC_{50}\% (t = 0)$ and $EC_{50}\% (t = t)$ are the 5 min and 15 min Microtox toxicity of the samples at times 0 and t. Relative toxicity results are given in figure 5.8.1 as a function of time. Toxicity ratings on the basis of percentage inhibition of luminescence towards Microtox for assessing toxicity of environmental samples are given as follows: (Yavuz and Koparal 2006); Pandey et al. 2003) $EC_{50} (\%) \leq 25$ = highly toxic; 25-50 = moderately toxic; 51-75 = toxic; >75 = slightly toxic; >100 = non-toxic. According to these ratings, toxicities of RB5 solution were reduced to more acceptable levels when the toxicities of the initial

solution were taken into consideration. Toxicity reduction was a significant success, and is an advantage of using BDD anodes. Toxicity is decreased rapidly by electrochemical process in first 5 min and then gives stable RTI values of about 0.333, corresponding to EC₅₀ values of about 30% for 5 min and 15 min Microtox toxicity. According to the toxicity ratings; initially highly toxic EC value of RB5 dye was decreased to moderately toxic value. In addition to the COD, TOC and spectra in the UV region, electrochemical process exhibited a limited performance for toxicity reduction.

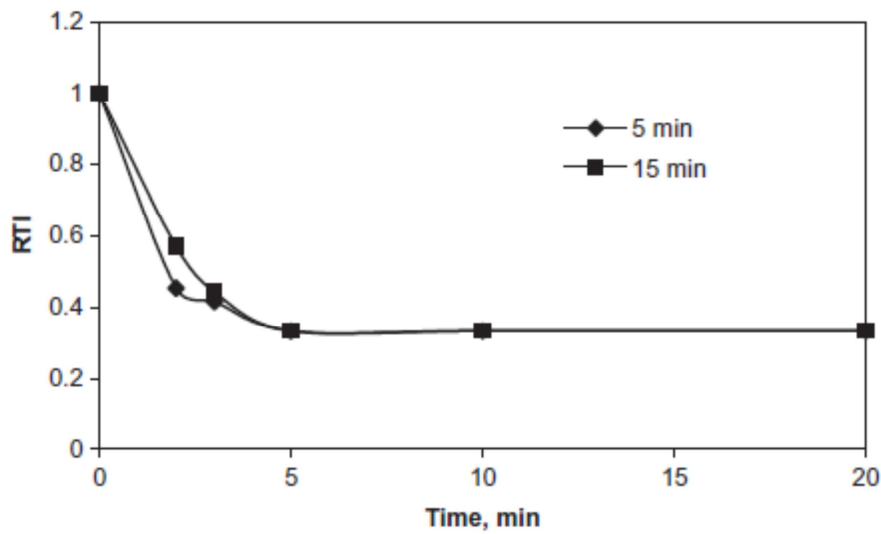


Figure 5.8.1. Variation of 5th min and 15th min toxicity of dye solution with time ($C_0=40$ mg/L RB5, $i=1$ mA/cm², $I=176$ A, S.E=0.02 M Na₂SO₄, $Q=100$ mL/min, rpm=37.1, Natural pH)

6. CONCLUSION

In this study, electrochemical oxidation of RB5 dye using BTT reactor and Raschig ring shaped BDD electrodes in recirculated batch mode was realized. Effects of flow rate, sodium sulfate concentration (Na₂SO₄) as supporting electrolyte, initial pH, current density and initial dye concentration on electrochemical treatment were investigated. The best experimental conditions obtained were as follows: current density 1 mA/cm², natural pH, flow rate 100 mL/min, Na₂SO₄ concentration 0.02 mol/L. Under these conditions, 97% color, ~51% COD and 29.3% TOC removal were achieved. It was observed that color removal was faster and easier than organics removal. UV-VIS spectra results of

the samples withdrawn under the best experimental conditions were also compatible with absorbance, COD and TOC analysis. Toxicity of RB5 solution was decreased to more acceptable level in comparison to its initial toxicity value. According to all results, in addition to COD and TOC removal, electrochemical process also exhibited a limited performance for toxicity reduction for this dye solution.

REFERENCES

Al-Bastaki, N. (2004), "Removal of Methyl Orange Dye and Na₂SO₄ Salt from Synthetic Wastewater Using Reverse Osmosis," *Chem. Eng. Process*, 43, 1561-1567.

Anonymous (1998), "The Microtox Acute Basic, DIN, ISO and Wet Test Procedures," Azur Environmental, Carlsbad, CA, USA.

Awad, H.S. and Galwa, N.A. (2005), "Electrochemical Degradation of Acid Blue and Basic Brown Dyes on Pb/PbO₂ Electrode In The Presence of Different Conductive Electrolyte and Effect of Various Operating Factors," *Chemosphere*, 61, 1327, 1335.

Bandala, E.R., Pelaez, M.A., García, A.J., Salgado, M.J. and Moeller, G. (2008), "Photocatalytic Decolorization of Synthetic and Real Textile Wastewater Containing Benzidine Based Azo Dyes," *Chem. Eng. Process*, 47, 169-176.

Bechtold, T., Turcanu, A. and Schrott, W. (2006), "Electrochemical Decolourisation of Dispersed Indigo on Boron-Doped Diamond Anodes," *Diam. Relat. Material*, 15, 1513-1519.

Bolton, J. and Cater, S.R. (1994), "*Aquatic and Surface Photochemistry*," Lewis Publishers, Boca Raton, Florida.

Brune, D.J., Mendlratta, A., and Singleton, D.A. (1985), "Reaction/Removal of Polychlorinated Biphenyls from Transformer Oil: Treatment of Contaminated Oil with Poly(ethylene glycol)/KOH," *Environ. Sci. Technol.* 19, 740.

Cañizares, P., Sáez, C., Lobato, J. and Rodrigo, M.A. (2004), "Electrochemical Treatment of 4-Nitrophenol-Containing Aqueous Wastes Using Boron-Doped Diamond Anodes," *Ind. Eng. Chem. Res.*, 43, 1944-1951.

Chang, C., Liao, Y., Wang, G.Z., Ma, Y.R. and Fang, R.C. (2008), *CVD Diamond Growth*, University of Science and Technology of China, Hefei, 230026 Anhui, China.

Chen, J., Liu, M., Zhang, J., Xian, Y. and Jin, L. (2003), “Electrochemical Degradation of Bromopyrogallol Red in Presence of Cobalt Ions,” *Chemosphere*, 53, 1131-1136.

Chen, X., Chen, G. and Yue, P.L. (2003), “Anodic Oxidation of Dyes at Novel Ti/B-Diamond Electrodes,” *Chem. Eng. Sci.*, 58, 995-1001.

Comninellis, Ch. (1994), “Electrocatalysis in The Electrochemical Conversion/Combustion of Organic Pollutants for Waste Water Treatment,” *Electrochem. Acta*, 39, 1857-1862.

Comninellis, Ch. (1994), “Electrocatalysis in the Electrochemical Conversion/Combustion of Organic Pollutants for Waste Water Treatment,” *Electrochem. Acta*, 39, 1857-1862.

Daneshvar, N., Oladegaragoze, A. and Djafarzadeh, N. (2006), “Decolorization of Basic Dye Solutions by Electrocoagulation: An Investigation of the Effect of Operational Parameters,” *J. Hazard. Mater.*, B129, 116-122.

Daneshvar, N., Rabbani, M., Modirshahla, N. and Behnajady, M.A. (2005), “Photooxidative Degradation of Acid Red 27 in A Tubularcontinuous-Flow Photoreactor: Influence of Operational Parameters and Mineralization Products,” *J. Hazard. Mater.*, B118, 155-160.

Davila-Jimenez, M.M., Elizalde-Gonzalez, M.P. and Pelaez-Cid, A.A. (2005), “Adsorption Interaction between Natural Adsorbents and Textile Dyes in Aqueous Solution,” *Colloid. Surf., A* 254, 107-114.

Dos Santos, A.B., Cervantes, F.J. and Van Lier, J.B. (2007), “Review Paper on Current Technologies for Decolorization of Textile Wastewaters: Perspectives for Anaerobic Biotechnology,” *Bioresour. Technol.*, 98, 2369-2385.

Dubpernel, G., "Selected topics in the history of electrochemistry," The Electrochemical Society, Princeton, 1978.

Farmer, J.C., Wang, F.T., Hawley-Fedder, R.A., Lewis, P.R., Summers, L.J. and Foiles, L. (1992), "Electrochemical Treatment of Mixed and Hazardous Wastes: Oxidation of Ethylene Glycol by Cobalt (III) and Iron (III)," *J. Electrochem. Soc.*, 139, 654-662.

Fernandes, A., Morão, A., Magrinho, M., Lopes, A. and Goncalves, I. (2004), "Electrochemical Degradation of C.I. Acid Orange 7," *Dyes Pigments*, 61, 287-296.

Fleet, B., "Evolution of electrochemical reactor system for metal recovery and pollution control," (Ed: Stock, J.T. and Orna, M.V.), *Electrochemistry, Past and Present*, American Chemical Society, Washington, DC, 1989.

Flox, C., Arias, C., Brillas, E., Savall, A. and Groenen-Serrano, K. (2009), "Electrochemical Incineration of Cresols: A Comparative Study between PbO_2 and Boron-Doped Diamond Anodes," *Chemosphere*, 74, 1340-1347.

Flox, C., Cabot, P.L., Centellas, F., Garrido, J.A., Rodriguez, R.M., Arias, C. and Brillas, E. (2006), "Electrochemical Combustion of Herbicide Mecoprop in Aqueous Medium Using a Flow Reactor with a Boron-Doped Diamond Anode," *Chemosphere*, 64, 892-902.

García-Montaña, J., Doménech, X., García-Hortal, J.A., Torrades, F. and Peral, J. (2008), "The Testing of Several Biological and Chemical Coupled Treatments for Cibacron Red FN-R Azo Dye Removal," *J. Hazard. Mater.*, 154, 484-490.

Grimau, V.L. and Gutierrez, M.C. (2006), "Decolourisation of simulated reactive dyebath effluents by electrochemical oxidation assisted by UV light," *Chemosphere*, 62, 106-112.

Harper, T.R. and Kingham, N.W. (1992), "Removal of Arsenic from Wastewater Using Chemical Precipitation Methods," *Water Environ. Res.*, 64, 200.

Jüttner, K., Galla, U. and Schmieder, H. (2000), "Electrochemical approaches to environmental problems in the process industry," *Electrochim. Acta*, 45, 2575–2594.

Kim, T., Park, C., Lee, J. ve Shin, E. (2002), "Pilot Scale Treatment of Textile Wastewater by Combined Process (Fluidized Biofilm Process-Chemical Coagulation -Electrochemical Oxidation)," *Water Research*, 36, 3979-3988.

Koparal, A.S., Yavuz, Y. and Öğütveren, Ü.B. (2002), "Electroadsorption of Acilan Blue Dye From Textile Effluents by Using Activated Carbon-Perlite Mixtures," *Water Environ. Res.*, 6, 521-525.

Koparal, A.S., Yavuz, Y., Gürel, C. and Öğütveren, Ü.B. (2006), "Electrochemical Degradation and Toxicity Reduction of C.I. Basic Red 29 Solution and Textile Wastewater by Using Diamond Anode," *J. Hazard. Mater.*, 145, 100-108.

Koparal, A.S., Yavuz, Y., Gurel, C. and Öğütveren, Ü.B. (2007), "Electrochemical Degradation and Toxicity Reduction of C.I. Basic Red 29 Solution and Textile Wastewater by Using Diamond Anode," *J. Hazard. Mater.*, B145, 100-108.

Körbahti, B.K. and Tanyolaç, A. (2008), "Electrochemical Treatment of Simulated Textile Wastewater with Industrial Components and Levafix Blue CA Reactive Dye: Optimization through Response Surface Methodology," *J. Hazard. Mater.*, B151, 422-431.

Kraft, A., Stadelmann, M. and Blaschke, M. (2003), "Anodic Oxidation with Doped Diamond Electrodes: A New Advanced Oxidation Process," *J. Hazard. Mater.*, B103, 247-261.

Kul'skii, L.A., Stokach, P.P., Slipchenko, V.A. and Saigak, E.I., *Water Purification by Electrocoagulation*, Budivel'nik, Kiev, 1978.

Leddy, J.J., "Industrial Electrochemistry," (Ed: Stock, J.T. and Orna, M.V.), *Electrochemistry, Past and Present*, American Chemical Society, Washington, DC, 1989.

Li, H., Zhu, X. and Ni, J. (2010), "Inactivation of Escherichia Coli in Na₂SO₄ Electrolyte Using Boron-Doped Diamond Anode," *Electrochim. Acta* 56, 448-453.

Lin, S.H. and Peng, C.F. (1994), "Treatment of Textile wastewater by Electrochemical Method," *Water Research*, 28, No: 2, 277-282.

Marselli, B., Garcia-Gomez, J., Michaud, P.A., Rodrigo, M.A. and Comninellis, C. (2003), "Electrogeneration of Hydroxyl Radicals on Boron-Doped Diamond Electrodes," *J. Electrochem. Soc.*, 150, D79-D83.

Martínez-Huitle, C.A. and Brillas, E. (2009), "Decontamination of Wastewaters Containing Synthetic Organic Dyes by Electrochemical Methods: A General Review," *Appl. Catal. B. Environ.*, 87, 105-145.

Matsumoto, S., Sato, Y., Tsumi, M. and Setaka, N. (1982), "Hot-filament CVD," *J. Mater. Sci.* 17, 3106.

Meriç, S., Kaptan, D. and Ölmez, T. (2004), "Color and cod removal from wastewater containing reactive black 5 using fenton's oxidation process," *Chemosphere*, 54, 435-441.

Michaels, A.S. (1990), "Membranes, Membrane Processes, and Their Applications: Needs, Unsolved Problems and Challenges of the 1990's," *Desalination*, 77, 5.

Muruganathan, M., Yoshihara, S., Rakuma, T., Uehara, N. and Shirakashi, T. (2007), "Electrochemical degradation of 17 β -estradiol (E2) at boron-doped diamond (Si/BDD) thin film electrode," *Electrochim., Acta* 52, 3242-3249.

Naumczyk, J., Szpyrkowicz, L. and Zilio-Grandi, F. (1996), "Electrochemical treatment of textile wastewater," *Water Sci. Technol.*, 34, 17-24.

Orozco, S., Bandala, E.R., Arancibia, C., Serrano, B., Suarez, R. and Hernández, I. (2008), "Effect of iron salt on the color removal of water containing the azo reactive blue 69 using photo-assisted Fe(II)/H₂O₂ and Fe(III)/H₂O₂ systems," *J. Photochem. Photobiol. A: Chem.*, 198, 144-149.

Panakoulias, T., Kalatzis, P., Kalderis, D. and Katsaounis, A. (2010), "Electrochemical degradation of reactive red 120 using dsa and bdd anodes," *J. Appl. Electrochem.*, 40, 1759-1765.

Pandey, A.K., Pandey, S.D., Misra, V. and Srimal, A. (2003), "Removal of chromium and reduction of toxicity to microtox system from tannery effluent by the use of calcium alginate beads containing humic acid," *Chemosphere*, 51, 329-333.

Panizza, M. and Cerisola, C. (2008), "Removal of Colour and COD from Wastewater Containing Acid Blue 22 by Electrochemical Oxidation," *J. Hazard. Mater.*, 153, 83-88.

Panizza, M. and Cerisola, G. (2005), "Application of diamond electrodes to electrochemical processes," *Electrochim., Acta* 51, 191-199.

Panizza, M., Michaud, P.A., Cerisola, G. and Comninellis, C. (2001), "Anodic oxidation of 2-naphthol at boron-doped diamond electrodes," *J. Electroanal. Chem.*, 507, 206-214.

Petricic, I., Andersen, N.P.R., Šostar-Turk, S. and Marechal, A.M. (2007), "The removal of reactive dye printing compounds using nanofiltration," *Dyes Pigments*, 74, 512-518.

Petrucci, E. and Montanaro, D. (2011), "Anodic Oxidation of a Simulated Effluent Containing Reactive Blue 19 on a Boron-Doped Diamond Electrode," *Chem. Eng. J.*, 174, 612– 618.

Rajeshwar, K. and Ibanez, J.G. (1997), "*Environmental Electrochemistry: Fundamentals and Applications in Pollution Abatement*," Elsevier Inc.

Raju, G.B. and Khangaonkar (1984), "Electroflotation-A Critical Review," *Trans. Indian Inst. Met.*, 37 (1), 59-66.

Riera-Torres, M. and Gutiérrez, M. (2010), "Colour removal of three reactive dyes by UV light exposure after electrochemical treatment," *Chem. Eng. J.*, 156, 114-120.

Sakalis, A., Mpoulmpasakos, K., Nickel, U., Fytianos, K. and Voulgaropoulos, A. (2005), "Evaluation of a novel electrochemical pilot plant process for azodyes removal from textile wastewater," *Chem. Eng. J.*, 111, 63-70.

Sawyer, N., McCarty, L. and Parkin, F. (2003), *Chemistry for environmental engineering and science*, 5th edition, New York: McGraw-Hill, 15-20.

Shu, H.Y. and Chang, M.C. (2005), "Decolourization effects of six azo dyes by O₃, UV/O₃ and UV/H₂O₂ processes," *Dyes Pigments*, 65, 25-31.

Soloman, P.A., Basha, C.A., Velan, M., Ramamurthi, V., Koteeswaran, K. and Balasubramanian, N. (2009), "Electrochemical Degradation of Remazol Black B Dye Effluent," *Clean-Soil Air Water*, 37, 889-900.

Swamy, J. and Ramsay, J. (1999), "The evaluation of white rot fungi in the decoloration of textile dyes," *Enzyme Microb. Technol.*, 24, 130-137.

Thomas, J.M. and Ward, C.H. (1998), "In Situ Bioremediation of Organic Contaminants in the Subsurface," *Environ. Sci. Technol.* 23, 760.

Vlyssides, A.G., Loizidou, M., Karlis, P.K., Zorpas, P. and Papaioannou, D. (1999), "Electrochemical Oxidation of A Textile Wastewater Using A Pt/Ti Electrode," *J. Hazard. Mater.*, 70, 41-52.

Walsh, F.C. (1993), *A first course in electrochemical engineering*, Alresford Press Ltd., Hants, Great Britain.

Walsh, M.A. and Morris, R. S. (1987), *Electrolytic Reactor and Method for Treating Fluids*. U.S.. Patent No: 4,690,741

Wang, C., Yediler, A., Lienert, D., Wang, Z. and Kettrup, A. (2003), "Ozonation of an Azo Dye C.I. Remazol Black 5 and toxicological assessment of its oxidation products," *Chemosphere*, 52, 1225-1232.

Wu, J., Liu, C., Chu, K.H. and Suen, S. (2008), "Removal of Cationic Dye Methyl Violet 2B from Water by Cation Exchange Membranes," *J. Membr. Sci.*, 309, 239-245.

Yavuz, Y. and Koparal, A.S. (2006), "Electrochemical Oxidation of Phenol in a Parallel Plate Reactor Using Ruthenium Mixed Metal Oxide Electrode," *J. Hazard. Mater.*, B136, 296-302.

Yavuz, Y. and Shahbazi, R. (2012), "Anodic Oxidation of Reactive Black 5 Dye Using Boron Doped Diamond Anodes in a Bipolar Trickle Tower Reactor," *Separation and Purification Technology*, 85, 130-136.

Yavuz, Y., Koparal, A.S. and Ögütveren, Ü.B. (2008), "Phenol Degradation in a Bipolar Trickle Tower Reactor Using Boron-Doped Diamond Electrode," *J. Environ. Eng.-ASCE*, 134, 24-31.

Yavuz, Y., Koparal, A.S. and Ögütveren, Ü.B. (2011), "Electrochemical Oxidation of Basic Blue 3 Dye Using a Diamond Anode: Evaluation of Colour, COD and Toxicity Removal," *J. Chem. Technol. Biotechnol.*, 86, 261-265.

Yavuz, Y., Koparal, A.S., Artık, A. and Ögütveren, Ü.B. (2009), “Degradation of C.I. Basic Red 29 Solution by Combined Ultrasound and Co^{2+} - H_2O_2 System,” *Desalination*, 249, 828-831.

APPENDIX-1 Calculations of Anode Surface Area of Each Electrode and Total Surface Area of BDD Electrodes

APPENDIX 1.1. Calculation of Anode Surface Area

Anode is the half of electrode's height. One BDD electrode height is 0.8 cm².surface area of the electrode is equal to sum of its outside and inside lateral surfaces.

$$\text{Outside surface area of the electrode} = \frac{D_L}{2} D_d \pi \quad (\text{Appendix 1.1})$$

$$\text{Inside surface area of the electrode} = \frac{D_L}{2} D_e \pi \quad (\text{Appendix 1.2})$$

$$\text{One electrode's surface area} = \frac{D_L}{2} D_d \pi + \frac{D_L}{2} D_e \pi = \frac{0.8}{2} 0.8\pi + \frac{0.8}{2} 0.55\pi = 1.696 \text{ cm}^2$$

$$\text{Total anode surface area} = 1.696 \text{ cm}^2 \times 26 \times 4 = 176.43 \times 10^{-4} \text{ m}^2$$

APPENDIX-2 Calculations for Determining Dye Concentration

APPENDIX 2.1. Concentration Calculations

First of all with using Appendix 2.1 formula the amount of dye in sample solution can be calculated in mg. Then, using Appendix 2.2 formula concentration of the dye solution can be calculated in mg/L.

$$y = 0.0233x \quad (\text{Appendix 2.1})$$

$$\text{mg dye amount/L} = \frac{x}{z} 1000 \quad (\text{Appendix 2.2})$$

In this formula:

- x = mg dye amount in sample
- z = mL original sample volume

For instance dye amount in a solution that its absorbance is (y) 0.250 can be calculated using Appendix 2.1 formula;

$$0.250 = 0.0233x$$

$$x = 10.72 \text{ mg dye amount}$$

Using this x value and replacing it in the Appendix 2.2 formula and replacing volume as 1000 mL it will be;

$$\text{mg dye amount/L} = \frac{10.72}{1000} 1000 = 10.72 \text{ mg/L}$$

APPENDIX-3 Sample Calculations

In sample calculations exposed results of table 5.5.2 have been used (CO=40 mg/L RB5, $i=1$ mA/cm², I=176 A, S.E=0.02 M Na₂SO₄, Q=100 mL/min, rpm=37.1, Natural pH, volume 0.5L, t=2).

Appendix 3.1. Decolorization Efficiency (%)

Using (Appendix 3.1.1) decolorization efficiency has been calculated.

$$\%Giderim = \frac{C_0 - C}{C_0} 100 \quad (\text{Appendix 3.1.1})$$

$$\%Giderim = \frac{37.339 - 19.657}{37.339} 100 = \%47.356$$

Appendix 3.2. Energy Consumption

Using (Appendix 3.2.1) energy consumption has been calculated for t=2 min.

$$(\text{kWhm}^{-3}) = \frac{I \cdot V \cdot t_b - t_a / 60}{V} \quad (\text{Appendix 3.2.1})$$

$$\frac{0.176 \text{ A} \times 265 \text{ V} \times 1 / 60}{0.5 \text{ L}} = 1.55 \text{ kWhm}^{-3}$$

APPENDIX-4 Chemical Oxygen Demand Test

APPENDIX 4.1. COD Test Procedure

To do the test Potassium dichromate, Silver nitrate, Ferroin Indicator and ferrous ammonium sulfate (FAS) were used. Potassium dichromate is a strong oxidizing agent under acidic conditions. In the process of oxidizing the organic substances found in the water sample, potassium dichromate is reduced (since in all redox reactions, one reagent is oxidized and the other is reduced), forming Cr^{3+} . The amount of Cr^{3+} is determined after oxidization is complete, and is used as an indirect measure of the organic contents of the water sample. Because COD measures the oxygen demand of organic compounds in a sample of water, it is important that no outside organic material be accidentally added to the sample to be measured. To control for this, a so-called blank sample is required in the determination of COD. A blank sample is created by adding all reagents (e.g. acid and oxidizing agent) to a volume of distilled water. The oxygen demand in the blank sample is subtracted from the COD for the original sample to ensure a true measurement of organic matter.

For all organic matter to be completely oxidized, an excess amount of potassium dichromate (or any oxidizing agent) must be present. Once oxidation is complete, the amount of excess potassium dichromate must be measured to ensure that the amount of Cr^{3+} can be determined with accuracy. To do so, the excess potassium dichromate is titrated with ferrous ammonium sulfate (FAS) until the entire excess oxidizing agent has been reduced to Cr^{3+} . Typically, the oxidation-reduction indicator Ferroin is added during this titration step as well. Once all the excess dichromate has been reduced, the Ferroin indicator changes from blue-green to reddish-brown. The amount of ferrous ammonium sulfate added is equivalent to the amount of excess potassium dichromate added to the original sample.

The following formula is used to calculate COD:

$$\text{COD} = \frac{8000 (b-s)n}{\text{sample volume}} \quad (\text{Appendix 4.1})$$

Where b is the volume of FAS used in the blank sample, s is the volume of FAS in the original sample, and n is the normality of FAS. If milliliters are used consistently for volume measurements, the result of the COD calculation is given in mg/L.